# QEX

March/April 2006

## A Forum for Communications Experimenters

Issue No. 235


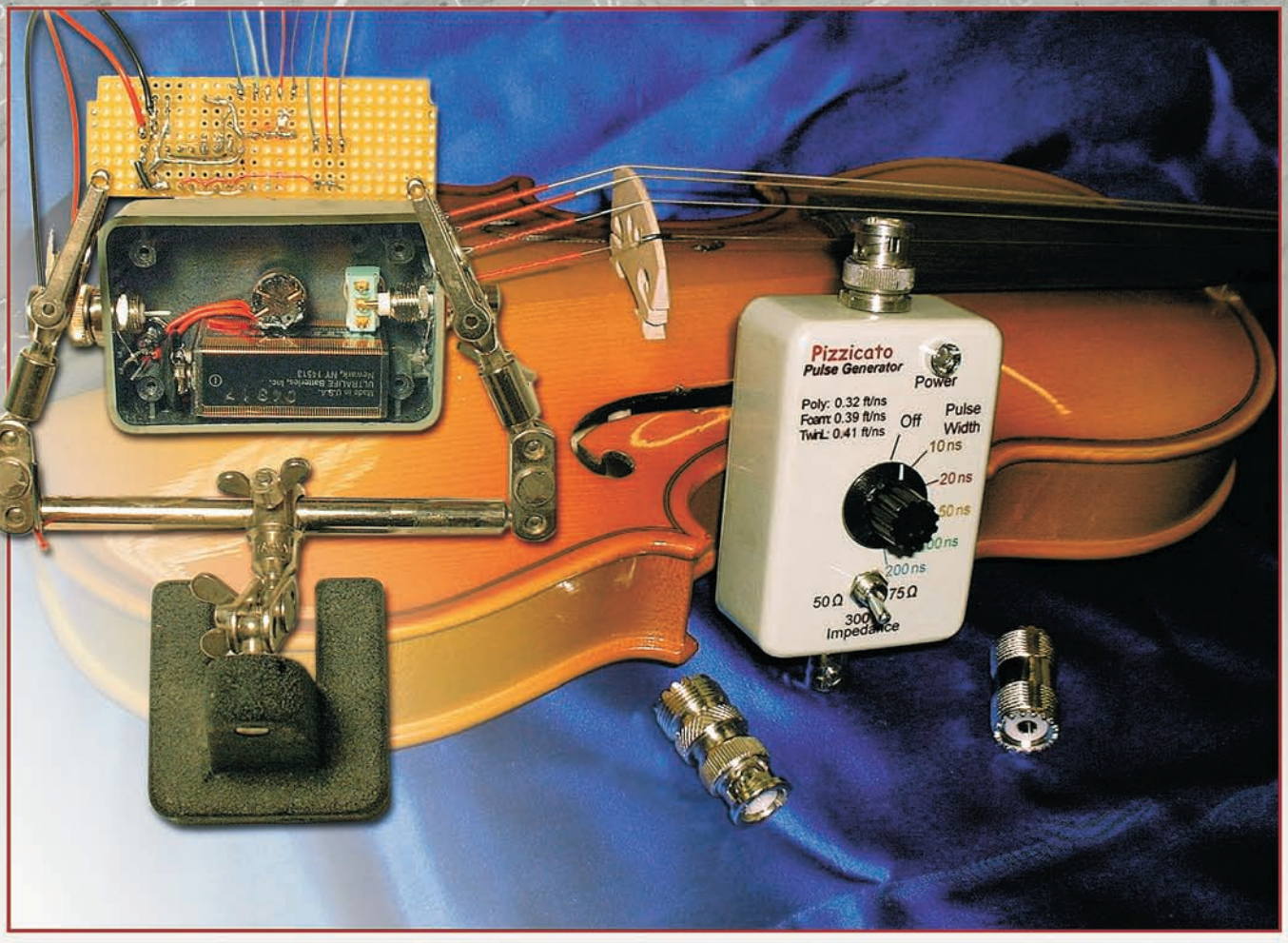


**AF8L** teaches us how to "pluck the strings" of a transmission line to hear the sweet music produced when we see the characteristics of that line on an o'scope.


**ARRL** *The national association for* ***AMATEUR RADIO***

225 Main Street
Newington, CT USA 06111-1494

# Continuing Education

**Register Online! www.arrl.org/cce**

**There's no better time to improve your skills**. **Online Classes are Available Now** through the ARRL Certification and Continuing Education Program. Complete 100% of your training via the Internet:

- **Self-paced (asynchronous) format**—you attend class when and where you want.
- **High quality web experience** enhanced with graphics, audio, video, hyper-linking and interactive modules.
- **Online Mentoring**. Individually assigned instructors help advance each student toward successfully completing the course material.
- **Register Now!** Classes open regularly.

## Available Courses

### Antenna Design and Construction...EC-009
Sample of subjects covered:
- Introduction and Basics
- The Ground-Plane Antenna
- The Dipole
- Transmission Lines
- Impedance Matching
- Loops and Quads

Suggested reading: *Simple and Fun Antennas for Hams*
**Member: $65 / Non-member: $95**

### HF Digital Communications...EC-005
Sample of subjects covered:
- Radioteletype
- PSK31
- Pactor II
- WinLink 2000
- Clover
- Chasing Digital DX
- HF Contesting

Suggested reading: *HF Digital Handbook*
**Member: $65 / Non-member: $95**

### Radio Frequency Propagation...EC-011
Sample of subjects covered:
- Electromagnetic Waves
- Sun Spots
- Ground waves and sky waves
- Solar Indices
- Gray line propagation
- Auroral Propagation
- Meteor Scatter

**Member: $65 / Non-member: $95**

### Radio Frequency Interference...EC-006
Sample of subjects covered:
- Filters
- RF Generators
- Power Line and Electrical Devices
- Automobiles
- Television
- Regulations

Suggested reading: *ARRL RFI Book*
**Member: $65 / Non-member: $95**

### VHF/UHF—Life Beyond the Repeater...EC-008
Sample of subjects covered:
- Amateur Satellites
- Direction finding
- APRS
- VHF Contesting
- Microwaves
- High Speed Multimedia Radio

**Member: $65 / Non-member: $95**

### Digital Electronics...EC-013
Sample of subjects covered:
- Basic Boolean
- Basic Gates
- Counters and shift registers
- Buffers and Latches
- Parallel Interfaces
- Input Devices
- Logic Families
- Microprocessors

**Member: $65 / Non-member: $95**

### Antenna Modeling...EC-004
Sample of subjects covered:
- Antenna modeling by computer
- *NEC-2* and other modeling "cores" in commercial software
- Language of modeling
- Antenna model outputs
- Frequency selection, sweeps and scaling
- Workarounds for *NEC-2* limitations
- Modeling by Equation
- Advanced and specialized modeling

Suggested reading: *ARRL Antenna Modeling Course*
**Member $65 / Non-member $85**

ARRL The national association for AMATEUR RADIO

**For the complete course catalog, visit www.arrl.org/cce**

Online courses are produced by American Radio Relay League, Inc. and are available through ARRL's partnership with the Connecticut Distance Learning Consortium (CTDLC), a nonprofit organization that specializes in developing on-line courses for Connecticut colleges and universities. Continuing Education Units (CEUs) are available for all ARRL Certification and Continuing Education courses. The ARRL Certification and Continuing Education Program is funded in part by course fees from interested hams who support public service and quality continuing education.

For further information, e-mail your questions to **cce@arrl.org**, or write to **ARRL C-CE**, **225 Main Street**, **Newington**, **CT 06111**.

*QEX* (ISSN: 0886-8093) is published bimonthly in January, March, May, July, September, and November by the American Radio Relay League, 225 Main Street, Newington, CT 06111-1494. Periodicals postage paid at Hartford, CT and at additional mailing offices.

POSTMASTER: Send address changes to: QEX, 225 Main St, Newington, CT 06111-1494 Issue No 235



**Offices**

225 Main St, Newington, CT 06111-1494 USA
Telephone: 860-594-0200
Fax: 860-594-0259 (24 hour direct line)
e-mail: **qex@arrl.org**

Subscription rate for 6 issues:

In the US: ARRL Member $24, nonmember $36;

US by First Class Mail: ARRL member $37, nonmember $49;

Elsewhere by Surface Mail (4-8 week delivery): ARRL member $31, nonmember $43;

Canada by Airmail: ARRL member $40, nonmember $52;

Elsewhere by Airmail: ARRL member $59, nonmember $71.

Members are asked to include their membership control number or a label from their *QST* when applying.

In order to ensure prompt delivery, we ask that you periodically check the address information on your mailing label. If you find any inaccuracies, please contact the Circulation Department immediately. Thank you for your assistance.




## About the Cover

**Gary Steinbaugh, AF8L, describes his *Pizzicato* Pulse Generator and teaches us how to observe the characteristics of a transmission line by watching the reflected pulses on an oscilloscope. This is one piece of test gear that could be music to your eyes!**

# Features



# Columns



# Mar/Apr 2006 *QEX* Advertising Index

THE AMERICAN RADIO RELAY LEAGUE

# Empirical Outlook



## Familiar Faces in New Jobs

Please join us in welcoming Larry Wolfgang, WR1B, as Managing Editor of *QEX*. Larry comes aboard with considerable experience as a technical editor. His ARRL duties also include being Senior Assistant Technical Editor of *QST*. Previously, he was a member the "Book Team" editorial staff. He was the handling editor for *Now You're Talking, ARRL's Tech Q&A, The ARRL General Class License Manual, ARRL's General Q & A, Your Introduction to Morse Code* — on cassettes and CDs — and *The ARRL Extra Class License Manual*. Larry was responsible for the video licensing courses, as well. He wrote *Understanding Basic Electronics*, a popular book among young hams and hams-to-be. Larry has also edited several chapters of *The ARRL Handbook*.

Larry formats articles and shepherds them through our production process, among other things. His attention to detail is a tremendous asset to our editorial team. You'll find him to be a technically savvy fellow with a positive attitude and some very good ideas about how to ensure that *QEX* remains the top periodical in its field. Give him the support you gave his predecessor and *QEX* will continue to improve.

On January 20, 2006, Joel Harrison, W5ZN, of Judsonia, Arkansas, was elected League President for the next two years. He succeeds Jim Haynie, W5JBP, who chose not to run for a fourth term in the uncompensated, volunteer post. Gathering in Windsor, Connecticut, for its annual meeting, the Board voted 10 to 5 to choose Harrison over ARRL Central Division Director Dick Isely, W9GIG, the only other nominee.

First licensed in 1972 as WN5IGF, Harrison says he's interested in virtually all aspects of Amateur Radio, from HF DXing and contesting to VHF/UHF/microwave and moonbounce. He's an ARRL Life Member. His wife, daughter and son all are Amateur Radio licensees. He's the League's 14th President since its founding in 1914.

Harrison also says he'll promote the League's *Petition for Rule Making* (RM-11306) to regulate Amateur Radio allocations by necessary (occupied) bandwidth. "Right now we do that by mode, and we're one of the few countries in the world that does that," he pointed out. "We need to change that and move forward with this initiative of regulation by bandwidth instead of mode." Related to that issue, the Board is in the process of developing effective band plans to support the rule changes it's requesting in RM-11306.

We feel RM-11306 is a much-needed change. The existing rules are arcane when it comes to allowing for the development of new modes and the efficient use of our spectrum, especially on HF. We hope you've sent your comments to the FCC.

The ARRL Board also elected Vice President Kay Craigie, N3KN, as First Vice President, succeeding Harrison, and Delta Division Director Rick Roderick, K5UR, to Vice President, succeeding Craigie. Both were unopposed.

As always, certain minor changes are afoot here, as well. Note that we've dropped *Communications Quarterly* from our banner. The effects of our merger with that erstwhile publication have long since reached equilibrium. Award-winning artist Sue Fagan has restyled our cover. We're eliminating the "In This Issue" portion of this editorial because it regularly delays finalization of the column, which in turn places undue last-minute deadline pressure on the staff. We'll occasionally comment on certain content as conditions warrant.

You've helped us fill these pages with some very interesting and informative pieces and we're not starving — good job! Our article acceptance criteria are *not* changing; but an increasingly important criterion is whether submitted manuscripts are in the standard form. We must be able to place your exhibits — tables, figures and the like — where they best fit within our published format. We therefore ask that you place tables and figure captions at the end of your manuscript, and place graphics in separate files.

We use Microsoft Word for most of our editing work but not for final page layouts. We'd rather devote our editing time to your text than to deleting embedded exhibits, reformatting what's left and begging for graphics files. Many magazines automatically return material not in standard form because of the extra work required. Give your articles their best chance of acceptance by reviewing "Preparing a Manuscript — The Standard Form" on our Web page at **www.arrl.org/qex**. To those of you who've been heeding that advice: Thank you! — *73, Doug Smith, KF6DX,* **kf6dx@arrl.org** □□

# Pizzicato *Pulse Generator*

*Your oscilloscope and the* Pizzicato *create a time domain reflectometer, a handy piece of test equipment for checking your transmission line's characteristics.*

By Gary Steinbaugh, PE, AF8L

An Amateur Radio station has much in common with a violin: the transmitter is like a bow, the transmission line is like the strings and the antenna is like the wooden body. Now, a violinist will recognize the musical term *pizzicato* as a direction to pluck the strings instead of using a bow. The pulse generator described in this article electrically "plucks" a transmission line; by observing the line's reaction on an oscilloscope, you can check the line's length, terminations, and possible defects.

The radio/violin similarity is actually mathematical, as both obey the wave equation,

9534 Appomattox Ct
Loveland, OH 45140-7140
**gsteinbaugh@yahoo.com**

$$\nabla^2 \times \Psi = \frac{1}{c^2}\frac{\partial^2 \Psi}{\partial t^2}$$

The Scottish scientist James Clerk Maxwell (1831-1879) collected, completed and combined the electromagnetic equations of Gauss, Ampère and Faraday, obtaining a wave equation for the electric field, and a corresponding wave equation for the magnetic field. Maxwell showed that the wave equation's constant $1 / c^2$ (the product of the permeability and permittivity of free space) is equal to the reciprocal of the square of the speed of light in a vacuum (c = 299,792,458 m/s). He correctly theorized that light is electromagnetic, and paved the way for the likes of Hertz, Marconi, and Einstein. The Nobel Prize-winning physicist Richard Feynman said, "From a long view of the history of mankind — seen from, say, 10,000 years from now — there can be little doubt that the most significant event of the 19th century will be judged as Maxwell's discovery of the laws of electrodynamics."[1]

You can think of a transmission line or a violin string as a row of little masses connected by springs (a *lumped-parameter* model). Any given mass is affected only by the two adjacent masses connected to it by springs. Look at the left column of Figure 1, which shows a wave being "launched" by giving the left end a tug upward, then an equal tug downward. You can see how the masses and springs yank each other up and down to form a wave that travels toward the right end (note that the

[1]Notes appear on page 8.

masses do not move sideways).

What happens when the wave reaches the right end depends on whether the end is fixed, free to move up and down, etc. The middle column of Figure 1 shows the fixed case; notice how the pulse becomes inverted (changes phase) during its reflection. You can try this yourself with a rope tied to a doorknob. The right column of Figure 1 shows the free case, where the pulse is reflected without a phase change. To verify this, add a length of light fishing line between the rope and the doorknob. If the right end is connected to a shock absorber with the right damping (matching impedance), the pulse will be completely absorbed; we aspire to this case for our antennas.

### Speed and VF

By measuring the time it takes for the wave to return and by knowing its speed, we can calculate the length of

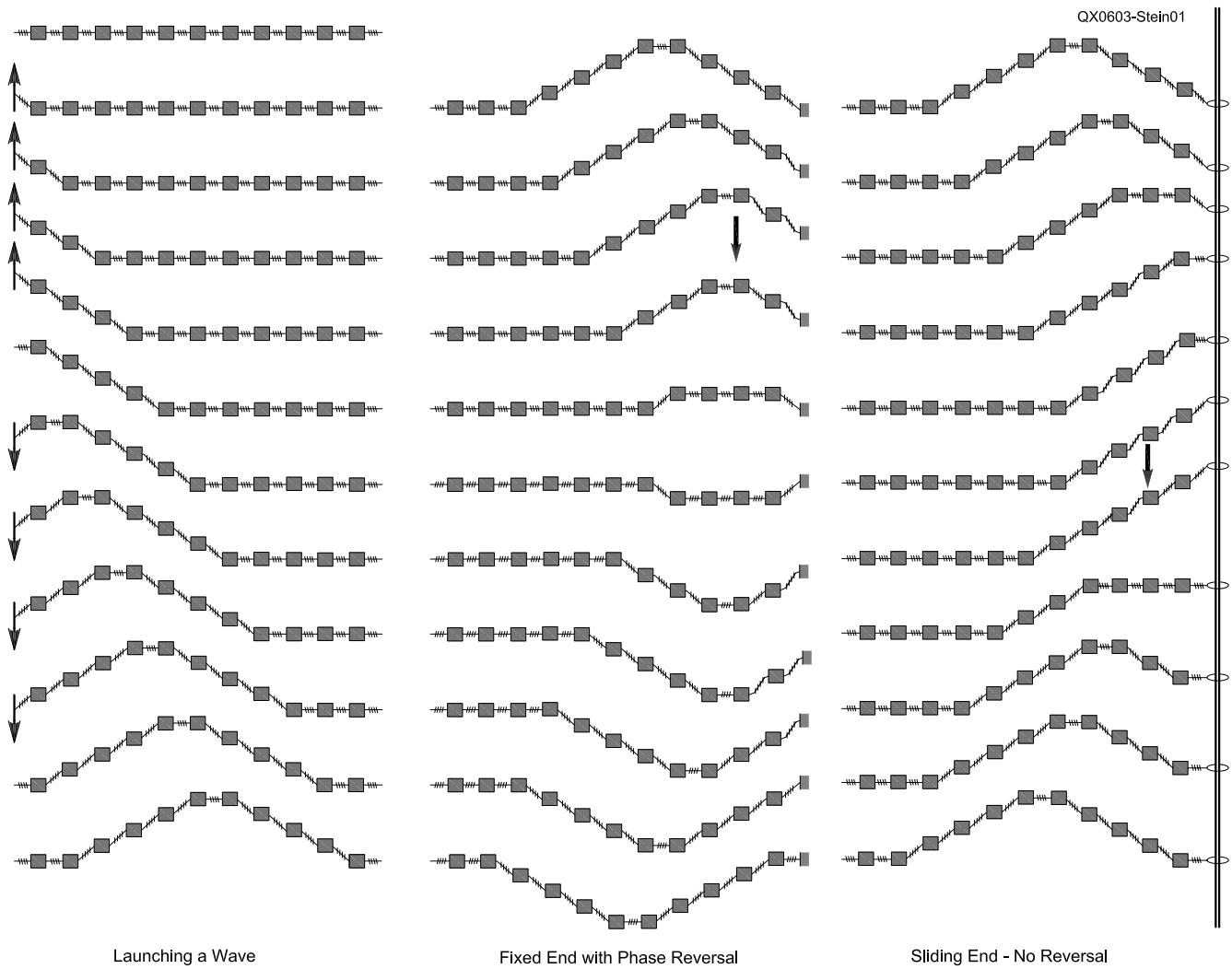


**Figure 1 — Wave in a lumped-parameter model.**

**Table 1**
**Velocity Factor Tabulation: Theoretical**

| *Transmission Line* | *meters / sec* | *feet / sec* | *Velocity Factor* | *Round Trip meters / ns* | *Round Trip feet / ns* |
|---|---|---|---|---|---|
| Space (vacuum) | 299792458 | 983571058 | 1.00 | 0.149896229 | 0.491785529 |
| Air, 600 Ω open wire | 293796609 | 963899637 | 0.98 | 0.146898304 | 0.481949814 |
| 450 Ω twinlead | 263817363 | 865542531 | 0.88 | 0.131908682 | 0.432771266 |
| 300 Ω twinlead | 245829816 | 806528268 | 0.82 | 0.122914908 | 0.403264134 |
| Coax (foam)[2] | 239833966 | 786856846 | 0.80 | 0.119916983 | 0.393428423 |
| Coax (polyethylene)[1] | 197863022 | 649156898 | 0.66 | 0.098931511 | 0.324578449 |

[1]RG-8, RG-11, RG-58, RG-59, RG-174, etc.
[2]Foam versions of above, and hardline.

the line. Electromagnetic waves travel slower in any material than in a vacuum (if they didn't, lenses wouldn't work), and this actual speed divided by c is called the *velocity factor*. Tables 1 and 2 show these speeds in common transmission media and their corresponding velocity factors; also shown is the out-and-back travel time, so distance may be calculated simply by multiplying the time between pulses by the appropriate speed. These numbers are too precise for real-world work, so practical values are also included. Some cable manufacturers publish measured velocity factors for their cables, and using their numbers would increase the accuracy of your results.

Resolution will be limited by the rise time of both the oscilloscope and the pulse generator. I began experimenting with a CMOS 555, but with a minimum pulse width of 100 ns and a rise time of about 15 ns, it was apparent that it would be too slow. I stumbled upon a pulse generator article in *Electronic Design*[2] that used Advanced CMOS, which is more suited to this application, having a rise time of 3.5 ns (yielding a resolution of about 1½ feet) and an output source/sink capability of 24 mA. Among other modifications to that design, I used a 74AC04 hex inverter in a three-gate ring oscillator circuit, with the remaining three gates as buffers. Figure 2 is the schematic diagram for the *Pizzicato*, essentially a square wave oscillator with a very low duty cycle. C1 charges through R1, but discharges through D1 and the parallel combination of R1 and R2 (and R3, R4, R5 or R6, depending on the setting of S1, a six-position miniature rotary switch that also serves as the power switch). This produces pulse widths useful for the line lengths that Amateur Radio operators are likely to encounter; the oscillator waveforms are shown in Figure 3. R8 is included to keep the 9 V and –3 V spikes from producing a gate input current that exceeds the limit of 20 mA. S2, an ON-OFF-ON toggle switch, provides the proper impedance for 50 Ω, 75 Ω and 300 Ω lines; obviously R9, R10 and R11 could be recalculated for other impedances. Although I have only used the *Pizzicato* for radio applications, it should be useful for any transmission line, eg, LAN cables and telephone wires.

### $LiMnO_2$ for Longer Life

My circuits often seem to design themselves. I had planned on using a common 9 V alkaline battery, but the AC logic series has an absolute maxi-

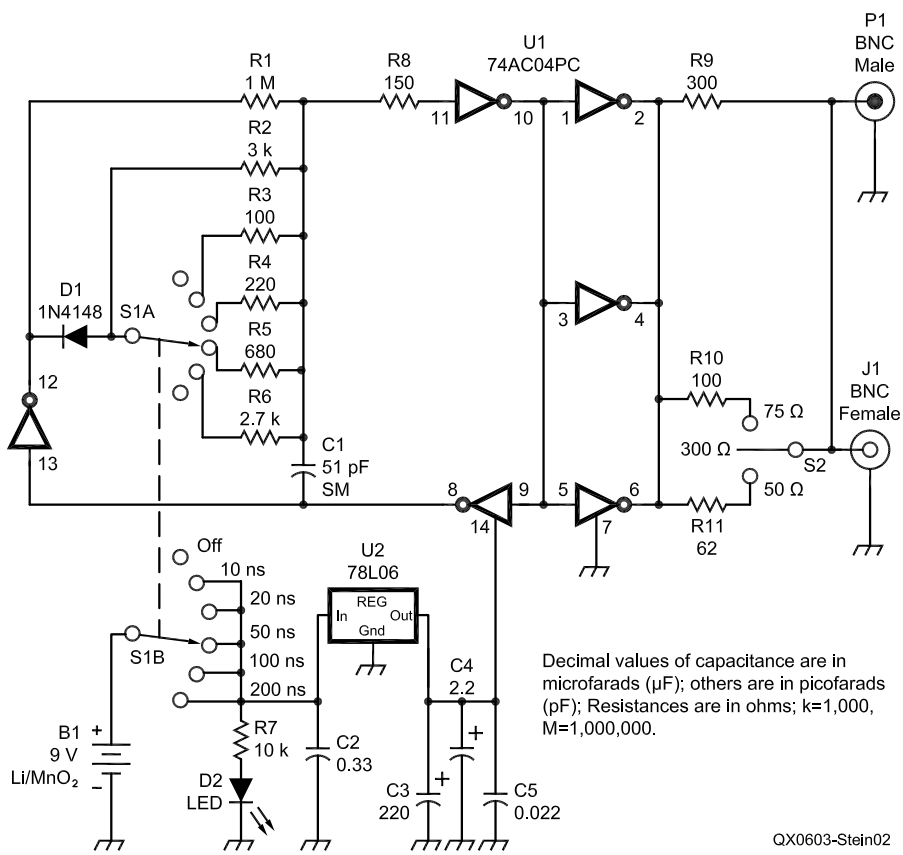


**Figure 2 — Schematic diagram of the Pizzicato Pulse Generator.**

**BT1 — 9 V lithium/manganese dioxide battery, NEDA 1604C.**
**P1 — BNC male panel mount, Alltronics CB111.**
**S1 — 0.5 inch rotary switch, 2 pole, 6 position, Mouser 633-MRK206A.**
**S2 — 0.5 inch toggle switch SPDT on-off-on.**

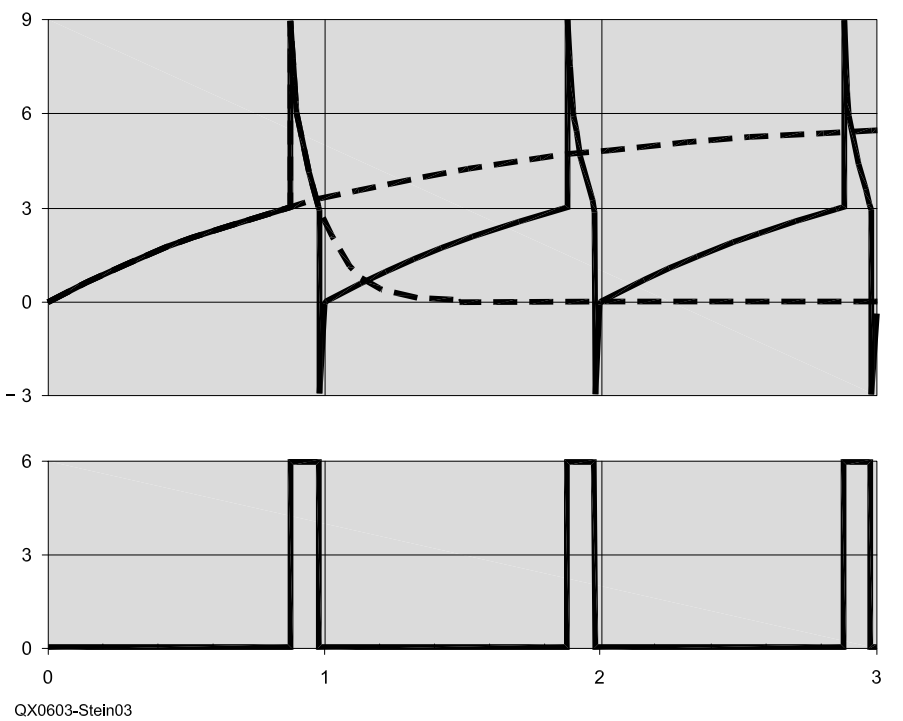


**Figure 3 — Oscillator waveforms.**

mum $V_{cc}$ of 7 V, so I added a 78L06 6 V regulator, with a 2 V dropout. This meant that the battery terminal voltage had to be a minimum of 8 V, but ordinary 9 V batteries discharge quickly to 7 V. This led me to lithium/manganese dioxide batteries, which have higher initial voltages and much longer lives. Figure 4 shows discharge curves for carbon/zinc, alkaline, and $LiMnO_2$ batteries. The battery is restrained by the box lid, and by the two switches, which are both 0.5 inch wide.

I built the circuit on a small scrap of perforated protoboard, trying to keep the leads as short as possible; Figure 5 shows the top of the board, while Figure 6 shows the bottom. The enclosure is a RadioShack 270-1801 ABS box, 3 × 2 × 1 inches with molded-in card slots. I had to do a little plastic surgery with a Dremel tool to remove some interfering bosses, and since the bottom would become the front, I sanded off the feet. Figure 7 is an inside view of the pulse generator. Ordinarily, I would not suggest such compact construction, but the high frequencies involved begged for an exception.

I had a RadioShack 276-068 red LED in a chrome holder, but I was appalled at the dim light level, even at 20 mA (the entire rest of the circuit draws 6 mA). Intending to substitute a brighter LED, I carefully removed the original, only to find that it was 4 mm in diameter instead of the standard 3 mm or 5 mm. Not to be thwarted, I bought a 276-320 white 5 mm LED, chucked it in my hand drill, and carefully sanded it down to 4 mm with an old emery board that my wife had discarded. I soldered a 10 kΩ resistor to the positive lead and glued the assembly in the empty holder. The result is a brilliant pilot light that draws only 500 µA.

Figure 8 is the front of the *Pizzicato*. I made the decal by printing the colored artwork on Micro-Mark Decal Paper (item 82272, from **www.micromark.com**), spraying it with Krylon Crystal Clear Acrylic Coating (1303A), and applying it like a common decal.

Figure 9 displays the oscilloscope screen with the *Pizzicato* "plucking" one end of a length of foam-insulated RG-8U with a 10 ns pulse; look closely

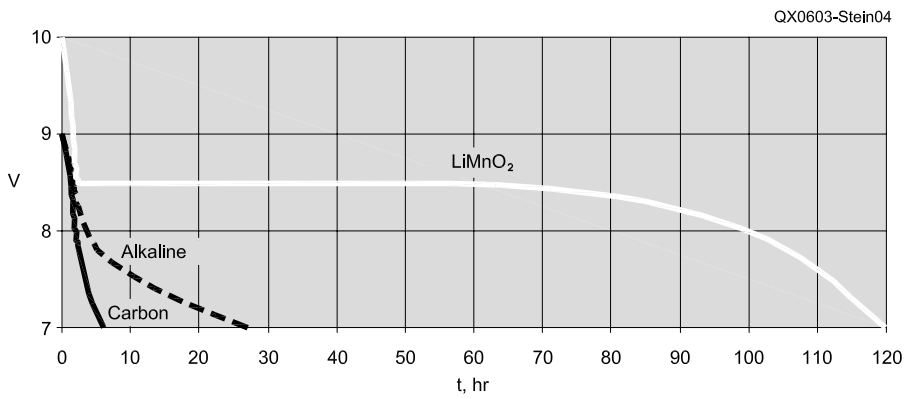


**Figure 4 — Battery discharge curves.**

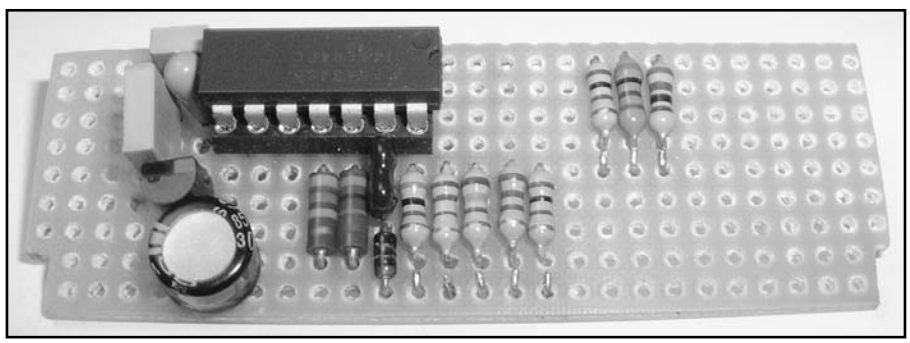

**Figure 5 — Top of board.**

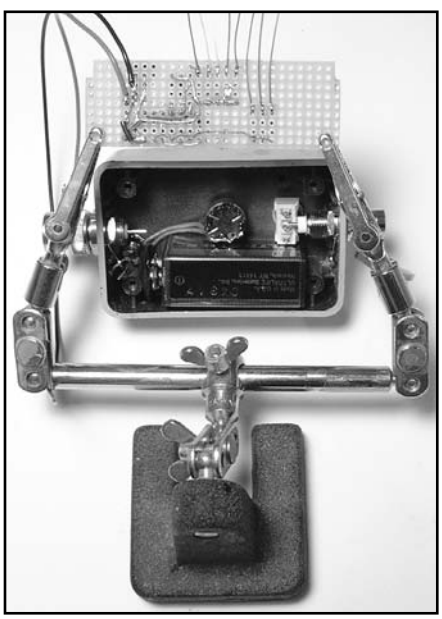

**Figure 6 — Bottom of board.**

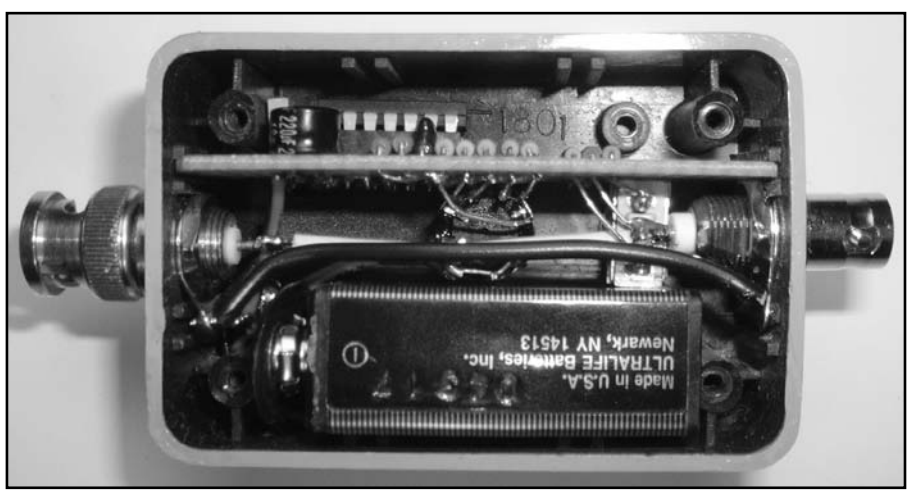


**Figure 7 — Inside view.**

at the end of the cable, and you can see that the other end is shorted. The reflected pulse is inverted, as predicted by the wave equation. The oscilloscope time base is set to 10 ns per division, and the time between the leading edges of the incident and reflected pulses is 45 ns. Multiplying this by 0.39 ns/ft, the length of this cable was calculated to be 17.55 feet long (a tape measure read 17.5 feet). Figure 10 is the same arrangement, but with an open end. Figure 11 is also an open end, but with a 20 ns pulse; in Figure 12, with a 50 ns pulse, you see the superposition that occurs if the reflected pulse returns before the incident pulse is over. Use whatever pulse width produces the best reflected pulse. As Figure 13 demonstrates, there is no reflected pulse when the cable is terminated in its characteristic impedance.

### One Practical Application

A practical application of the *Pizzicato* is shown in Figure 14. This is my Butternut HF6V vertical antenna at the end of 110 feet of direct-bury feed line. Note that the oscilloscope time base has been changed to 100 ns per division, and that the pulse width is 100 ns. The step at 100 feet is the beginning of a length of 75 Ω cable that matches the vertical's radiation resistance of 35 Ω to the feed line.

**Table 2**
**Velocity Factor Tabulation: Practical**

| *Transmission Line* | *Velocity Factor* | *Round Trip m / ns* | *Round Trip ft / ns* |
|---|---|---|---|
| Space (vacuum) | 1.00 | 0.15 | 0.49 |
| Air, 600 Ω open wire | 0.98 | 0.15 | 0.48 |
| 450 Ω twinlead | 0.88 | 0.13 | 0.43 |
| 300 Ω twinlead | 0.82 | 0.12 | 0.40 |
| Foam coax, hardline | 0.80 | 0.12 | 0.39 |
| Polyethylene coax | 0.66 | 0.10 | 0.32 |

**Figure 8 — Front view with violin.**

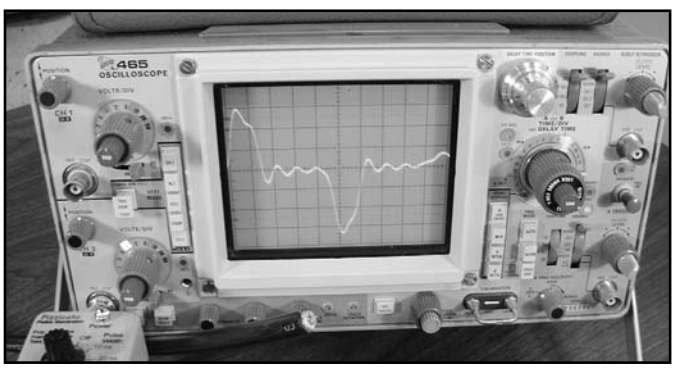

**Figure 9 — Shorted 10 ns pulse.**

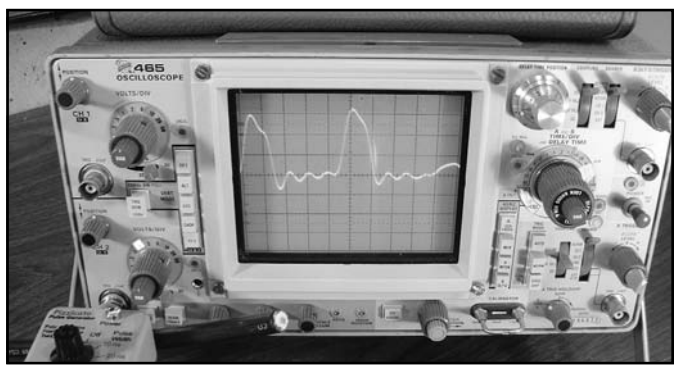

**Figure 10 — Open 10 ns pulse.**

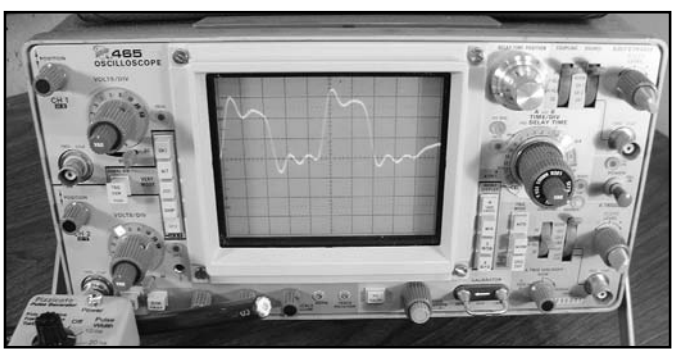

**Figure 11 — Open 20 ns pulse.**

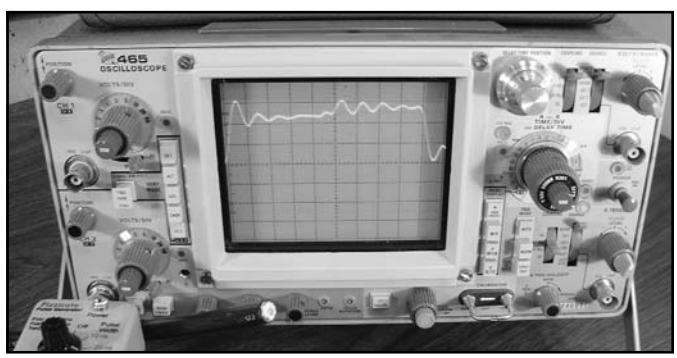

**Figure 12 — Open 50 ns pulse.**

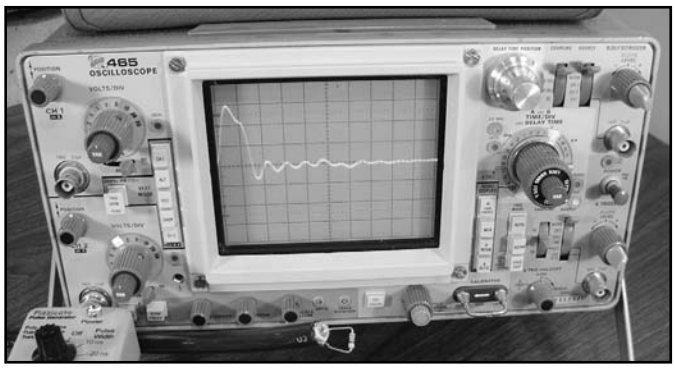


**Figure 13 — Terminated with resistor.**

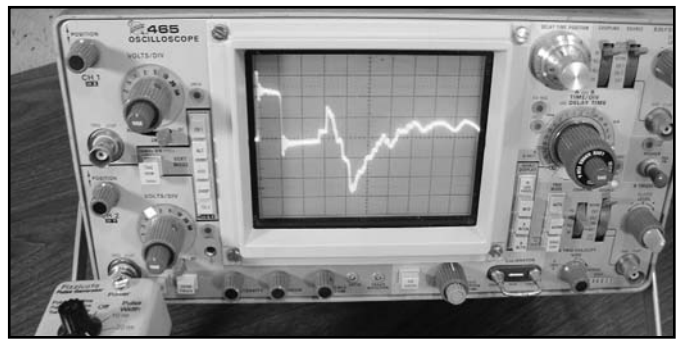


**Figure 14 — Vertical antenna.**

An S-shape is characteristic of an antenna, and the additional ornamentation is produced by the HF6V's bandswitching capacitors and coils. If the feed line ever develops a flaw, I will know within a foot or so where to start digging!

If your transmission lines have UHF connectors, a UG-255 BNC-to-SO-239 adapter will be a handy accessory, as will an extender made of a PL-258 double-female adapter (see Figure 8) and a length of line with PL-259 connectors. Be careful to support the transmission line so its weight does not overstress the ABS enclosure. Happy plucking with your *Pizzicato*!

**Notes**

[1]Feynman, Richard Phillips. *The Feynman Lectures on Physics*. Reading, MA: Addison-Wesley, 1965.

[2]Englund, Gunnar. "Build your own 'cable radar,'" *Electronic Design*, October 1, 1998.

*Continuously licensed since 1964, Gary Steinbaugh, AF8L, is an ARRL Life Member and a licensed Professional Engineer. He holds a BSEE from Case Institute of Technology, plays (using the word advisedly) many different musical instruments, and is a Certified Flight Instructor. He may be reached at* **gsteinbaugh@yahoo.com**. □□

# Book Review

**Practical RF Circuit Design for Modern Wireless Systems, Vol. 1 and 2**

*by Rowan Gilmore and Les Besser, Artech House Publishers, ISBN 158053-522-4, $95 each volume.*

Browsing one of my electrical engineering trade magazines, my eye caught on the publication notice for this two-volume set. In recent years, the RF designer's world has expanded well beyond what can be captured in a single handbook, leading to a blizzard of books on various specialties, but few that capture "the big picture." Would this be the answer? I borrowed two copies from the library to find out. The two weeks I had the books was obviously not enough time for an exhaustive review, but I believe I was able to assess the books' coverage.

The two volumes divide the RF world into passive circuits and systems (Volume 1) and active circuits and systems (Volume 2). Computer-aided techniques get extensive coverage in each volume and go hand-in-hand with each topic. The books assume that the reader understands the fundamentals of RF design and has access to RF computer-aided design, such as the limited-edition of *Super-Compact* from Compact Software that can be downloaded by hams (**www.arrl.org/ard/**).

Volume 1 starts with the basics, surveys common radio architectures, lays out the Smith chart and s-parameters and then dives into impedance-matching techniques. A section on the techniques used to simulate and optimize RF circuits is followed by a full 70 pages on component models, an often-neglected topic. The compromise is that the next section, on filters and resonant circuits, must cover much ground at a medium to high level. There is so much literature on filters that it would be unreasonable to expect that depth to be reproduced here. The volume concludes with a welcome discussion of the RF characteristics of high-speed digital designs, something that often comes as a surprise to digital designers.

Volume 2 gets into the serious details of RF amplification. It starts with linear RF amplifiers and continues to optimization and comparisons of the different designs. Modeling of active devices and nonlinear circuits is then covered as a detailed survey. Special concerns of high-power amplifier design are presented along with a design example. Oscillators, mixers and multipliers each get an overview. The final section covers several system-level examples, such as mobile telephony, software-defined radios and radio chipsets.

Even at 500 pages per volume, there still isn't enough space to reach a detailed examination of many topics. For example, there aren't enough example problem-and-solution sets to really learn a subject exclusively from these books. However, each section has an extensive set of references for further study. In numerous areas, the authors present a useful set of design equations and principles, but available space prevents them from covering the interactions and sensitivities that inevitably occur in actual designs. For these, readers must do additional research. Nevertheless, there is enough solid foundation material for an engineer to create a basic design and enough references to deal with some secondary considerations. My only complaint is that the graphic style is erratic, as is typical with heavy use of reprinted material. Many of the graphics would benefit as well from a more refined use of line width, style, and density, but these are minor distractions, at worst.

These texts are available through inter-library loan, so you can evaluate them before making the investment. At nearly $100 per volume, these are professional tools. Yet, if you work in the RF field and want a solid handbook to unify your niche references and theoretical textbooks, the set would be a good use of your book budget or a good addition to the company library. — *H. Ward Silver, N0AX, 22916 107th Ave SW, Vashon, WA 98070;* **n0ax@arrl.net** □□

# A 100-W Class-D Power Amplifier for LF and MF

*Get high efficiency from a complementary pair of inexpensive MOSFETs.*

By Frederick H. Raab, W1FR; Mike Gladu, N1FBZ, and Dan Rupp

**Introduction**

This paper describes a simple, high-efficiency transmitter for LF and MF experimental operation. The power amplifier (PA) is a class-D design using a complementary pair of MOSFETs.[1] It operates from 165 V and delivers 100 W with an efficiency of 89%. The PA is configured for operation at 500 kHz, but can be adapted to any frequency from 100 kHz to 3 MHz by changing the output filter. The driver is a single gate-driver IC, and a one-transistor circuit keys the drive for CW operation. The finished project is shown in Figure 1.

*Note:* This is a project for experienced experimenters. The 165-V dc-supply voltage can be lethal. Treat this circuit with the same respect you would give a vacuum-tube amplifier.

[1]Notes appear on page 13.

Frederick H. Raab, W1FR
240 Stamford Rd
Burlington, VT 05401
**f.raab@ieee.org**

**Driver**

The driver (Figure 2) operates from +12 V and requires about 50 mA. The signal input can be a sine wave of 3 V (peak) or more (20 dBm), TTL, or a square wave of about 1 V peak or more. Resistor R101 provides a load for the signal source. It should be removed for TTL or if necessary to get a sufficient output from the signal source. An insufficient input signal can lead to chaotic oscillations at high power due to transients from the final entering the input to the driver.

U101 is a standard 4-A gate driver that converts the input signal into square-wave drive for the final. It is biased near the threshold by adjustment of R103; hence, any input signal pushes the output of U101 into either a high or low state. To adjust the threshold, remove the signal input and look at the drive output with a scope or voltmeter. Adjust R103 to increase the bias voltage until a change is observed in the drive output, then back off R101 slightly so the output of U101 rests in the low state. The resultant bias voltage is about 1.5 V. (Alternately, R101 can be adjusted so that U101 rests in the high state.)

Keying for CW operation is accomplished by turning the drive on and off. This is done by Q101 and the related components. An open circuit or greater than +9 V at the key input

J102 results in no drive, while a short circuit or 0 V turns the drive on. This allows operation from either key or a programmable waveform generator with a range of 0 to 10 V. Capacitor C110 and resistors R105 and R106 control the shape of the waveform to avoid key clicks. The value of 10 µF produces a rise/fall time of about 10 ms.

### Final Amplifier

The final amplifier (Figure 3) consists of a complementary pair of 200-V power MOSFETs Q201 and Q202. The MOSFETs are biased near the threshold of conduction by R205 and R206 so that any RF drive pushes one into an on state and the other into an off state.

Gate biases are supplied by two Zener-regulated supplies. The bias for *n*-channel MOSFET Q202 is derived directly from the +12 V supply. The source of *p*-channel MOSFET Q201 is connected to the main supply $V_{DD}$, which may be variable. Consequently, the bias supply for Q201 floats against $V_{DD}$. This is accomplished by coupling the square-wave drive signal through C205 to the floating supply consisting of D203, D204 and C206, which provides a voltage of approximately $V_{DD}$ – 12 V to operate the bias circuit.

Turning both Q201 and Q202 on simultaneously produces a short circuit. Therefore, it is important to set the biases via the following procedure. Begin by disconnecting C210 and C211 and setting $V_{DD}$ to 0. Connect the +12-V supply, then adjust R205 to produce 0 V. Apply drive, verify that the floating bias supply is working, and set R206 to produce $V_{DD}$ – 0 V. Increase $V_{DD}$ and make sure no drain current flows, then return to zero. Temporarily connect a resistor of approximately 100 Ω from the two drains to ground. Set $V_{DD}$ to about 25 V. Slowly adjust R206 until approximately 5 mA is flowing in Q201. The resultant bias voltage is about $V_{DD}$ – 2.7 V for the VP1220N5, but may be different for other MOSFETs. Turn off $V_{DD}$, remove the 100-Ω resistor from the drains, and connect a voltmeter in its place. Return $V_{DD}$ to 25 V and slowly adjust R205 until the drain voltage is about 12.5 V, which implies equal quiescent currents in the two MOSFETs. The resultant bias voltage is about 3.5 V for the IRF610. The drain voltage will drift and vary with temperature, but the MOSFETs will remain sufficiently close to their thresholds of conduction for proper operation when drive is applied. Finally, reconnect C210 and C211.

The output network provides a 50-Ω load to the drains, high imped-

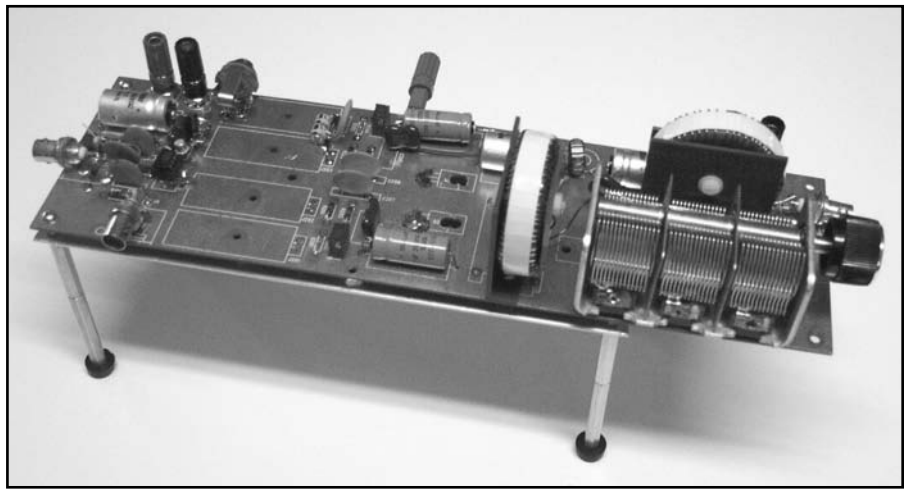

**Figure 1 — The LF/MF complementary class-D transmitter.**

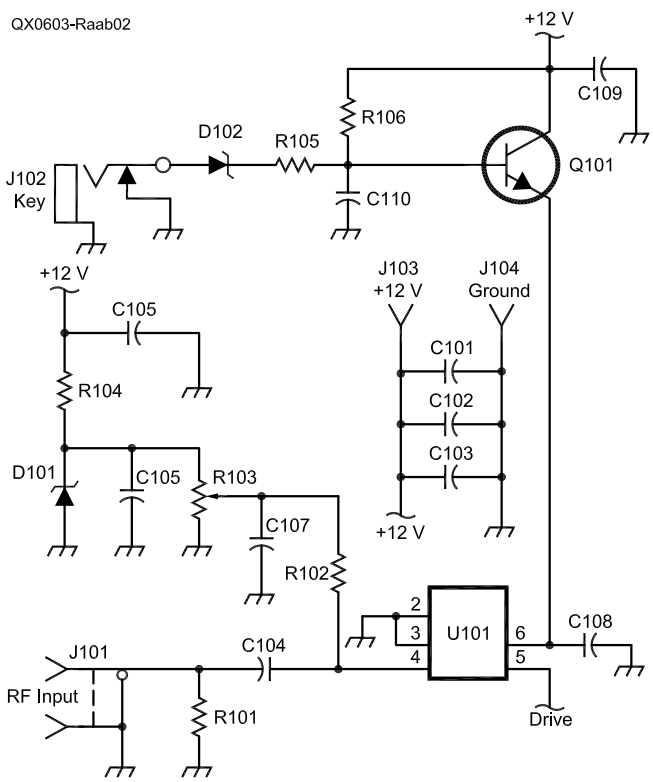


**Figure 2 — Circuit of driver.**

**C101 — 20-µF, 250-V electrolytic.**
**C102 — 3300-pF mica.**
**C103 — 0.1-µF, 50-WV chip, ATC 200B104NP50X.**
**C104 — 0.1-µF disk.**
**C105-C109 — 1-µF, 50-WV X7R chip, Kemet 1210C105K5RATCU.**
**C110 — 4.7-µF, 25-V electrolytic.**
**D101 — 1N751A, 5.1-V, 0.25-W Zener.**
**D102 — 1N746A, 3.3-V, 0.25-W Zener.**
**J101 — BNC jack.**
**J102 — Key jack, shorting.**
**J103 — European-style binding post, red, E.F. Johnson 111-0102-001. Mount vertically.**
**J104 — European-style binding post, black, E.F. Johnson 111-0103-001. Mount vertically.**
**R101 — 51-Ω RC07 (omit for TTL input).**
**R102 — 4.7-kΩ RC07.**
**R103 — 5-kΩ trimpot, Bournes 3006P-1-502.**
**R104 — 620-Ω RC07.**
**R105, R106 — 2.2-kΩ RC07.**
**Q101 — PNP BJT, 2N2907.**
**U101 — 4-A gate driver, TI UCC32325P or equivalent.**

ances to the harmonics, adequate suppression of the harmonics in the output, and single-knob tuning to the frequency of operation. The T configuration may be regarded as two back-to-back L networks that match upward to about 150 Ω at the center. Inductor L201 has a $Q$ of 3, which is sufficient to ensure that third-harmonic current circulating in the drains is no more than 10% of the fundamental-frequency current.

Adjustment is quite simple, since maximum RF output, maximum dc input, and maximum efficiency occur so close to each other that the settings are indistinguishable. Begin with $V_{DD}$ set to 25 to 50 V. Adjust C214 for either the maximum dc power or maximum RF output. Make a quick check on the RF output (Figure 4) and the efficiency to ensure the PA is operating correctly. Then increase $V_{DD}$ to 100 V and tweak C214 slightly to allow for any variation of drain capacitance with voltage. Then increase $V_{DD}$ to its full value of about 165 V without readjustment. The dc-input current should be about 0.72 A.

## Performance

The waveforms are shown in Figure 4 for operation at 500 kHz from $V_{DD}$ = 100 V. In this case, the input $v_i$ is a TTL signal. The drive signal $v_{DR}$ produced by U101 is a square wave that ranges from 0 to 12 V. The drain voltage $v_D$ produced by the two MOSFETs is a clean square wave. The complementary configuration eliminates most of the transients associated with charging drain capacitance through the inductance of a transformer.[2,3] The small droops are the result of drain current flowing through the on-state resistances of the MOSFETs. The output $v_O$ is a pure sine wave.

The output and efficiency characteristics for operation at 500 kHz are shown in Figure 5. Output voltage $V_{om}$ varies linearly with supply voltage $V_{DD}$. The transfer curve fits a straight line with an rms error of only 0.2%, indicating excellent amplitude-modulation linearity (IMDs less than –50 dBc). The efficiency is about 89% over most of the output range. It drops slightly at high levels because of increased MOSFET resistance and slightly at low levels because of increased drain capacitance.

The PA can be used at frequen-

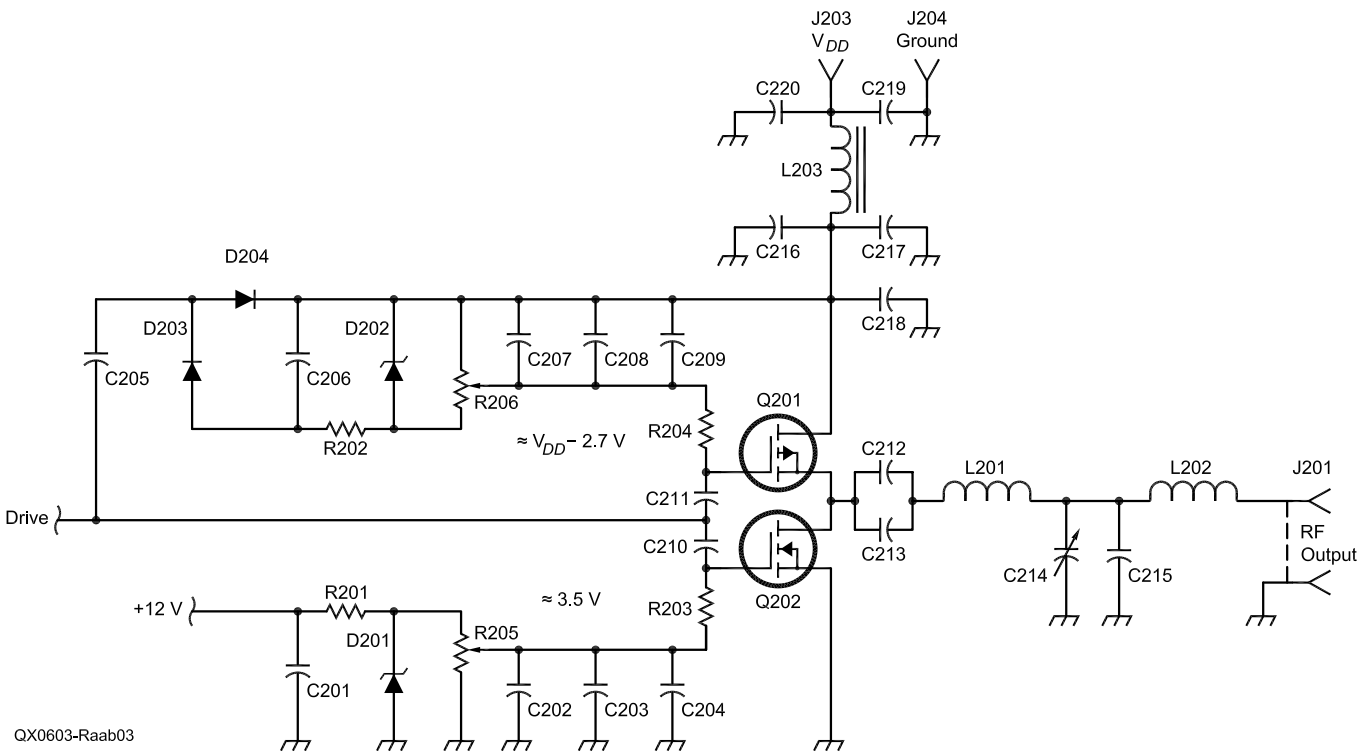


**Figure 3 — Circuit of final amplifier.**

**C201 — 1-µF, 50-WV X7R chip, Kemet 1210C105K5RATCU.**
**C202, C207, C111 — 0.1-µF, 50-WV chip, ATC 200B104NP50X.**
**C203, C208, C215, C217, C219 — 3300-pF mica.**
**C204, C209 — 5-µF 25-V electrolytic.**
**C205, C210, C211 — 0.022-µF disk.**
**C206 — 10-µF 25-V electrolytic.**
**C212, C213, C218 — 0.1-µF, 200-WV chip capacitor (American Technical Ceramics 900C104NP200).**
**C214 — Three-gang breadslicer, 15-525 pF per section, 70% closed at 500 kHz.**
**C216, C220 — 20-µF, 250-V electrolytic.**
**D201, D202 — 7.5-V 0.25-W Zener, 1N755A.**
**D203, D204 — MUR120 60-V 1-A ultra-fast switching diode.**
**J201 — BNC jack.**
**J202 — European-style binding post, green, E.F. Johnson 111-0104-001.**
**J203 — European-style binding post, red, E.F. Johnson 111-0102-001. Mount vertically.**
**J204 — European-style binding post, black, E.F. Johnson 111-0103-001. Mount vertically.**
**L201, L202 — 47.7 µH. 61 turns #24 AWG enameled wire on Micrometals T200-2 toroid.**
**L203 — 30 turns #24 AWG on Ferroxcube 768XT188 3E2A toroid.**
**Q201 — Supertex VP1220N5 200-V, 2-A P-channel MOSFET.**
**Q202 — IRF610 200-V, 2-A, N-channel MOSFET.**
**R201, R202 — 1-kΩ RC07.**
**R203, R204 — 10-kΩ RC07.**
**R205, R206 — 10-kΩ trimpot, top-adjustable, Bournes 3299X-1-103.**
**Heat sink — Extruded aluminum, 3.75-in wide, Aavid 60675.**
**Insulating pads for Q201, Q202 — Thermalloy 43-77-2.**

cies from 100 kHz to 3 MHz. Its performance is shown in Figure 6 as a function of frequency. These tests are based upon $V_{DD}$ = 165 V and simple series-tuned output circuits instead of the T network shown in Figure 2. The power drops from about 100 W at 500 kHz to 92 W at 3.5 MHz, and efficiency drops from about 90% to 83%.

### Adaptation to Different Voltages and Powers

The basic design presented here can be adapted to other MOSFETs, supply voltages and output powers. The output power of a complementary class-D PA is:

$$P_o = 2\ V_{\text{eff}}^2 / (\pi^2\ R_{PA}) \qquad \text{(Eq 1)}$$

where $R_{PA}$ is the drain-load resistance. The effective supply voltage is:

$$V_{\text{eff}} = V_{DD}\ R_{PA} / (R_{PA} + R_{on}) \qquad \text{(Eq 2)}$$

where $R_{on}$ is the on-state resistance of the MOSFETs. These equations allow determination of the drain-load resistance $R_{PA}$ for a desired output power $P_o$ and supply voltage, or vice versa.

The T network can be regarded as two back-to-back L networks (Figure 7) that match upward to an intermediate resistance $R_{\text{m}}$, which must be larger than either the input or output resistance. The capacitor in the T network is the sum of the capacitances in the two Ls. The equations for design of the L networks (from the reference cited in Note 1, Table 3-3.1) are

$$X_L / R = -X_C / R_m = Q \qquad \text{(Eq 3)}$$

and

$$Q^2 + 1 = R_m / R \qquad \text{(Eq 4)}$$

Above, $R$ is $R_{PA}$ or $R_{\text{o}}$ as appropriate for the input or output L. The design process can begin either by

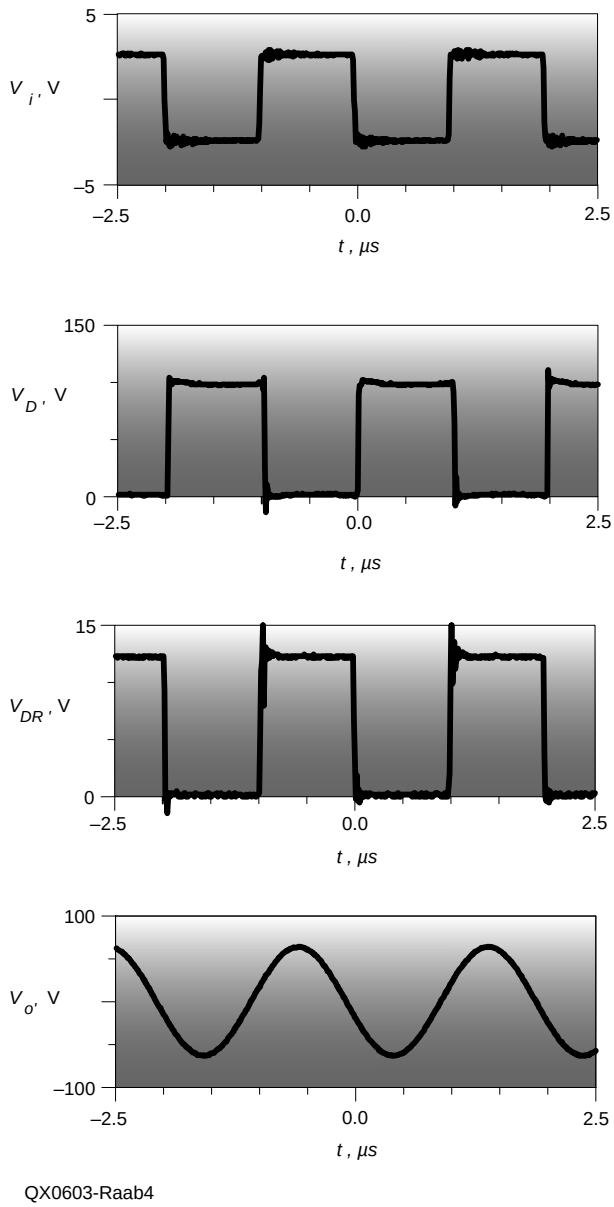


**Figure 4 — Waveforms at 500 kHz.**

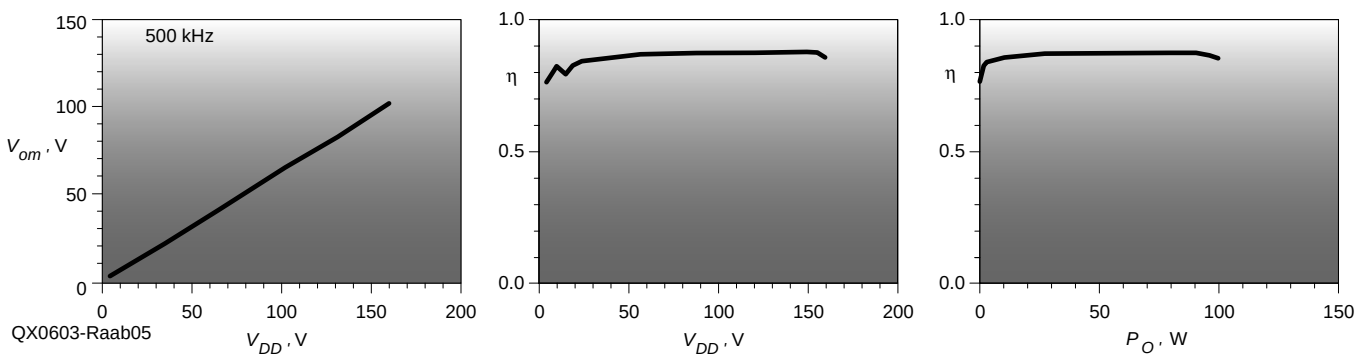


**Figure 5 — Power and efficiency at 500 kHz.**

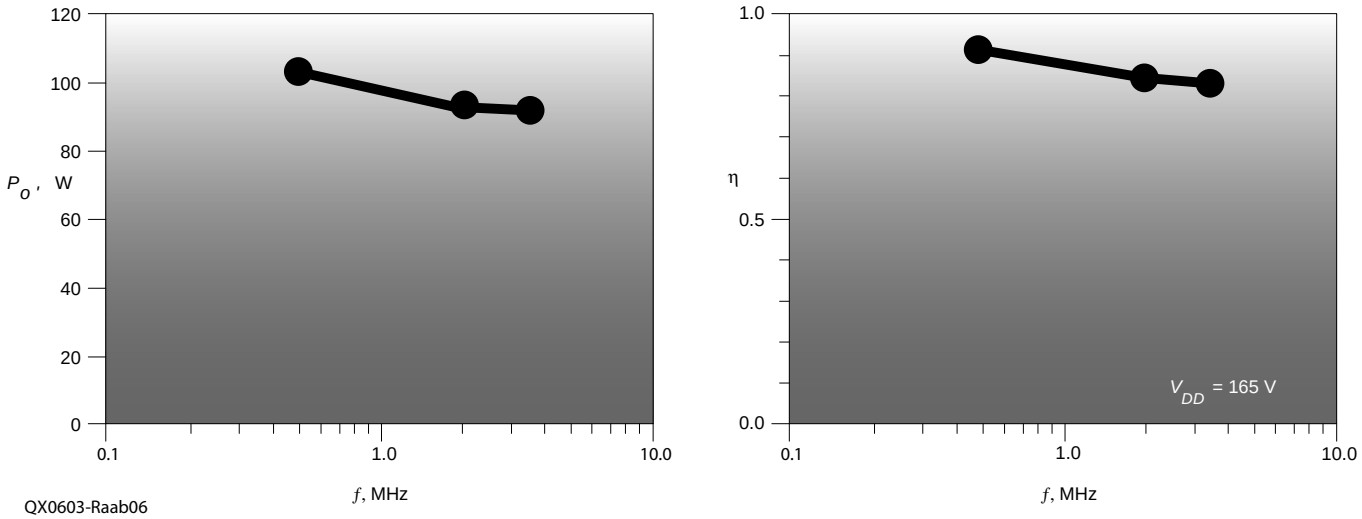


**Figure 6 — Output and efficiency as functions of frequency.**

specifying $Q$ and determining $R_{on}$ or by specifying $R_{on}$ and determining $Q$.

In the previously presented design, the drain-load resistance is 50 Ω, which is the same as the output resistance; hence, L1 and L2 are the same. Operation at higher power or from a lower $V_{DD}$ may require transformation of the output resistance, hence different values of the inductors. Many different T networks can be designed that provide the desired drain-load resistance. For proper operation of the class-D amplifier, however, the reactance of L1 at the third harmonic must be at least nine times the drain-load resistance. Consequently, the reactance of L1 at the fundamental frequency must be three times the drain-load resistance. Generally, nothing is gained by making L1 larger than necessary, so its value should be the minimum that provides the desired transformation and the minimum harmonic impedance.

## Recommendations

This amplifier was made by adapting an existing prototype. Consequently, the layout is somewhat of a kludge and not recommended. Improvements in the layout include:

- Elimination of about 2 inches between the driver and final;
- Installation of 1-μF chip capacitors right at the points to be bypassed;

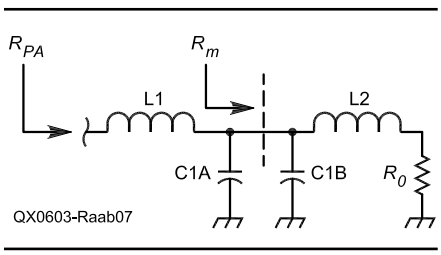


**Figure 7 — T network viewed as back-to-back L networks.**

- Shortening of all leads, and
- Elimination of the 3300-pF bypass capacitors.

A better layout and closer bypassing should allow operation from sinusoidal inputs of less amplitude. This can also be accomplished by placing a TTL line receiver to hard-limit the input before driving U101.

*Note:* A shorter version of this article appeared in the May/Jun 2005 issue of *The AMRAD Newsletter*.

### Notes

[1]H. L. Krauss, C. W. Bostian, and F. H. Raab, *Solid State Radio Engineering*. New York: Wiley, 1980.

[2]F. H. Raab, "Switching transients in class-D RF power amplifiers," *Proc Seventh Int Conf HF Radio Syst and Techniques (HF'97)*, Nottingham, UK, pp 190-194, Jul 7-10, 1997.

[3]F. H. Raab, "Simple and inexpensive high-efficiency power amplifier for 160-40 meters," *Communications Quarterly*, vol 6, no. 1, pp 57-63, Winter 1996.

*"Fritz" (Frederick H.) Raab, W1FR, has been licensed since 1961 and holds an Amateur Extra class license. He primarily operates CW on the 160 through 10 meter bands. Fritz received BS, MS and PhD degrees in electrical engineering from Iowa State University. He is an electronics engineer and designs RF power amplifiers through his consulting company Green Mountain Radio Research in Colchester, Vermont. A number of his designs have appeared in Amateur Radio publications. A recent activity is the ARRL-sponsored 500 kHz experimental license. He can be reached at* **f.raab@ieee.org**.

*Michael Gladu holds the amateur call sign of N1FBZ. He upgraded from a Technician Plus ticket to Amateur Extra class in 2005. He has been a licensed amateur since 1987. In his spare time he enjoys homebrewing and repairing anything electronic (just for the fun and challenge of it). He is a member of the ISCET (International Society of Certified Electronic Technicians) and holds a GROL (General Radiotelephone Operator License). He provides Consulting Technician Services to small electronics companies and consultants through his company, MikeTek. He resides in Hewitt, New Jersey, and can be reached at* **mgladu@miketek.com**.

*Dan Rupp received a BS degree in electrical engineering from Iowa State University and worked briefly for Green Mountain Radio Research. He is now a priest in Barton, Vermont.* □□

# An Expanded Reflection-Coefficient Equation for Transmission-Line Junctions

*When the familiar reflection coefficient is applied to a discontinuity in a transmission line, erroneous conclusions may result. W7WKB offers a revised formula and demonstrates how reflections become zero when a match is achieved.*

By Roger Sparks, W7WKB

It is very unusual to see two knowledgeable men quarrel about technical matters in Amateur Radio publications, but that is exactly what has happened with a series of three articles from Steven Best, VE9SRB,[1] and one from Walt Maxwell, W2DU.[2] This unusual occurrence prompted me to study both articles and learn more about transmission lines and reflections than I really wanted to know! Nonetheless, it was very interesting, and I think my results are worth sharing.

Rather than siding with either of these gentlemen, I will present a different way of looking at the situation with an expanded equation to find the reflection coefficient for a discontinuity. The result for a 1/4-wave matching section will be the same as Steven Best presented except for the canceling waves. The concept of complete reflection is more like Walt Maxwell's but without the idea of open or short circuits created by wave interference.

[1]Notes appear on page 19.

4780 Cove Rd
Ellensburg, WA 98926
**rsparks@elltel.net**

### Begin with Basics

Our radio transmitters send a wave down a wire to the antenna. We will begin by forming an idea of how that invisible wave might look if we could see it.

My favorite analogy is to look at a canal or channel filled with water. The canal is very long and narrow, filled with some depth of water. Initially quiet, we see waves generated when we drop a rock into the water. The waves travel each way from the point of impact but leave the water surface quiet at the point of impact. If it were not for friction and if the canal were infinitely long, the waves could travel forever in both directions, carrying the energy from the initial splash to distant regions. The waves have a velocity and frequency, and carry energy just like electromagnetic waves traveling on a wire.

We can place our transmitter at the center of an infinitely long wire (I am not sure how we would find the center!) and generate waves which go in each direction. We would be creating a series of matching troughs and peaks paired as they fly off down the wire in opposite directions. By paired, I mean that one trough going to the

left will be paired with a peak going to the right. The wave motion will be away from the initial point but the current for each trough-peak pair will be in the same direction. See Figure 1A.

Next, we can take our infinitely long wire and bend it into a U with the transmitter at the bend. We have now formed a transmission line. A wave generated at the bend in the U will travel down each side of the line with current going in opposite directions. See Figure 1B. In this situation the magnetic fields from the two currents cancel, as do the electrical fields, so long as you are measuring them from some distance away. If you measure really close to either wire, you will find the fields very much present.

If we use our transmission-line configuration but use a battery to generate the electrical pulse, we can ask "How much current would flow down the line when we make the battery connection?" If the line is infinitely long, will an infinitely large current flow? No, it turns out that a wave front is formed that charges the capacity between the wires to the battery voltage. The wave just travels along the wire charging the wire to the battery voltage at some rate of current. The speed of the wave is the speed of light (in air) or the velocity of propagation in a cable or insulated line. This velocity limit allows the capacity of the line to be charged only so fast, which means that a ratio of voltage to current can be found. Because the ratio of voltage to current is resistance, every transmission line will have a characteristic resistance.

The familiar equation for the resistance or impedance of a transmission line is

$$Z = \sqrt{LC}$$

where $Z$ is the impedance, $L$ the inductance, and $C$ the capacity. The equation can also be written as

$$Z = \frac{1}{cC}$$

where $c$ is the velocity of the wave, and $C$ is the capacity per unit distance. This second form of the equation provides a rich insight into how the wave moves to fill the available capacity of the transmission line as it travels, and gives mathematical form to the previous wave description.

When an electrical wave travels down a wire in the real world, it always reaches a destination or end. How does the source (the battery or transmitter) know that the wave has reached the end of the wires? Feedback to the source cannot travel faster than the speed of light so the source just keeps putting power into the transmission line until the *reflected wave* arrives back at the source. That means that two waves are on the line at one time if we consider the reflected wave as a new wave as if it were from a second source.

When the wave is reflected from an open end, the current reverses but the voltage retains polarity. When measured, we see that the forward and reflected currents oppose but the voltages add. In terms of impedance, an open ended transmission line would measure capacitive impedance.[3]

If the wave travels to a short circuit, then an inverted wave is reflected, with the reflected current adding to the forward current but the voltages opposing and canceling. Thus you measure a high current but no voltage at end of a shorted transmission line. (Off subject, but this is why a loop antenna always has a low voltage point when measured equal distance from each side of the feed point.) A short-circuited transmission line would measure as an inductive impedance.[3]

Both reflected and source waves will have the impedance of the transmission line carrying them. If the wave travels to a resistance (terminated with a resistance), there will be no reflection *if the resistance is the same as the characteristic impedance of the line*. There will be a partial reflection of an open line type (capacitive) if the termination is a resistance higher than the line impedance, and a partial reflection of a short circuit type (inductive) if the termination resistance is less than the line impedance.

A transmission line terminated with a matching resistor appears to be infinite in length because there are no reflections. On the other hand, a mismatched line has reflections and is said to be discontinuous (or to contain a discontinuity).

### Preparing to Derive a General Reflection Coefficient

Now let's ask a hard question: What will the reflected voltage be if some part of the power is delivered to a resistor?

As we work toward an answer, we will begin by selecting a circuit or visual model. The reflected wave travels back down the wire it just came

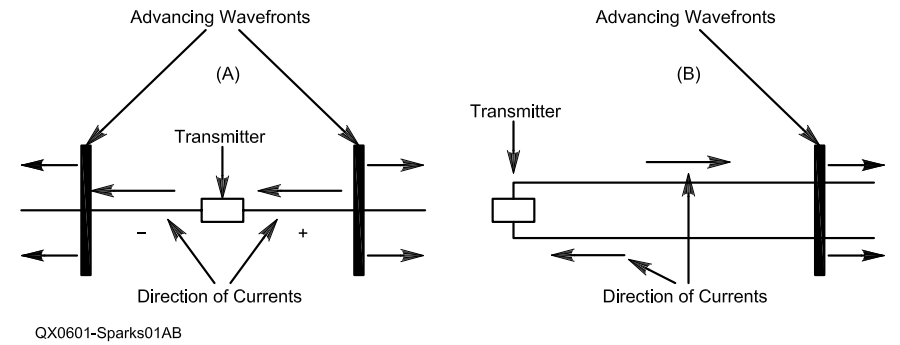


**Figure 1 — (A) A transmitter at the center of an infinitely long wire generating wave pulses that go in each direction creates a series of matching troughs and peaks paired as they fly off down the wire in opposite directions. At B, the ends of the wire have been folded together to make it a feed line.**

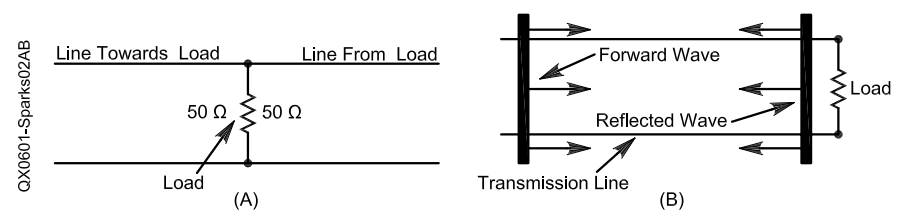


**Figure 2 — Which circuit is the correct representation for a reflected wave? It depends upon how the waves interact. If there was no interaction at all, then circuit A would be correct. By measuring voltages and currents, we find that the two waves interact in a manner to result in equal voltage at all junctions, but the current will divide between two (or more) resistive paths with the result that current into the junction equals current leaving the junction. The division of leaving current depends upon both the resistance of each possible path and upon the incoming current from each possible path. Circuit B is the correct representation.**

from. Will the circuit look like Figure 2A or 2B? If we use circuit 2A to build our mathematical model, the line picked to carry the reflection would look like a second resistance placed in parallel to the load resistance. In fact, circuit 2A is the circuit for a resistor placed into a transmission line. The line carrying the reflected wave has the same impedance as the source line, so the parallel combination of load and reflection carrying transmission line would always result in an inductive reflection.

Based on measurements, we can see that something else is happening when reflections occur. The reflected voltage or current adds or subtracts from the source power depending upon the resistive ratios. "Circuit" 2B must be used. It doesn't look like a circuit does it? It is more like a graphical description of the wave movement. This is how we will depict two waves flowing in opposite directions on a transmission line.

The familiar antenna reflection coefficient equation was derived from the "circuit" in Fig 2B.

$$\frac{Vfr}{Vf} = \frac{\frac{Zl}{Zf} - 1}{\frac{Zl}{Zf} + 1} \qquad \text{(Eq 1)}$$

where *Vfr* is the reflected part of the forward voltage, *Vf* is the forward voltage, *Zf* is the line impedance and *Zl* is the load impedance.

This equation was used very effectively by Steve Best in his article as he traced the multiple reflections that ultimately result in a stable transmission-line condition.[1]

The "circuit" in Figure 2B works fine for a transmission line terminated in either a resistor or antenna, but it must be expanded to include wave fronts coming from two directions if there is a discontinuity within the transmission line. Power coming from a second source will change the amount of primary power reflected from the discontinuity. Figure 3 is a representation of the wave flow from two directions at a discontinuity; it shows both forward and reflected waves.

We can use the familiar equation (Eq 1) for inline discontinuities (as Steven Best did), but the result leads us to the conclusion that a reflected wave from the discontinuity combines with a reflected wave from the antenna, which then cancels under matched conditions. We are left with the decidedly unsatisfactory notion that positive power cancels negative power. The power just seems to disappear, which we know to be impossible, from the laws of physics.

We can remove this unsatisfactory notion of canceled power by deriving the antenna reflection factor from a more general condition that includes power coming from a second direction on a conductor. To do this, we must break from the traditional premise that waves traveling in opposite directions pass through each other without effect. We substitute a premise that the waves always interact so that the resultant measurable voltage or current at any point is the sum of the voltages or currents of all the waves traveling in any direction on any one conductor.

If you are reluctant to give up the premise that opposite traveling waves pass without effect, look carefully at Figure 1A and Figure 1B to consider the differences between the two "circuits." If the reflected wave were to pass without effect, circuit (A) would apply. Instead, consider how waves travel when one wave rides "on top" of the other wave. Comfort may come after you understand how the expanded reflection coefficient is developed and actually works.

The general version of the reflection coefficient is developed in the sidebar "A Derivation of the Expanded Voltage-Ratio Equation."

The assumption that the voltage at any point is the sum of four waves rather than two deserves some explanation. When we consider a discontinuity, waves may source from both the right and left sides and meet at the point of consideration. A reflection will occur at the discontinuity for both waves. Thus, at the discontinuity, we have source waves arriving from both directions and reflected waves moving away in both directions, four waves. The voltage at the discontinuity is the sum of the two waves on each respective side, which becomes a single voltage at the single examination point.

Each reflected wave contains energy from both source waves but no instrument can identify from which source wave the energy actually came. Yes, it can be mathematically traced, but for all practical purposes, the

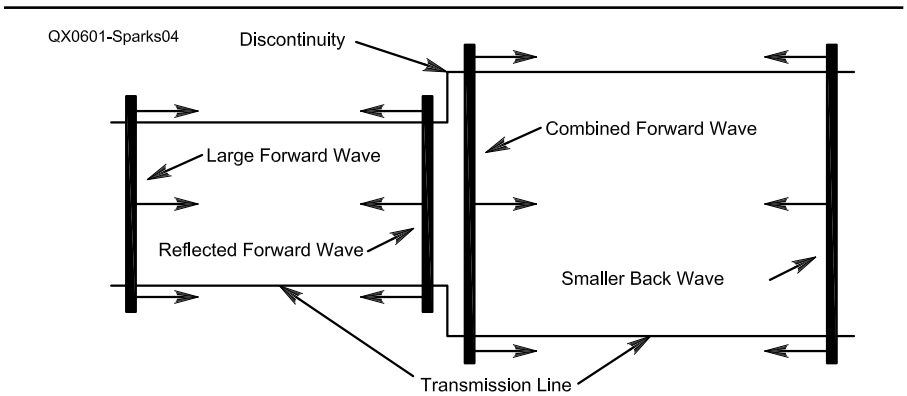


**Figure 3 — A representation of the wave flow from two directions at a discontinuity; it shows both forward and reflected waves.**

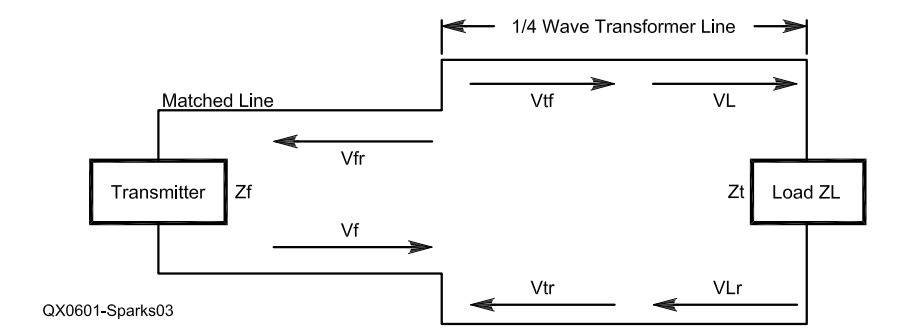


**Figure 4 — Matched transmission line using 1/4 wave transformer.**

source waves have been reformed into two new waves with a life of their own. The waves have been re-formed.

Here is the general reflection coefficient equation which was developed in the sidebar,

$$\frac{Vfr}{Vf} = \frac{\frac{Zl}{Zf} + 2\frac{Vlr}{Vf} - 1}{\frac{Zl}{Zf} + 1} \qquad \text{(Eq 2)}$$

where *Vlr* is the voltage reflected from the load and *Vf* is the forward source voltage.

One of the first things to notice about Eq 2 is that it reduces to Eq 1 if there is no reflected power. This is to be expected if it is a more comprehensive version of Eq 1.

The second thing to notice is that Eq 2 reduces to the pre-existing load reflection coefficient if there is no discontinuity in the transmission line. This is also to be expected if Eq 2 is a more comprehensive version of Eq 1.

### Using the Expanded Reflection Coefficient

An analysis of the frequently used 1/4 wave matching transformer is a good way to show how the expanded reflection coefficient is used. I have attempted to use an example with the same characteristics as used in both the Best and Maxwell articles. This makes comparisons to the previous articles easier. Figure 4 shows the symbols used in the analysis. The results are shown in spreadsheet format as Table 1.

Assume that the impedance of the source line is 50 Ω, the impedance of the load is 150 Ω, and the transforming line is 86.6 Ω. The input power will be 100 W, which makes the forward voltage in the source line to be 70.711 V. The entire system will be assumed to be without losses so that we can focus on the principles of the problem.

The beginning source wave, *Vf*, will travel to the input of the 1/4-wave transformer where it has the first reflection. Part of the wave, *Vtf*, will continue forward to the load where it will divide between load, *Vl*, and backward reflection, *Vlr*. The second part of the source wave, *Vf*, will reflect from the input of the 1/4-wave section back to the source and will be identified as *Vfr*. (The effects of *Vfr* on the source will be ignored in this analysis for sake of simplicity.) The part of the wave reflected back from the load, *Vlr*, is relabeled *Vtr* so that *Vlr* = *Vtr* when we move to the next wave sequence. This is done to clarify the sequence of events as we trace the forward wave. The entire sequence of events is recorded on line 1 of Table 1.

When the leading edge of the reflected part of the initial wave reaches the input of the quarter wave line (when *Vtr* first contacts the leading edge of the second half wave *Vf* at the discontinuity), a new wave is formed at the input to the 1/4-wave line. Now we will use Eq 2 to find a new reflection coefficient that accounts for the power input from *Vtr*. The sequence of voltages for the second 1/2-wave is recorded on line 2 of Table 1.

This sequence of successive 1/2-wave events continues and is recorded on lower lines in Table 1 until the reflection coefficient *Vfr/Vf* becomes zero. At that point, stability is reached.

Steven Best will be gratified to notice that the steady state power excess in the 1/4-wave transformer is 7.736 W, the same as he discovered. Walt Maxwell will be glad to see that there is no power reflected back toward the source from the input of the 1/4-wave transformer once a steady state is reached. All of the power is properly directed by means of voltage division among resistive loads.

It is appropriate to emphasize the role of the 1/4-wave transformer in this example. In the 1/4-wave transformer, the leading wave edge has traveled exactly 1/2 wavelength before a portion of it returns to the input as a reflected wave (having entered the transformer, traveled 1/4 wavelength to the load, and 1/4 avelength back to the input point). On arrival back at the input, the leading edge "encounters" the second half of the wave, which is always inverted from the first half wave. We must account for this inversion by reversing the sign for *Vtr*. This reversal allows the reflection coefficient to reduce to zero after several half waves have occurred.

We have already mentioned that in the steady state, the transforming section of the 1/4-wavelength line always contains more power than the matched section of line (per unit

**Table 1**

Results of a spreadsheet to calculate the ratio of reflected voltage to source voltage (power is also calculated) using Eq 2 to analyze a 1/4-wavelength impedance transformer. A stable reflection factor, Vfr/Vf = 0, is reached after five reflection events. The voltage symbols for this spreadsheet/table are shown in Figure 4. The power associated with each voltage has a prefix "P"and a suffix identical to the associated voltage "V."

***Input***

| | |
|---|---|
| Source impedance | 50 Ω |
| Load impedance | 150 Ω |
| Matching impedance | 86.6 Ω |
| Source voltage | 70.711 |

***Calculations***

*Input*

| *Pulse Number* | *Vtr* | *Vfr/Vf* | *Vfr* | *Pfr* | *Vtf* | *Ptf* | *Vlr/Vl* | *Vlr* | *Plr* | *Vl* | *P* | *Sum P* |
|---|---|---|---|---|---|---|---|---|---|---|---|---|
| 1 | 0.000 | 0.268 | 18.946 | 7.179 | 89.657 | 92.822 | 0.268 | 24.025 | 6.665 | 113.682 | 86.157 | 100.001 |
| 2 | 24.025 | 0.019 | 1.358 | 0.037 | 96.094 | 106.629 | 0.268 | 25.750 | 7.656 | 121.844 | 98.973 | 106.666 |
| 3 | 25.750 | 0.001 | 0.096 | 0.000 | 96.556 | 107.657 | 0.268 | 25.873 | 7.730 | 122.430 | 99.927 | 107.657 |
| 4 | 25.873 | 0.000 | 0.005 | 0.000 | 96.589 | 107.731 | 0.268 | 25.882 | 7.736 | 122.472 | 99.996 | 107.731 |
| 5 | 25.882 | –0.000 | –0.002 | 0.000 | 96.592 | 107.736 | 0.268 | 25.883 | 7.736 | 122.475 | 100.001 | 107.736 |

## A Derivation of the Expanded Voltage-Ratio Equation

A junction in a real transmission line often carries waves traveling in both directions. What is the reflection factor — expressed as a ratio of reflected voltage to forward voltage — when power is flowing in both directions at a junction between two mismatched transmission lines?

*Assumptions*

1. Power entering the junction is equal to power leaving the junction.
2. Current entering the junction is equal to current leaving the junction.
3. The voltage developed at the junction is common to all conductors making the junction.
4. The voltage at the junction is the sum of the forward and reflected voltages for both the source and load sides of the junction. These voltages could be measured by a directional voltmeter.

*Derivation*

Refer to Figure A for a diagram and symbol description.

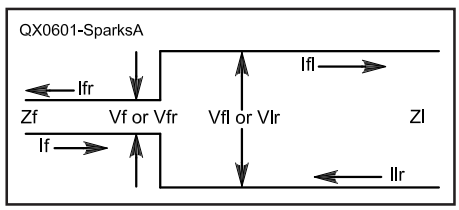


$Zf$ = Impedance of the transmission line carrying forward power
$Zl$ = Impedance of the transmission line carrying reflected power
$Vf$ = Voltage of the forward wave
$Vfr$ = Voltage of the reflected portion of the forward wave
$Vlr$ = Voltage of the reflected wave traveling rearward from the load
$Vfl$ = Voltage of the re-formed wave traveling forward to the load
$If$ = Forward current
$Ifr$ = Reflected current from junction
$Ilr$ = Reflected current from the load
$Ifl$ = Forward current of the re-formed wave traveling forward to the load

Based on our assumptions, we have:

$$Vf + Vfr = Vfl + Vlr \qquad \text{(Eq S1)}$$

Voltage on the forward side equals voltage on load side, and

$$If + Ilr = Ifr + Ifl \qquad \text{(Eq S2)}$$

current flowing into the junction equals current flowing out of it.

First, we find another definition for $Vfl$ to reduce the number of unknown terms. The basic transmission line impedance is $Z = V / I$, where $V$ is the input voltage and $I$ is the input current. Therefore, we can say

$$Vfl = IflZl$$

We can define $Vfl$ in terms of $Zf$ and $Zl$ by using Eq S2 and the basic impedance relationship to substitute and rearrange terms.

$$Vfl = Zl(If + Ilr - Ifr)$$

$$Vfl = Zl\left(\frac{Vf}{Zf} + \frac{Vlr}{Zl} - \frac{Vfr}{Zf}\right) \qquad \text{(Eq S3)}$$

The reflection ratio is defined as $Vfr / Vf$. We can substitute, using Eq S1, to get

$$\frac{Vfr}{Vf} = \frac{Vfl + Vlr - Vf}{Vf}$$

Next, multiply both sides by $Vf$ and substitute $Vfl$ by using Eq S3.

$$\frac{Vf\ Vfr}{Vf} = Vlr - Vf + Zl\left(\frac{Vf}{Zf} + \frac{Vlr}{Zl} - \frac{Vfr}{Zf}\right)$$

Carry out the multiplication

$$\frac{Vf\,Vfr}{Vf} = Vlr - Vf + \frac{Zl\,Vf}{Zf} + \frac{Zl\,Vlr}{Zl} - \frac{Zl\,Vfr}{Zf}$$

then simplify and combine terms.

$$Vfr = 2Vlr - Vf + \frac{Zl\,Vf}{Zf} - \frac{Zl\,Vfr}{Zf}$$

Divide both sides by $Vf$.

$$\frac{Vfr}{Vf} = \frac{2\,Vlr}{Vf} - 1 + \frac{Zl}{Zf} - \frac{Zl\ Vfr}{Zf\ Vf}$$

Group all the terms containing $Vfr$ on the left side and factor out $Vfr / Vf$.

$$\frac{Vfr}{Vf}\left(\frac{Zl}{Zf} + 1\right) = \frac{Zl}{Zf} - 1 + \frac{2Vlr}{Vf}$$

Leave only $Vfr / Vf$ on the left side to get the voltage reflection ratio:

$$\frac{Vfr}{Vf} = \frac{\frac{Zl}{Zf} - 1 + 2\left(\frac{Vlr}{Vf}\right)}{\frac{Zl}{Zf} + 1} \qquad \text{(Eq S4)}$$

Equation S4 is the voltage reflection ratio for a transmission line discontinuity with power coming from two directions. Notice that the ratio is dependent upon the ratio of reflected load voltage (from the load) to the forward voltage, as well as the ratio of impedances on each side of the junction. Notice also that the ratio becomes the familiar

$$\frac{Vfr}{Vf} = \frac{\frac{Zl}{Zf} - 1}{\frac{Zl}{Zf} + 1} \qquad \text{(Eq S5)}$$

if the reflected voltage from the load is zero.

length). The reflected wave is entirely reformed during each half cycle to contain just enough reflected power (extracted from the power going to the antenna) to cause the natural power division at the discontinuity to be zero in the source direction. At the same time, the reflected power is re-reflected from the discontinuity back to the antenna in phase with the source power. As a result, the transforming section always contains power from both the source wave and the reflected wave. In the example, the excess power is 7.736 W.

It is tempting to picture the reflections in the matching section as waves bouncing between mirrors. I would argue that it is more intellectually correct to say that the reflected wave is actually re-forming at each end using the power from both the forward and previously reflected waves. I must admit that the vision of mirrors has an appeal that is seductive, but it does not conjure an accurate conceptual framework.

**Conclusion**

We can take some of the mystery out of transmission-line reflections by using the expanded version of the reflection coefficient. The problem reduces to a sequence of voltage divisions that are easily calculated.

**Acknowledgment**

I would like to thank Mr Jon Pollock, KØZN, for reviewing the text and making many constructive suggestions.

**Notes**

[1]S. R. Best, VE9SRB, "Wave Mechanics of Transmission Lines," Part 1, *QEX*, Jan/Feb 2001, pp 3-8; Part 2, Jul/Aug 2001, pp 34-42; Part 3, Nov/Dec 2001, pp 43-50.

[2]W. Maxwell, W2DU, "A Tutorial Dispelling Certain Misconceptions Concerning Wave Interference in Impedance Matching," *QEX*, Jul/Aug 2004, pp 43-50.

[3]Whether the measured impedance of a transmission line is capacitive or inductive also depends on the distance between the measurement point and the line termination. For a purely resistive load, the first point of reversal is 1/4-wavelength toward the source from the load. If the transmission line is long enough, additional reversals will occur each 1/4 wavelength closer to the source from the first reversal point.

*Roger was born in Jan 1937 and obtained his first Amateur Radio license in 1954. He graduated from Wallace High School in Wallace, Idaho, in 1955, and obtained an Agricultural Engineering degree from the University of Idaho in 1959. From 1959 through May 1962, Roger served in the US Navy, achieving the rank of Lieutenant JG. From September 1962 through February 1963, he was in General Dynamics' Centaur program. From March 1963 to present, he has worked in irrigated farming at Second Century Farms, Inc, at Ellensburg, Washington.*

*From 1974 to present, he has been an elected Commissioner of Kittitas County Public Utility District, providing electrical power.*

*In about 1989, Roger was elected to the Board of Directors of the Washington Public Power Supply System. In about 1998, he was elected to the Executive Board of Energy Northwest, which operates the Columbia Nuclear Generating Station at Richland, Washington.*

*Roger's hobbies include Amateur Radio, Amateur Seismology and the study of physics and mechanics. He has previously published "The C-T Quad" (in* QST *and* The 1988 ARRL Antenna Anthology*) and "The Super Sloper" (Dec 1995* QST*).* □□

# *Perfecting a QSK System*

*A reed relay and a sequence timing circuit allow the author to hear received audio between dots and dashes at 30 wpm.*

By Markus Hansen, VE7CA

The first item listed under The Amateur's Code in *The ARRL Handbook* is "CONSIDERATE …never knowingly operates in such a way as to lessen the pleasure of others." When we are operating CW, trying to work a rare country and the DX station is listening, "up 2," we often hear stations continuing to call the DX station even though the DX station has already begun an exchange with another station. This is either the result of bad manners or the offending station is not equipped with a transceiver that is capable of QSK operation.

674 St Ives Crescent
North Vancouver, BC V7N 2X3
Canada
**ve7ca@rac.ca**

Full break-in operation, or QSK, has its roots in the early days of radio communication and CW traffic handling. When an operator sent QSK?, he was asking if the other operator had the ability to hear between CW characters when he was sending. If both operators had QSK capability, then they could easily interrupt each other if they missed a word while copying a message.

In the early 1960s I worked as a commercial radio operator in the high arctic. Our station employed separate receive and transmit antennas spaced a considerable distance apart. Our station was thus capable of QSK operation, and it was a feature that I really learned to appreciate.

When I built my own transceiver, which I named the HBR-2000, one of the features I decided to incorporate was full break-in keying. My design goal was to be able to hear other stations between CW elements at 30 words per minute. At 30 wpm the length of a space between character elements is 40 ms.[1] I decided to aim

[1]ARRL Technical Information Service, Morse Transmission Timing Standard, **www.arrl.org/files/infoserv/tech/code-std.txt**. For purposes of specifying code speed, the "PARIS" 50-unit standard is used. From that standard, the following relationship is derived:

$$u = (1.2)/c$$

where:

u = period of one unit, in seconds
c = speed of transmission, in words per minute (wpm)

The length of a DOT and the space between elements of a character is one unit. The length of a dash is 3 units and the space between words is 7 units.

for a "transmit to full audio recovery time" of 10 ms or less. At 30 wpm that means the receiver is operating for 75% of the time between elements. As an example, when sending the letter "A," the receiver will be fully recovered from transmitting the dot for 30 ms or 75% of the length of the break time before beginning transmission of the dash.

To fulfill this requirement, a friend helped me design a TR switching circuit to do the following:

1. On key-down: activate audio and IF mute, CW sidetone and TR reed relays.
2. 3 ms after key-down: turn on carrier oscillator.
3. On key-up: turn off carrier oscillator and sidetone oscillator.
4. 4 ms after key-up: TR relays switched to receive position.
5. 10 ms after key-up: audio and IF stages unmuted.

There is nothing unusual in this design approach. After building the circuit and implementing it in the transceiver, however, I was greeted with thumping/popping sounds in the audio output when keying the transmitter. It was very unpleasant to listen to. The thumping/popping sound became even more objectionable when I switched to my narrow 250 Hz IF filter. Connecting an oscilloscope to the audio output of my receiver, I was able to clearly see the distortion. See Figure 1.

I was able to reduce the annoying thumping by doing what commercial Amateur Radio manufacturers do: lengthening the time that the audio stage remains muted after key-up to about 27 to 30 ms rather than the 10 ms I desired. I tried this for a while but I was not happy, as I could not hear between dots when I was sending CW at 30 wpm. Actually, it was just about the same as using semi-break-in. Obviously, I had to do something if I wanted to meet my original design goal of a full-break-in TR system.

To understand what is happening you have to know a little about my HBR-2000 architecture. The receiver is a single-conversion receiver with no RF amplifier. The receiver mixer is a high-level +17 dBm double-balanced mixer followed by a single-stage classic W7ZOI-design 2N3688 post-mixer amplifier, then a 6 dB pad. Five selectable, relay-switched, crystal IF filters are located between the post-mixer amplifier and the input to the IF stage. I enclosed the different stages in boxes constructed of circuit-board material, and used BNC connectors for all RF runs and feedthrough insulators for all dc and control lines between the different boxes.

I use one reed relay for switching the antenna between transmit and receive (TR switching) and two more reed relays to switch band-pass filters (BPFs) between the receiver front end and the transmitter low level amplifier section. Since TR relays do not provide 100% isolation between contacts, there is some leakage of the transmit signal through to the receiver mixer and post mixer preamplifier when transmitting.

To get an idea of the level of signal at the receiver mixer port when in the transmit mode, I measured the RF level with a power meter when trans-

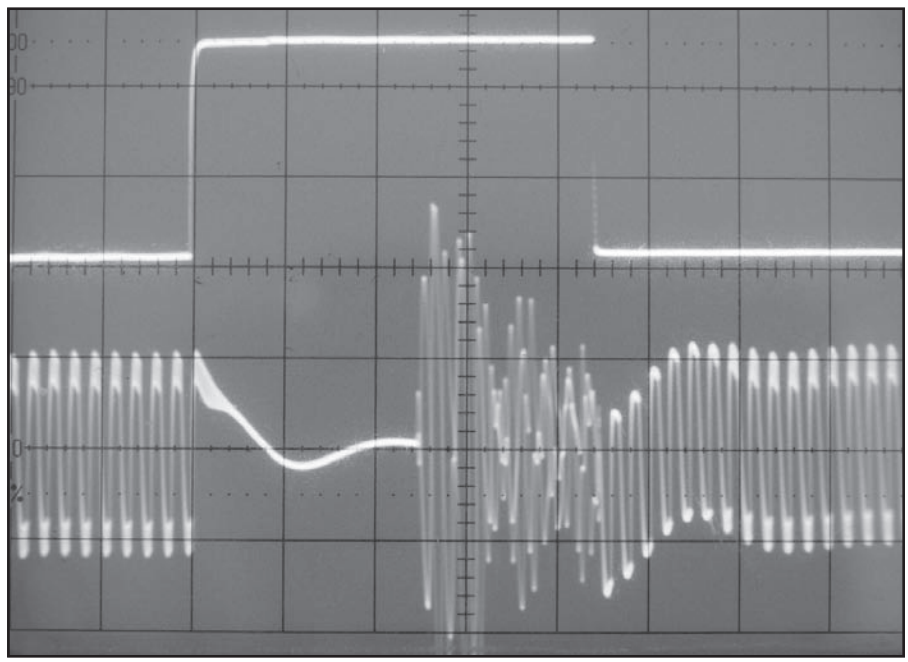

**Figure 1 — This is the oscilloscope trace of keying line and audio output, showing the loud thumps when the receiver recovers. The oscilloscope time base was set to 5 ms per division.**

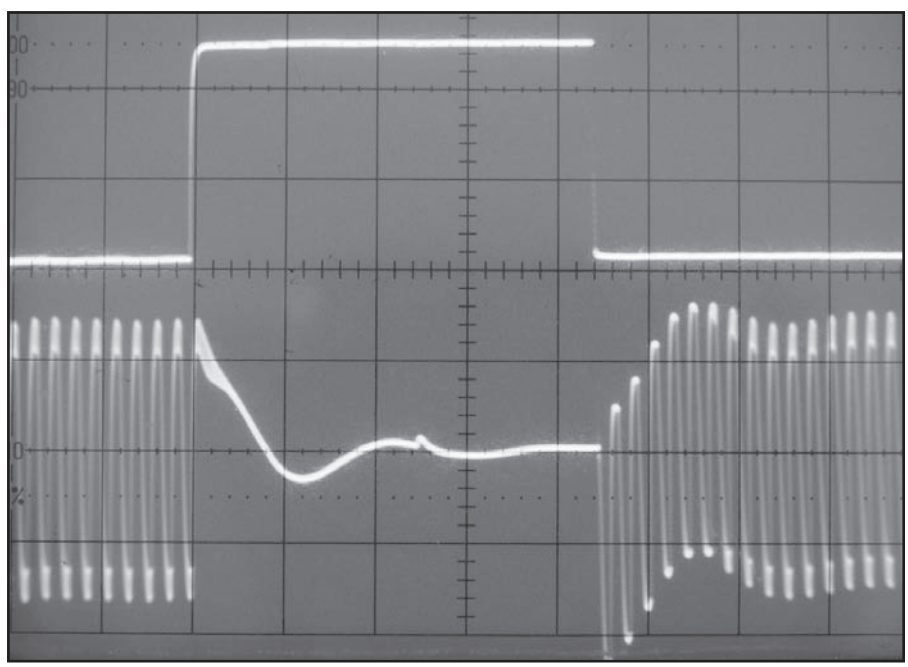

**Figure 2 — Here you can see the sine wave on the break of the CW sidetone. That was the cause of the low sounding thump.**

mitting at 5 W. It was –59.6 dBm. I switched my 100 W amplifier in and out with separate input and output reed relays. Five watts is equivalent to +37 dBm; therefore there is about 77 dB of isolation between the transmitter output and receiver input when transmitting. This means that the receiver front end is being exposed to a very loud 10-dB-over-S9 signal when transmitting.

As mentioned above, after key-up, the TR relays do not switch from transmit to receive until 4 ms has passed. Relays do not switch instantaneously and though the relay specifications call for a switching time of less than 1 ms, the contacts bounce a little, producing a transient pulse. Since it takes about 3 ms for the CW carrier to diminish to zero, 4 ms is sufficient time to ensure that I am not hot switching the TR relay.

Transients produce the thumping/popping sound in the receiver audio output when switching between transmit and receive. The transients are produced by a combination of events all happening very quickly: the TR relay switching, the carrier oscillator turning on and off and so on. The transients flow between the TR relay contacts and on to the mixer, post-mixer amplifier and crystal filters before reaching the IF input.

Previously I mentioned that the thumping sound was particularly bad when choosing the narrow CW IF filters. What I discovered was that when a wide IF filter (2.5 kHz BW) was selected, I only needed an audio mute time of 10 ms after key-up to achieve no thumping sound in the audio output. When I selected my narrow 250 Hz IF filter, however, I had to increase the audio mute time to 27 ms to achieve the same clean sound.

The length of time that it takes RF transients to diminish to zero varies with the bandwidth of the stage through which they pass. Compared to a 2.5 kHz wide filter, a narrow filter such as my 250 Hz filter increases the time that it takes a transient to diminish to zero by a considerable amount. That is why there is still some RF energy at the IF input after the TR relay and carrier oscillator have switched to receive when listening with a narrow filter. In my particular case it takes about 17 ms longer for a transient to diminish to zero for the 250 Hz filter compared to the 2.5 kHz filter.

It became obvious after the initial investigation that if I wanted to achieve my original goal of being able to hear between CW dots, then another course of action had to be taken.

I reasoned that if I could come up with another method of providing further isolation between the TR switch and the mixer input, I could achieve my goal. One thought was to incorporate a diode attenuator in conjunction with the TR reed relays to obtain additional isolation. This in turn would reduce the level of the transients before they reached the IF filters. I was not keen on this idea, because I had purposely avoided using diodes in the receiver signal path. I wanted to avoid the possibility of introducing diode-associated IMD problems.

After explaining my problem to my friend, who has helped me a lot when I ran into problems while building the HBR-2000, he suggested I should switch off the LO power to the receiver mixer while transmitting. Our first thought was to use electronic switching but since I had an extra reed relay on hand we decided to use the relay instead, as it was easier and quicker to incorporate than a diode switch. When there is no LO power applied to a double diode balanced mixer, it is actually an electronic attenuator. The LO power forward biases the mixer diodes and causes the diodes to conduct.

Upon adding a reed relay in series with the LO to the first mixer, I was able to reset the audio mute time after key-up to 12 ms when listening with the 250 Hz filter. The sound of

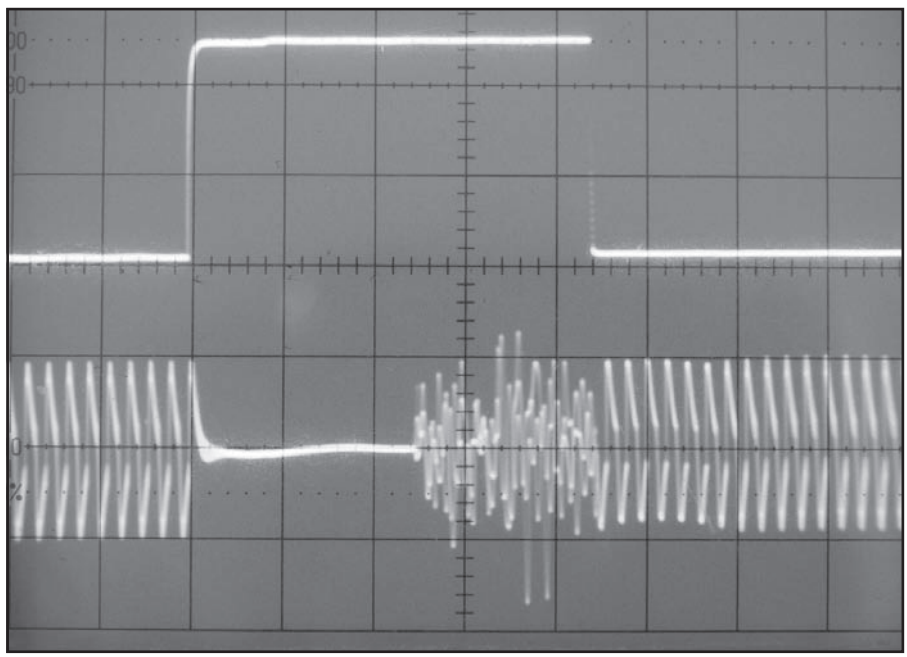

**Figure 3 — Here the low frequency sine wave has been eliminated. No transient in the audio output, just receiver noise.**

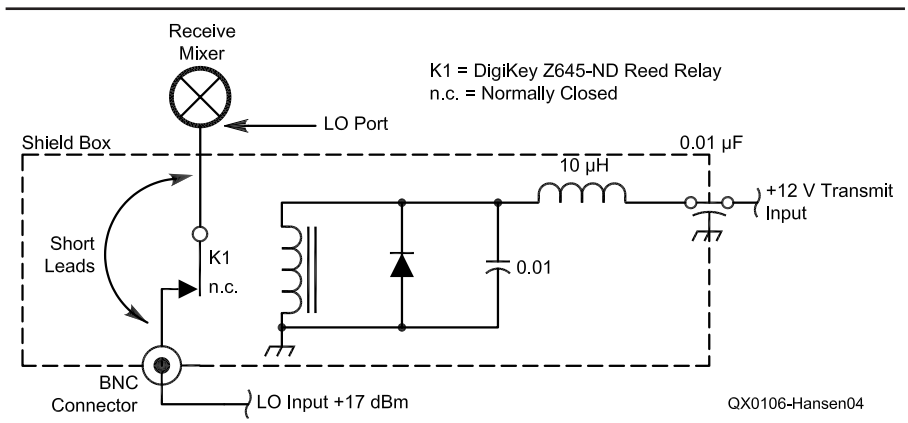


**Figure 4 — This is the wiring diagram of the LO relay.**

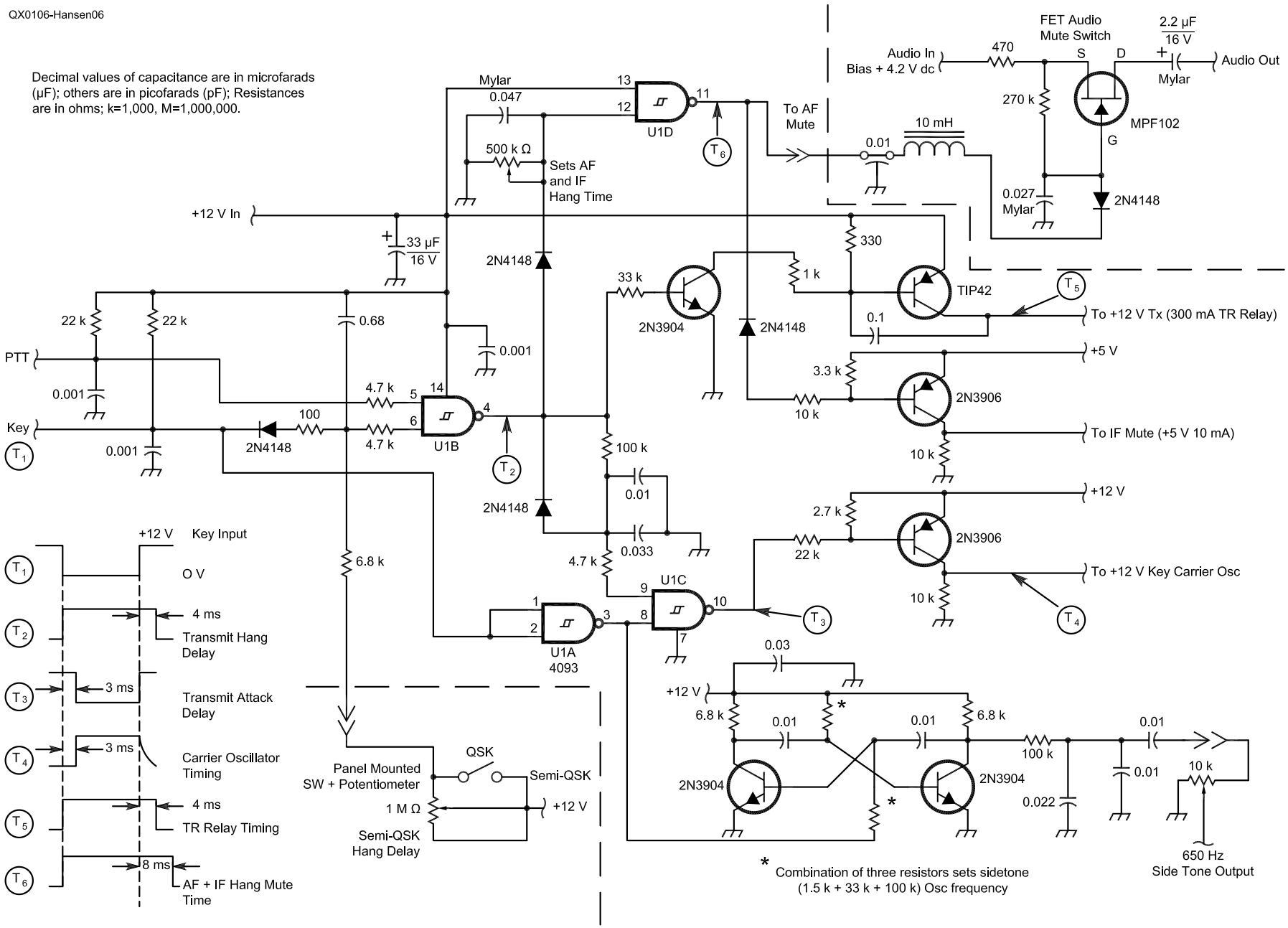


**Figure 6 — TR System Diagram.**

the audio output was considerably improved. The relay contacts switch between the LO and a 50 Ω resistor so that the mixer LO port is looking at a 50 Ω impedance on transmit. However, there is still a little low frequency thump when the CW sidetone breaks, as Figure 2 shows.

The problem is that the sidetone oscillator (a switching astable oscillator) produces a supply-to-ground square wave having a half-supply bias that produces a transient. This is the low-frequency thump heard in the audio output, upon key up. The combination of the LP and HP filters between the oscillator output and 10 kΩ level control will cause thumping if their time constants aren't matched. By installing a coupling (0.01 µF) capacitor with a value matched for the time constant of the LPF, the low frequency thump was eliminated. Figure 3 shows the result of our efforts.

I still had not reached my goal of a 10 ms receive recovery time, though. As mentioned previously, I had wired the LO reed relay so that when transmitting, the receiver mixer LO port was connected to a 50 Ω resistor. I decided to change the wiring of the relay so that when transmitting, the LO port was grounded instead of being connected to a 50 Ω resistor, hoping to achieve further isolation in the mixer stage. See Figure 4 for the revised wiring. Very short leads from the BNC LO input connector to the reed relay and a shield between the relay and the mixer all play a roll in improving the isolation when the mixer port is grounded by the relay.

This wiring change improved the LO-to-mixer port isolation, and I was able to reduce the receive recovery time to 10 ms. By adding 0.01 µF capacitors across the coil contacts of all the reed relays as well as a 10 mH choke in series with the +12 V dc supply line on the inside of the box to the post mixer amplifier, I was able to further reduce the receive recovery time to 8 ms. Could it be improved further? If I had used better quality RF reed relays I may have been able to achieve an even shorter receive recovery time. I believe that there comes a point of diminishing returns, however. Remember that we are dealing with a transmitter and a very sensitive receiver in the same box. Figure 5 shows the receive audio waveform for the final circuit.

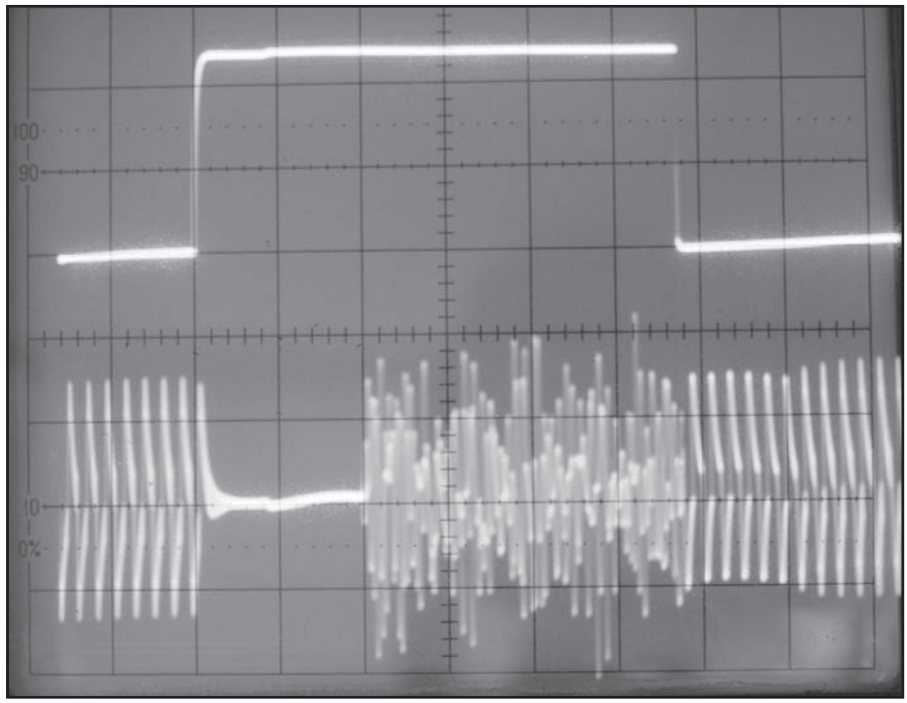

**Figure 5 — The final result.**

How does the QSK system sound after making the above-mentioned changes? Wonderful! In fact, when I am listening to a CW pileup, if I set the CW sidetone oscillator level so that it is at the same level as the incoming signals, I am not even aware that I am transmitting (because I still hear the other signals). The CW sidetone oscillator blends in with the incoming signals.

Figure 6 is a diagram of the final version of the TR switching system and sidetone oscillator. The sidetone oscillator frequency is 650 Hz, which corresponds to my transmit frequency offset. Also shown is the audio FET mute switch that is located in the audio module box, which is in a separate enclosure from the TR circuit board.

Recently I had the opportunity to make side-by-side comparisons of my HBR-2000 with three different commercial Amateur Radio transceivers. Not one of the commercial transceivers was capable of hearing signals between CW dots when operating at 30 wpm, using narrow CW IF filters. Two transceivers in particular produced objectionable thumping sounds that would be very difficult to bear for any length of time. I suppose that explains why many operators still use semi break-in when operating CW.

When you build your own equipment, you have the option of optimizing it for your own use. With careful measurements and some help from my friend, I was able to achieve my goal for a smooth and pleasant sounding full break-in QSK system.

*Markus Hansen has been an Amateur Radio operator since 1959. He has no formal electronics training but likes experimenting and writing articles about his experiences. He has had articles published by ARRL in* QST, QEX *and the* Antenna Compendium *series. You will find Markus in many of the HF CW contests as well as on 6 meters. He is always on the lookout for the last few countries that he needs for DXCC honor roll. His Web site describes more technical details of the HBR-2000 plus other homebrew projects and antennas that he has built.* ☐☐

# An L-Q Meter

*Build this 21st-century equivalent of a Boonton Q Meter.*

By Jim A. Koehler, VA7DIJ

Every radio experimenter will, at one time or another, want to measure inductance. Some multimeters have some ranges for doing this, and there are even better and more inexpensive tools for doing so, such as the AADE capacitance-inductance meter.[1] However, none of these measures the Q of the inductance, and that attribute may be as important as the value of the inductance for the design of things like filters.

The term "Q" comes from the word "quality" and is a measure of how closely the inductor approaches an ideal inductor; that is, one with no losses. A real inductor has losses and, so, a real inductor can be represented by a resistance in series with an ideal, lossless inductor. The value of $Q$ is defined by Eq 1:

$$Q = \frac{\omega L}{r} \qquad \text{(Eq 1)}$$

where $\omega$ is the angular frequency ($2\pi f$), $L$ is the inductance of the ideal inductor, in henrys, and $r$ is the equivalent series resistance of the inductor at that frequency. For any real inductor, the value of $Q$ depends on the frequency of operation, which means that $r$, itself, varies with frequency. An ideal inductor would have a $Q$ approaching infinity because $r$ would be zero. Real inductors have $Q$s that vary depending on the geometry and the core. Typical inductor $Q$s range from 10 to 200.

So, how does one measure $Q$? To start with, you cannot just measure the resistance of the inductor with a dc multimeter and say that is $r$. The true value of $r$ depends on the frequency because, at radio frequencies, $r$ is greater than the dc resistance. This is due to skin effect, radiation losses, eddy-current losses and core losses. You must measure $r$ at the frequency of operation, and that can only be done indirectly by *measuring* $Q$ and then using that to calculate $r$. Surprisingly, it is not difficult to measure $Q$.

### Theory of *Q* Meter Operation

The classic instrument for measuring $Q$ is the Boonton Q Meter, Model 260-A, later manufactured by Hewlett-Packard in the 1950s and 1960s. When I was a student in the late 1950s, the lab in which I worked

[1]Notes appear on page 34.

2258 June Rd
Courtenay, BC V9J 1X9
Canada
**jark@shaw.ca**

had one of these instruments and, over a period of several years, I often used this instrument to measure both the inductance and the *Q* of inductors I was making for various circuits. Many years later, I came across this very instrument in a university sale of surplus assets, so I bought it and have it at home. It is slow and tedious to operate, very heavy (40 pounds), takes a lot of bench space, but it still works as well as it did 50 years ago.

The instrument consists, essentially, of a signal generator and an RF voltmeter. The signal-generator output is connected to the inductor under test in series with a variable capacitor. The RF voltage across the capacitor is measured by the RF voltmeter as shown in Figure 1. If the output voltage of the signal generator is $v_g$ volts and the voltage measured across the capacitor, *at resonance*, is $v_c$ volts, the *Q* of the inductor at that frequency is given by the ratio

$$\frac{v_c}{v_g}.$$

The dial for the variable capacitor has two scales on it; one shows capacitance and the other, inductance. At specific frequencies, this inductance scale is appropriate to show the value of the inductance, in microhenrys, of the inductor under test. Did you ever wonder why the *Q* values for inductors in catalogues are always shown for frequencies of 2.5 MHz, 7.9 MHz or 25 MHz? The Boonton Q Meter dial was calibrated in inductance values for those frequencies. Figure 2 shows the Boonton Q Meter; notice the variable capacitor dial showing both capacitance and inductance scales.

To measure *L* and *Q* with the Boonton meter, one clamps the inductor to be tested between the two terminals, sets the signal generator to one of the standard frequencies and sets the output level of the signal generator as shown on one meter. One then tunes the capacitance dial through its range while looking for a peak on the other meter. If it is the correct frequency range for the particular inductor, the inductor *Q* value is shown as the peak voltage on the other meter, while the value of the inductance can be read from the capacitance dial. If one doesn't get a peak, it means that either the *Q* was too low to measure or, more likely, that one needs to change the frequency (either up or down) to the next standard frequency and try the procedure again. It is a tedious procedure, and the novelty of measuring inductance this way soon wears off.

This article describes a modern version of an L-Q meter that is a small, fast and accurate means of measuring both the *L* and *Q* of an inductor. This instrument is shown in Figure 3. It uses a modern direct digital synthesizer (DDS) instead of a tunable oscillator and a single Analog Devices AD8307 RF detector IC instead of an RF voltmeter. These two components are controlled by a microprocessor that also provides the human interface to the instrument.

## Revised Theory of Operation

The relationship

$$Q = \frac{v_c}{v_g} \qquad \text{(Eq 2)}$$

is true if the source resistance of the RF source is zero and if the voltmeter impedance is infinitely large. For the Boonton Q Meter, the oscillator was quite powerful; it used a 5763 tube with a plate voltage of over 300 V. Older hams may recall that the 5763 was often used as a driver for PA stages in transmitters or even as the final amplifier in low-power transmitters. In each of the eight switched frequency bands covering the range from 50 kHz to 50 MHz, the output of this oscillator was transformer coupled to provide a low-impedance output source, which the manufacturer specified at just 0.02 Ω! The high-power oscillator was required to provide a reasonably high-voltage output, even with this

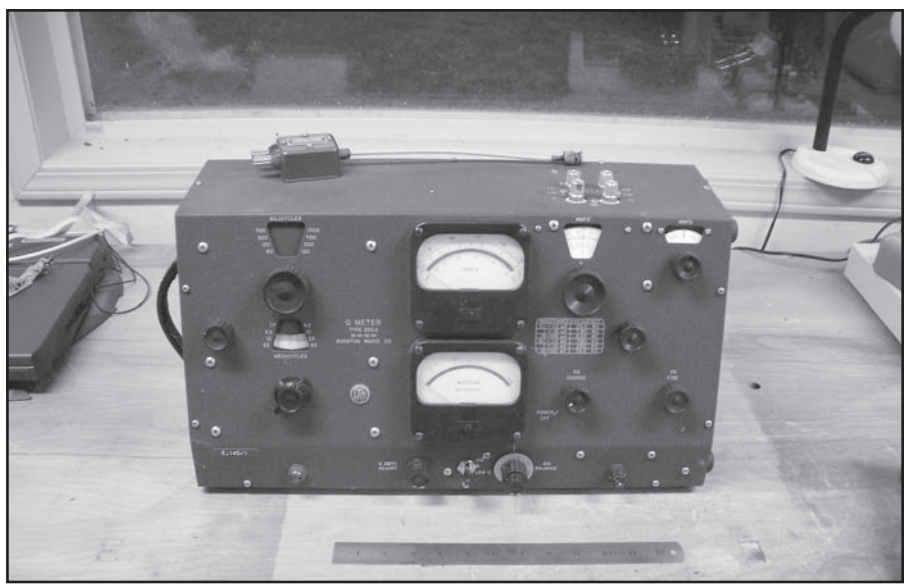

(A)

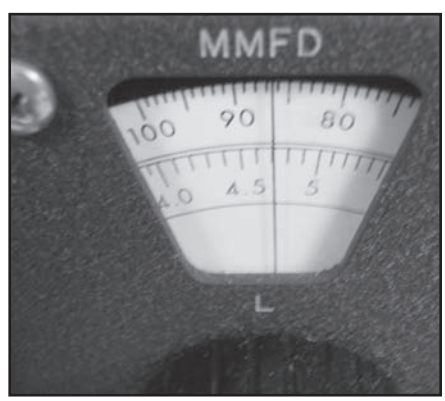


(B)

**Figure 2 — (A) The Boonton Q meter. (B) A close-up of the capacitance dial: capacitance is read on the top scale and inductance on the bottom scale.**

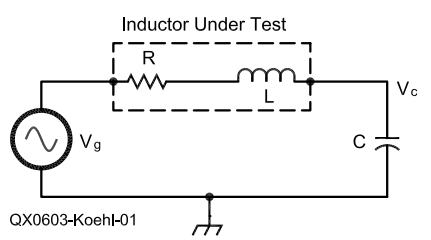


**Figure 1 — A circuit for a simple *Q* meter.**

low impedance. The RF voltmeter used a specially fabricated triode vacuum tube with very high input impedance, and the grid-leak resistance was 100 MΩ, so this voltmeter appears as a capacitance of a few picofarads in parallel with 100 MΩ. So, in the Boonton Q Meter, the two requirements of zero source impedance for the generator and infinite input impedance for the RF voltmeter were almost perfectly realized in practice.

In my modern version of the Q Meter, the basic equation is no longer true because, firstly, the output impedance of my DDS module is not close to zero; and, secondly, the input impedance of the AD8307 RF detector chip is finite. However, one can compensate for these two factors in a way the original Boonton designers probably never conceived: we can use a microprocessor to calculate the correction factors necessary to calculate *L* and *Q* for this much more imperfect instrument.

A block diagram of the instrument is shown in Figure 4. The details of the calculations needed to determine the actual *Q* of the inductor are given in Appendix A. The calculation is complex but the microprocessor doesn't care, and the calculation only takes a fraction of a second.

**Basic Operation**

The instrument has two sets of terminal/banana jacks on top (see Figure 3): one pair for the external capacitor and one for the inductor to be measured. In normal practice, the external capacitor will have some fixed value appropriate for the frequency range and inductance to be measured. I have made up two small circuit boards with banana plugs on them that plug into the capacitor jacks, one with an 82 pF silver mica capacitor and the other with a 470 pF silver mica capacitor

The inductance to be measured is connected to the inductor terminals and a push-button switch is pressed. The microprocessor then causes the DDS module to scan through the range from 0.1 to 100 MHz in 201 logarithmically spaced steps, while looking at the output of the RF detector. If it finds a peak, it steps around this peak in 15 steps, either side, with a logarithmic step-size one tenth of those in the original scan. It then uses the frequency of the highest peak in this range to calculate the value of the inductance, knowing the value of the external capacitor. Then, using the equations shown in Appendix A, it calculates the true *Q* value of the inductor. The whole


**Figure 3 — The L-Q meter in operation. The external capacitance is connected between the terminals at the back, while the inductor under test is connected between the terminals at the front. In this photo, two component clips are inserted in the inductor terminals to allow quick and easy placement of inductors.**

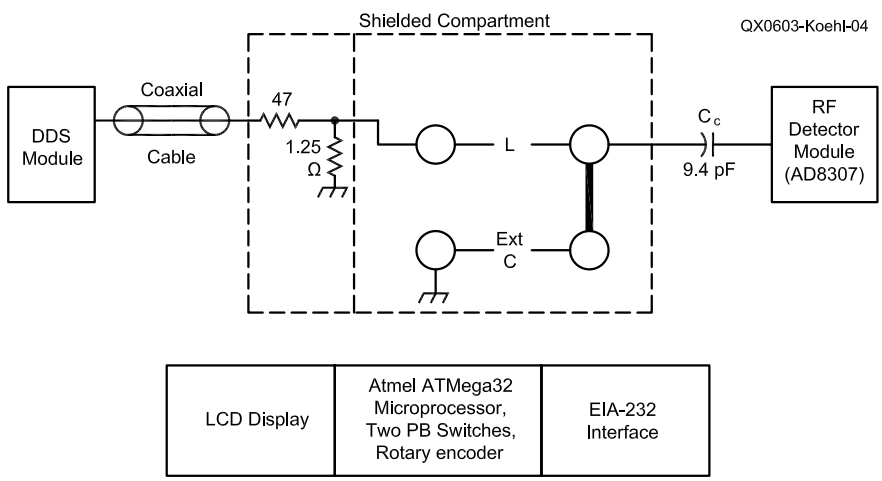


**Figure 4 — Block diagram of *Q* meter, connections between units not shown.**

process, including the calculations takes about 2 seconds, most of this time being taken by the scan. At the end of the process, the inductance — in microhenrys — is shown on the top line of the display. The bottom line shows the true $Q$ of the inductance and the resonant frequency.

There are two push-button switches on the instrument panel, along with a rotary optical encoder. One switch, labeled SELECT, changes mode of operation while the other, labeled SET, does an action. For example, when the instrument is turned on, it is in a "measurement" mode and pressing the SET button causes a measurement of inductance, as described above, to take place. Pressing the SELECT button once moves the instrument to a capacitance mode, where one can use the rotary encoder to tell the instrument the value of the external capacitance. When you've got the correct capacitance on the LCD display, pressing the SET button causes the instrument to store that value of capacitance in its internal EEPROM non-volatile memory, which ensures that this entry will be available for later use, as appropriate.

The next mode, accessed by pressing the SELECT switch again, is one in which the rotary encoder changes the frequency of operation. In this mode, with an inductor in place, the bottom

## Appendix A — Circuit theory

### 1. Calibration mode

In the calibration mode, a low-inductance strap is placed across the inductance terminals, thereby connecting the output of the low-impedance signal generator to the detector. The simplified circuit diagram for this is shown in Figure A.

$R_s$ is the internal RF source impedance, which was 1.24 Ω. $C_t$ is the stray capacitance of the fixture (which was measured to be 13.5 pF in my case). $C_c$ is the coupling capacitance from the fixture to the AD8307 detector (9.4 pF in my case). $C_i$ and $R_i$ are the parallel input capacitance and resistance, respectively, of the AD8307 RF detector.

This circuit can be redrawn to show the components all as impedances. This is shown in Figure B.

Here, the source resistance, $R_s$, is replaced by an impedance, $Z_s$, and so on. $Z_a$ is the impedance of the AD8307. Let the voltage appearing across the AD8307 detector be $v_c$. Then it is easy to show that it is related to the source voltage, $v_s$, by the following equation:

$$\frac{v_c}{v_s} = \frac{Z_a Z_{pc}}{(Z_a + Z_c)(Z_{pc} + Z_s)} = F_c \qquad \text{(Eq A1)}$$

where $Z_{pc}$ is the parallel combination of $Z_t$ with $Z_c$ and $Z_a$ in series.

### 2. Measurement Mode

In this mode, an inductor is placed between the low-impedance signal generator and the detector. An external capacitor is placed in parallel with the stray capacitance. The equivalent circuit is exactly as in Figure A2, except that now, $Z_s$ is the source resistor $R_s$ in series with the inductor. The inductor can be represented by a perfect inductance, $L$, in series with a resistance, $r$. $Z_t$ is now a parallel combination of the stray capacitance and the external capacitor; let us name it $Z'_t$. The equivalent of $Z_{pc}$ will be called $Z_m$; it consists of $Z'_t$ in parallel with the series combination of $Z_a$ and $Z_c$.

The analysis is simplified because, at resonance, the inductive reactance cancels out the capacitive reactance of $Z_m$, which we calculate. This allows us to then calculate the value of the inductance, $L$. It is easy to show that, at resonance, the voltage appearing at the detector, $v_m$, is related to the source voltage, $v_s$, by the following equation:

$$\frac{v_m}{v_s} = \frac{Z_a Z_m}{(R_s + r + R_m)(Z_a + Z_c)} = \frac{F_m}{R_s + r + R_m} \qquad \text{(Eq A2)}$$

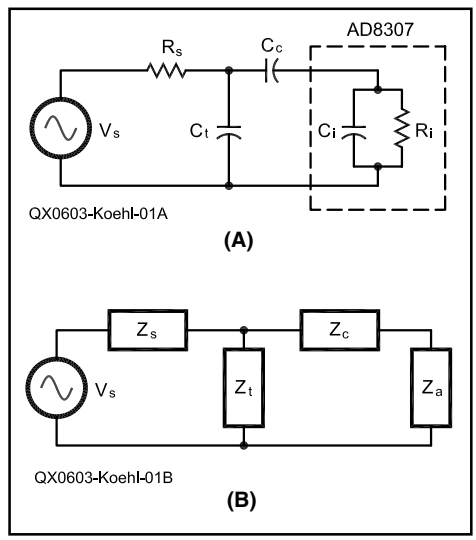


Here, $R_m$ is the resistive component of $Z_m$.

In both equations the voltage ratios have both real and quadrature components. The AD8307 detector, however, only measures magnitude, so we really need only calculate the magnitude of $F_c$ and $F_m$ in these equations *after* the multiplications and additions have been done, taking into account the phase relationships. Fortunately, complex-number manipulations are available as a library of functions in *C*, and these were used in the microprocessor program.[4] Then at any frequency, all values are known except $r$ and we can solve for this as follows: We substitute the value for $v_s$ from Eq A1 into Eq A2 and, after rearranging, get the final equation:

$$r = \frac{F_m}{Q_m F_c} - (R_s + R_m) \qquad \text{(Eq A3)}$$

where $Q_m$, the measured $Q$, is the measured ratio of $v_m / v_c$. The true value of $Q$ for the inductor is, then, just the inductive reactance divided by $r$.

To summarize, the L-Q meter determines the inductance and $Q$ by scanning through the frequency range, looking for a peak in the detected RF voltage. When that frequency is found, a series of calculations are done to determine a value for the reactive component of $Z_m$. This gives us the inductance. The ratio of the peak voltage detected at resonance to the voltage measured during the calibration cycle is the measured $Q$; $Q_m$. Then, using Eq A3, we can calculate $r$, and hence, the true $Q$ of the inductor.

line of the LCD display acts as a bar graph showing the voltage across the external capacitor. In this mode, one can vary the frequency and see the peak at resonance. Pressing the SET switch when the frequency has been set to the peak causes the instrument to display the *Q* at that frequency. This mode is useful if one wants to know the *Q* of an inductor at a particular frequency.

I have made a variable capacitor fixture that plugs into the capacitor jacks and has a dial calibrated in pF. You set the frequency with the rotary encoder and use the variable capacitor connected to the external C terminals to get a peak on the bar graph. Then, press the SET button to choose a mode where you can use the rotary encoder to set the value of the capacitance at resonance and press the SET button again to measure the *Q* at this frequency.

Finally, the fourth mode is used to calibrate the instrument. In this mode, one connects a very low inductance strap between the two "inductance" terminals and presses the SET button, which causes the instrument to scan through its frequency range and store, internally, the value of the detected voltages at those frequencies. These are the source generator voltages, $v_c$, as described in Appendix A. This procedure is needed only once, when the instrument is first powered up, or if some of the internal circuit components have been changed. The calibration values are stored in EEPROM.

Because EEPROM is used to store the calibration and capacitor values, the instrument keeps these values for the next time it is turned on.

### The DDS Module

The DDS module is based on an Analog Devices AD9951 DDS integrated circuit. Tom Alldread, VA7TA, and I designed the module, and it provides an output from zero to 200 MHz in steps of 1 Hz. The components are all surface-mounted on a $^1/_{32}$-inch-thick circuit board that is 2.65×1.4 inches (6.7×3.6 cm). This DDS module has been the basis of several instruments that Tom and I designed and built; it is a very nice little unit. This module actually has two AD9951s and is controlled by its own built-in Atmel ATTiny26 microprocessor. The DDS module was designed to be driven either by an external oven-controlled crystal clock (OCXO) or an internal crystal. For this application, the accuracy and stability of an OCXO isn't needed and an internal crystal clock is used. For this application, only one of the AD9951s is installed. The interface to the built-in controller is

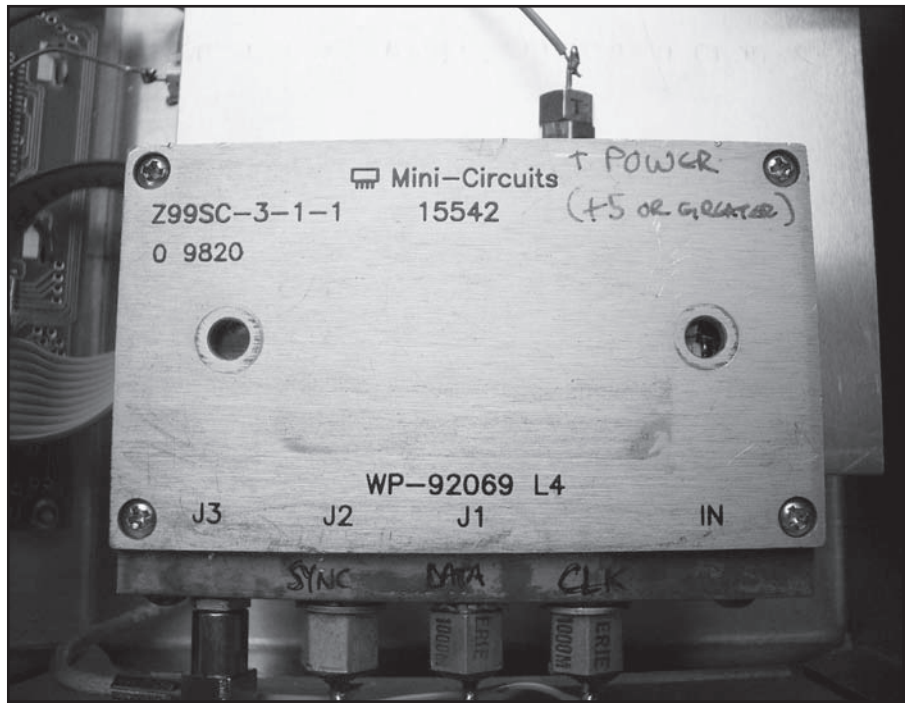


**Figure 5 — A photo of the DDS module. Frequency control is provided by a serial protocol via three wires going through three feed-through capacitors along the bottom side of the unit. Power is provided through a feed-through capacitor at the top side of the unit. RF comes out the SMB connector on the bottom-left side.**

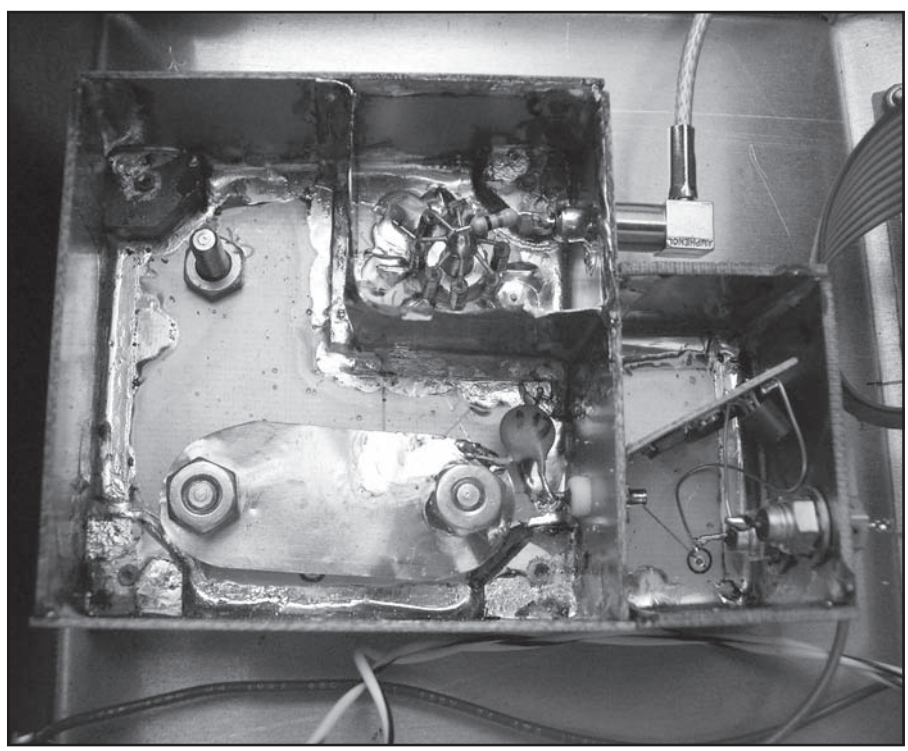

**Figure 6 — A photo showing the interior of the RF compartment. Note the eight 10-Ω resistors soldered symmetrically around the L terminal at the top right. A 47 Ω resistor goes from that terminal to the SMB connector providing RF input to the unit.**

via a three-wire serial protocol. Figure 5 is a photograph of this unit, built into a small, surplus Mini-Circuits milled enclosure with the RF output on an SMB connector.

### The Shielded RF Compartment

This enclosure was built with double-sided pc-board material all soldered together. The RF input from the DDS module comes in at an SMB connector. The center pin of this connector is connected to a series 47 Ω resistor that connects directly to the banana-jack/terminal, which is for one side of the inductor under test. Soldered to this jack are eight 10 Ω, 1/4-W resistors arranged symmetrically around the jack. The other ends of the resistors are soldered to the pc-board ground plane. This arrangement may be seen in Figure 6. After this photo was taken, I soldered some copper foil to the enclosure walls completely around the terminal jack to shield it and the input SMB connector from the rest of the enclosure.

The connection between the other terminal of the inductor pair and one side of the external capacitor was made from a strap of copper foil material, to minimize its inductance. The stray capacitance of this strap (and the terminals connected to it) to ground is about 13.5 pF, as measured with a capacitance meter. This capacitance value is needed in the calculations.

The coupling capacitor — a nominal 10 pF ceramic disc — goes from this strap, with very short leads, to a feed-through lead (*not* a feed-through capacitor!) into a separate compartment that holds the AD8307 RF detector IC. I measured the value of the coupling capacitor with a capacitance meter before soldering it in place.

### The RF Detector

The RF detector is the AD8307 IC. I had built some very small boards that have nothing on them but this IC, a few components and a 5 V regulator; I used this board as the detector. The board is 1/32-inch thick and has a

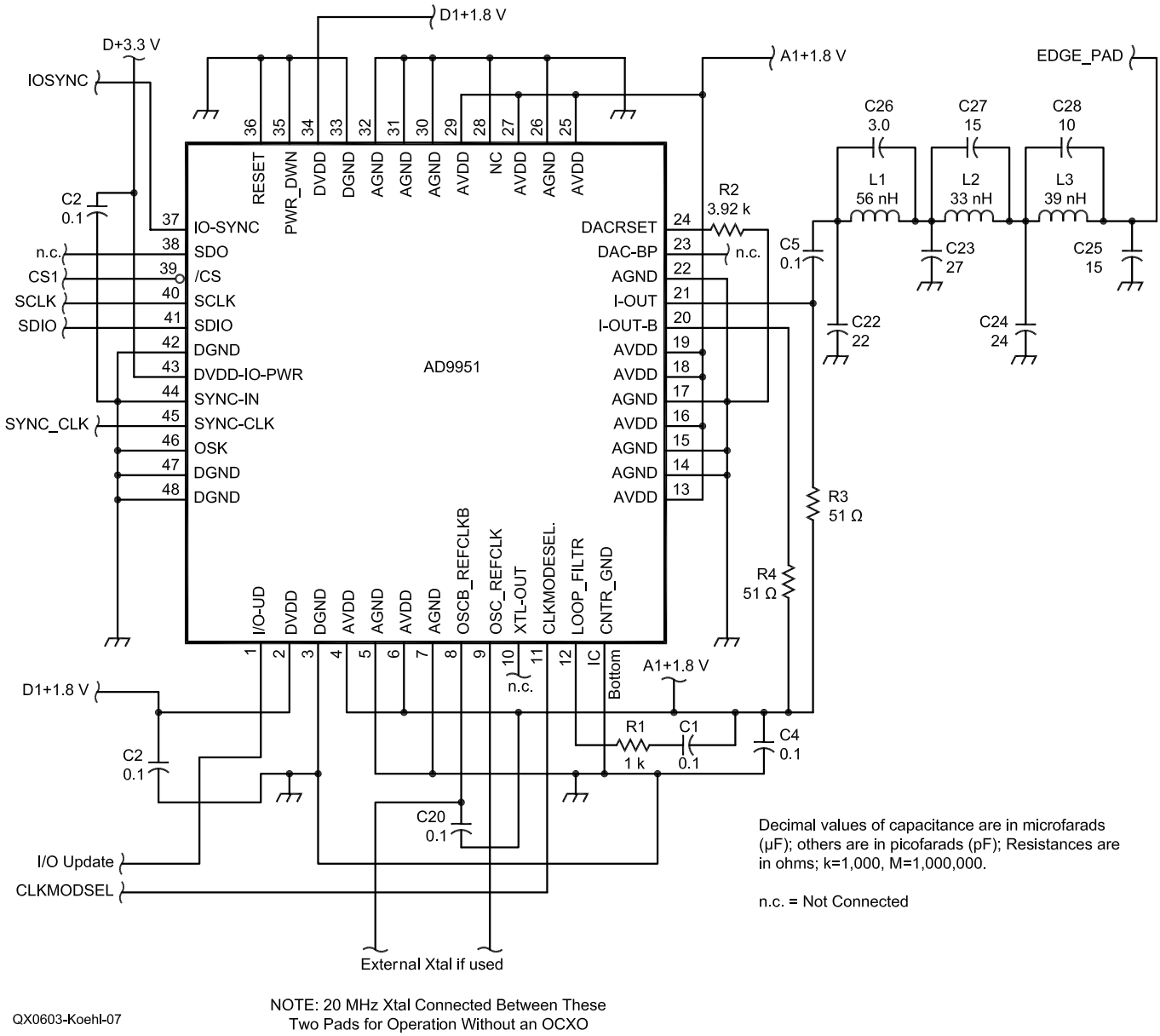


**Figure 7 — Schematic of the master DDS circuit.**

groundplane on the bottom side. The board is mounted by just soldering its groundplane to the enclosure. The AD8307 input is equivalent to a 1.2 pF capacitor in parallel with a 1.1 kΩ resistance; these are the values used for $C_i$ and $R_i$, respectively.

### The Microprocessor, LCD Display, Switches and Rotary Encoder

I used the Atmel ATMega32 microprocessor for this unit. This inexpensive IC has 32 k bytes of flash memory, 1k bytes of EEPROM, 2 k bytes of RAM and four eight-bit I/O ports. The internal A/D converter has eight channels of 10 bits each. The internal clock runs at up to 16 MHz, and most instructions are executed in one clock cycle. The firmware was all written in *C* using the *GNU GCC* compiler for the Atmel AVR series of microprocessors. This is a very mature *C* compiler and it's completely free! The code produced by this compiler is very good and the price cannot be beat. There is a very nice package (consisting of the GCC-AVR compiler, an editor, debugger and other utilities) that was written to run on *Windows* machines; it is called *WinAVR*.[2]

I added a serial EIA-232 interface to the microprocessor, mainly for debugging. It is not used in the normal operation of the instrument.

The LCD display is a standard two-line, 16-character per line LCD display. It is connected to one port of the microprocessor. The push-button switches are simply each connected to ground and to one line of a port. The microprocessor has provision to provide internal pull-up resistors, so a switch push is detected by the line going low. The rotary encoder is connected so that one phase generates an interrupt; the direction of motion is then detected by looking at the other phase in the interrupt routine.

### Other Considerations

There is a potential problem when using the instrument with very high-*Q* inductors, and Appendix A discusses it in detail. For these inductors, the RF resistance, *r*, of the inductor is very small. We calculate what it is by subtracting two calculated values from a measured value of resistance. Because of measurement errors, it may turn out that our calculated *r* is negative, which is not possible for a real inductor. For these cases, I have written the

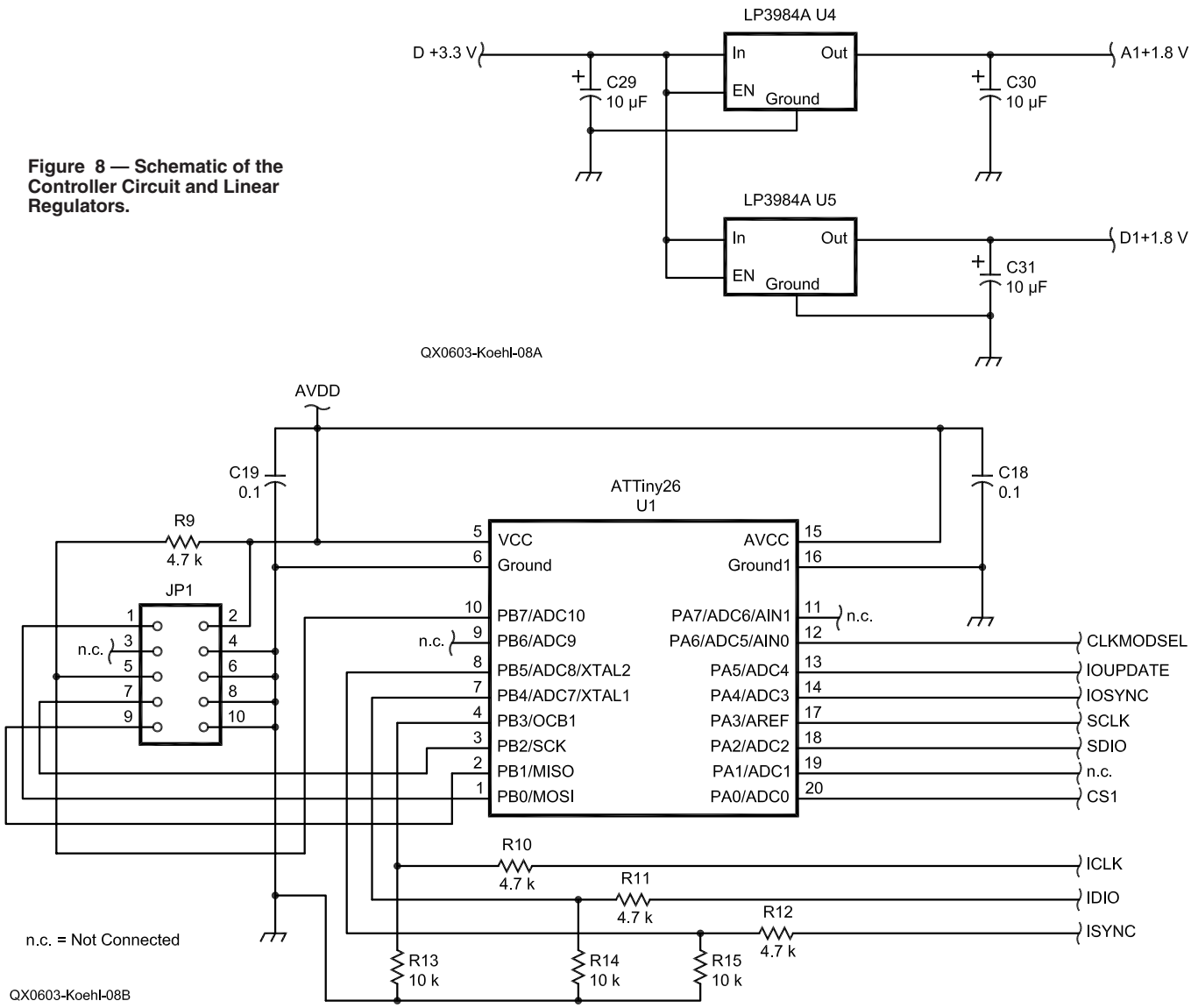


**Figure 8 — Schematic of the Controller Circuit and Linear Regulators.**

program so that the instrument shows the *apparent Q*, not the calculated *Q*, and indicates that it is apparent, not true, by a comment on the display. This is an annoyance more than a problem since, if the *Q* is very high, we can normally treat the inductor as if it were perfect anyway.

Finally, I would like to point out that if you already have a good signal generator with some way of setting the frequency from a serial or other port, it is possible to make an L-Q meter using that generator and just building a test "pod" consisting of the RF compartment and AD8307 RF detector. If you control the generator with a PC and can read the output voltage of the AD8307 into the PC, you can effectively make an L*Q* meter without having a dedicated microprocessor controller as I have used here.

Figures 7 and 8 are the schematic diagram of the DDS module. Figures 9

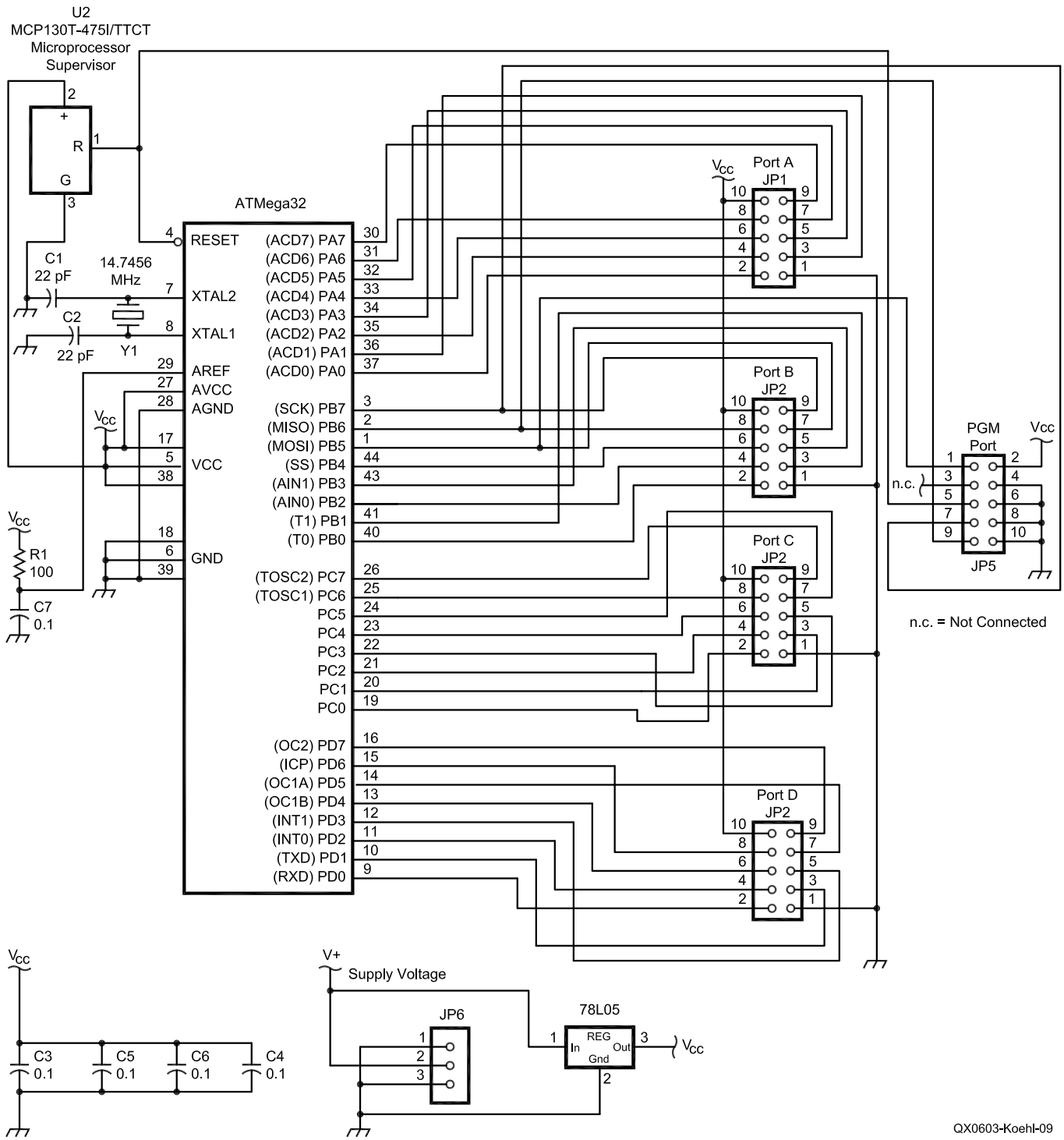


**Figure 9 — Schematic of the ATMega32 board used in the L-Q meter.**

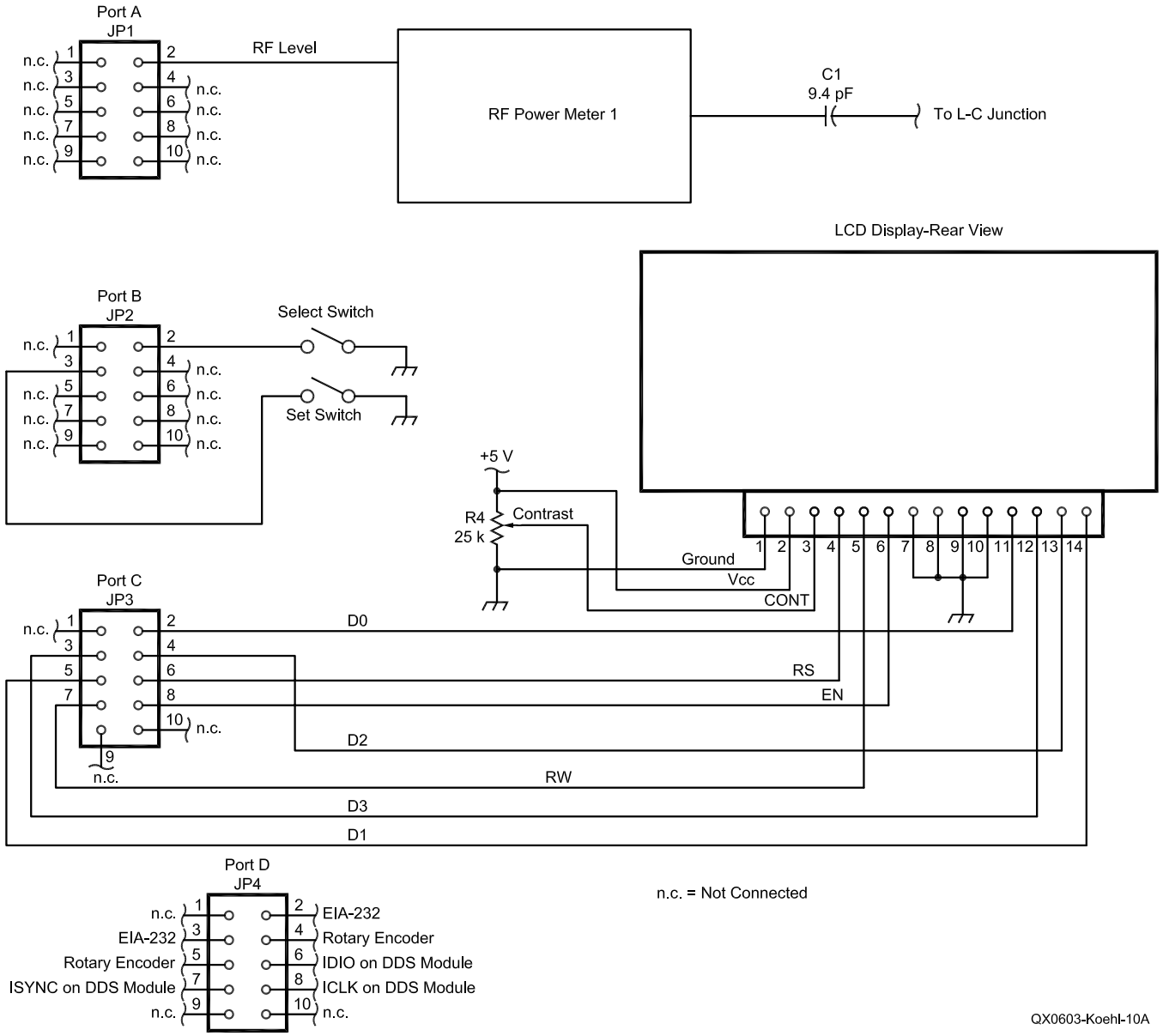


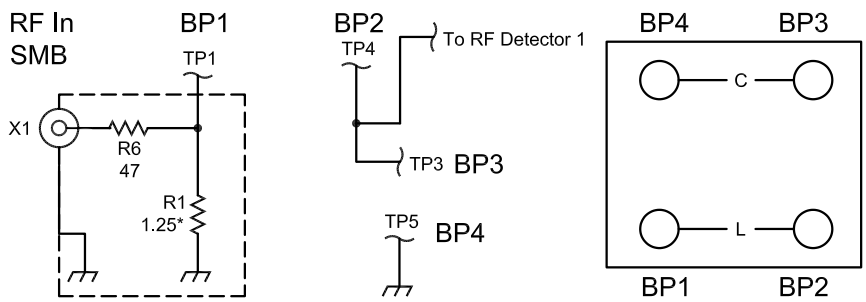


**Figure 10 — Interconnections of the microprocessor to the rest of the instrument.**

Decimal values of capacitance are in microfarads (μF); others are in picofarads (pF); Resistances are in ohms; k=1,000, M=1,000,000.

* This resistor is really eight 10 Ω resistors in parallel.

QX0603-Koehl-10B

and 10 show the controller and interassembly wiring. Figure 11 is the schematic of teh RF detector module. A copy of the source code, written in *AVR-GCC C*, is available on the ARRL Web site.[3]

## Conclusion

It is worth saying a few words about accuracy. The calculated value of $r$ is the result of a subtraction of two calculated numbers based on measurements, which can never be absolutely accurate. Because of measurement errors, especially when $r$ is small (that is, when $Q$ is high), it is possible for the final error in true $Q$ to be very high. For this reason, whenever the calculated value of $Q$ is greater than about 300 (or if $r$ is calculated to be negative — which is impossible), I wrote the program to display just the measured value of $Q$ and to indicate that the true $Q$ of the inductor will be greater than this measured value. Unlike $Q$ meters such as the Boonton 260A, the accuracy of the true $Q$ determined by this instrument gets better as the $Q$ of the inductor decreases!

For the particular value of coupling capacitor I used, at frequencies lower than about 250 kHz, the measured voltage ratio will not be very accurate, because the voltage going into the AD8307 is too low, when calibrating, to give a useful measurement. Therefore, at these frequencies, the displayed $Q$ is just an estimate. I am not usually interested in winding inductors for these lower frequencies. If I were, I would have increased the value of the coupling capacitor and thereby increased the accuracy at the lower-frequency end of the range at the expense of reduced accuracy at the upper end.

The accuracy of the value for the inductance is not affected by any of these errors; its accuracy depends only on the accuracy with which the capacitances have been measured previously and the accuracy of the resonant frequency found by the instrument. I used an AADE *L/C* meter (see Note 1) to measure the various capacitances, and I believe they are accurate to about ±2%. The algorithm used to find the peak frequency of resonance is accurate to better than 0.5%, and the frequencies generated by the DDS are accurate to about one part in 100,000. In general, I would expect $L$ to be determined with an accuracy of about ±2%.

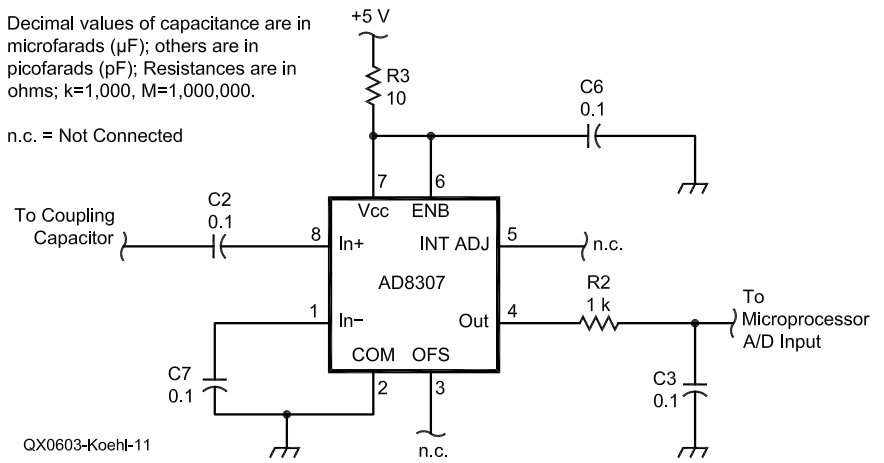


**Figure 11 — Schematic of the AD8307 RF detector.**

### Notes

[1]AADE Electronics L/C Meter IIB; **www.aade.com**.

[2]**winavr.sourceforge.net**.

[3]You can download this package from the *ARRLWeb* at **www.arrl.org/qexfiles/**. Look for 3x06Koehler.zip.

[4]**www.phanderson.com/complex/cplx_c.html**.

*Jim was first licensed as VE5AL in 1952 at age 15. He became VE5FP in 1966 when he returned from living abroad for a few years. He spent most of his professional life as a Professor of Physics and Engineering Physics at the University of Saskatchewan, both teaching and doing research in upper-atmospheric physics. He retired in 1996 and moved to Vancouver Island in British Columbia, where he indulges in his hobbies and generally enjoys the good life, the superior weather and the complete absence of mosquitoes.* ☐☐

# Blocking Dynamic Range in Receivers

*An explanation of the different procedures and definitions that are commonly used for blocking dynamic range (BDR) measurements.*

By Leif Åsbrink, SM5BSZ

**Introduction**

Blocking dynamic range (BDR) may actually mean quite different things at different laboratories. Circumstances and what definition of BDR is being used affect performance comparisons among receivers in the presence of a strong, off-channel interfering signal.

Dynamic range in general is the ratio (or difference in decibels) between the weakest signal a system can handle and the strongest signal the same system can handle simultaneously — without an operator switching attenuators or turning volume potentiometers. The concept is quite general and by no means limited to radio receivers. Human sensors like the ears and the eyes have very large dynamic ranges, for example. The undamaged ear can detect a 1 kHz sound wave at a level of $10^{-12}$ W/m$^2$ while the upper limit is about 1 W/m$^2$, where we start to feel pain. The dynamic range of our ears is thus about 120 dB. Our eyes can detect the light from a star in the dark sky when about ten photons per second reach the retina, which converts to something like $10^{-13}$ W/m$^2$. The Sun, with its 300 W/m$^2$, does not damage our eyes unless we look straight into it.

Another example of dynamic range is the dynamic range of a vinyl music record. It may be on the order of 60 to 80 dB only, much less than the dynamic range of our ears.

The above examples show the dynamic range for a single signal. The corresponding dynamic range for a receiver is not particularly interesting. It relates the strongest on-channel signal the radio can handle, without serious distortion (or damage), to the weakest signal it can receive. We may observe that a local very strong SSB station sounds severely distorted when we tune to it even though the same station does not cause any interference when we listen to other stations on the same band. This is not likely to be any problem to a radio amateur. The example is given just to show the wide meaning of the concept of dynamic range.

The rest of this article will deal with the dynamic range pertinent to situations where a single strong signal is causing interference to the desired sig-

Jaders Prastgard
63505 Eskilstuna
Sweden
**leif@sm5bsz.com**

nal. This kind of dynamic range — blocking dynamic range (BDR) — may be the most important figure of merit for some radio amateurs while others may find that the interference created by the simultaneous presence of two or more strong signals is the limiting factor. In such cases, the intermodulation-free dynamic range is the number to look for when selecting what receiver to use.

The intermodulation-free dynamic range is discussed frequently in amateur publications. It may be technically challenging to measure properly but there is no controversy about what it means.

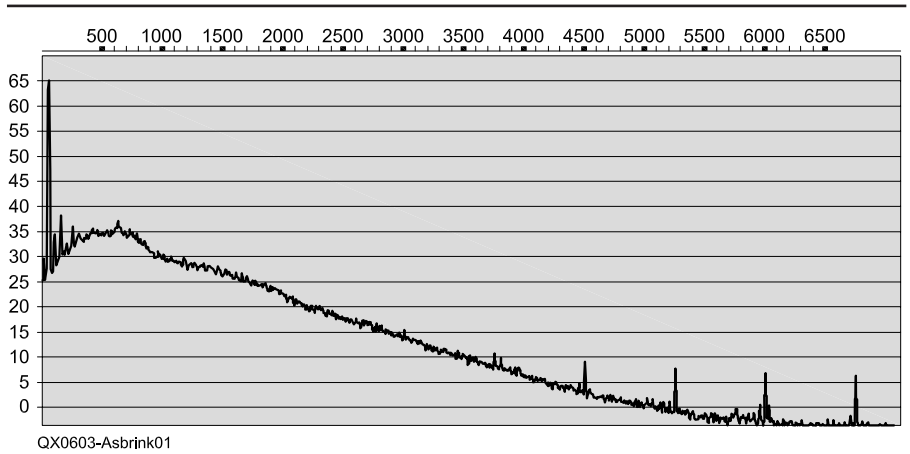


**Figure 1 — The loudspeaker output from a Yaesu FT-1000D transceiver with a very leaky transformer close to it causing a fairly strong, but still absolutely inaudible, 50-Hz hum signal.**

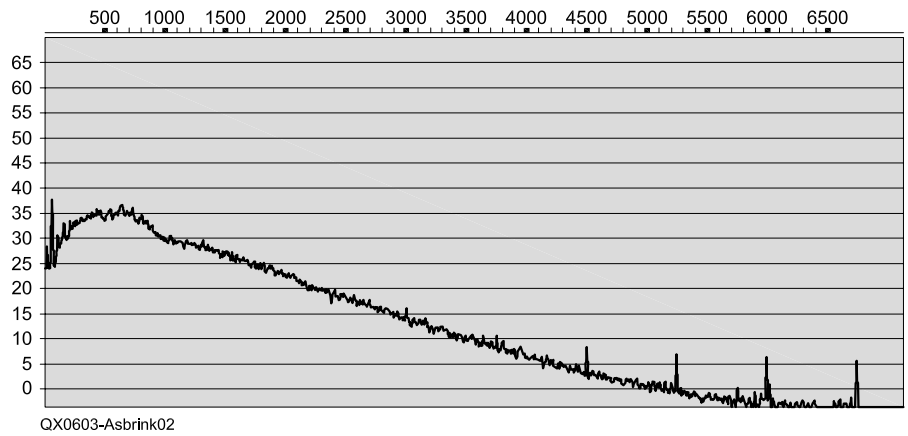


**Figure 2 — The loudspeaker output from an FT-1000D with a dummy load at the antenna input. All settings are identical to those of Figure 1.**

### The Weakest Signal

The weakest signal a receiver can handle is usually taken as the total noise power that reaches the output as measured with a true RMS voltmeter. This means that the low end of the dynamic range is taken as the signal at the antenna input that doubles the output power from the receiver. The measurement has to be done without AGC, and the doubled power output means that the weak signal power equals the noise power at the output. Any room-temperature resistor produces a noise voltage that would transfer –174 dBm/Hz to a matched cold resistor. With the RF preamplifier disabled, a typical HF receiver may produce 20 dB more noise with a room-temperature dummy load at the input than would an ideal receiver that would not add any noise of its own (only amplifying the noise from the dummy load). A receiver adding 20 dB of noise is said to have a noise figure of 20 dB. If the bandwidth were 500 Hz, the noise floor referenced to the antenna input would be –174 + 20 + 27 dBm = –127 dBm. (Note that 10 log 500 ≈ 27.) This signal level is sometimes improperly called MDS (minimum discernible signal) for such a typical receiver, even though a CW operator would easily copy a signal that is 10 dB weaker.

Picking the noise floor as the low end of the dynamic range is typical for all dynamic ranges, not only in radio receivers. The noise floor power is proportional to the bandwidth and therefore a receiver will have 10 dB more dynamic range when measured at a bandwidth of 200 Hz compared to when it is measured at a bandwidth of 2 kHz. It is the same receiver, though, and the dynamic range differences that depend on bandwidth should not be included when different receivers are compared.

For that reason, receivers should be measured at a standardized bandwidth. It could be 1 Hz, 500 Hz, 2.4 kHz, or something else. Since there is no de-facto standard, each laboratory has to specify what bandwidth they use to allow correct comparisons to results from other labs.

### The Strongest Signal

There are two vastly different BDR definitions that may give completely different, although perfectly reproducible, results. Michael Tracy, KC1SX, described them in *QST*.[1] He writes: "BDR as a lab measurement normally refers to the point at which the weak (presumed desired) signal is reduced by 1.0 dB ('blocked') by the presence of a strong (presumed undesired) signal." The procedure followed at the ARRL Lab for BDR measurements is set up to find the point of 1 dB gain loss.[2] A quite different definition defines the strong signal as the signal that causes a predetermined degradation of signal-to-noise ratio (SNR) for a weak signal (1 dB or 3 dB). In some cases, the two different definitions may give the same result; but in other cases, the resulting BDR may differ by 40 dB or more.

The two different phenomena that lie behind the two definitions are called *saturation* and *reciprocal mixing*, although the physical phenomena in the receiver may be something else. A receiver that uses front-end AGC to avoid saturation, and that compensates for the gain loss after the bandwidth-defining filters, will lose sensitivity when the off-channel signal turns the front-end AGC on. As a result, the noise

[1]Notes appear on page 39.

floor will increase to cause a reduced SNR for a weak signal even though the total gain is unchanged. An RF amplifier that is supplied with inadequately decoupled dc voltage or that has a high impedance for audio frequencies on the base and very low impedance for audio frequencies on the emitter will amplitude-modulate the strong off-channel signal. Both these examples would be classified as reciprocal mixing even though the mechanism is quite different from what the classification implies.

The ARRL Lab definition of BDR through the procedure in Note 2 translates to this definition in plain English: "The BDR is the amount above the noise floor for an off-channel signal that degrades the receiver for strong signals." It may be appropriate for crowded HF bands where the desired signal typically is high above the internal noise floor of the receiver. A receiver with a very high number according to this definition is convenient to use because the operator does not have to use an attenuator to shift the dynamic range up and down as conditions change. Radios that reach 150 dB in the ARRL test reports are not uncommon. The other definition translates to this in plain English: "The BDR is the amount above the noise floor for an off-channel signal that degrades SNR for a very weak signal." This BDR is typically about 100 dB.

The first definition is similar to the dynamic range for ears and eyes as defined above. It is the total useful signal range but it does not contain any information about the ability to detect a weak signal in the presence of a strong undesired signal. The second definition is the true dynamic range in the case of a single dominating off-channel signal. It defines *the strongest signal* that may be present simultaneously while *the weakest signal* is detected.

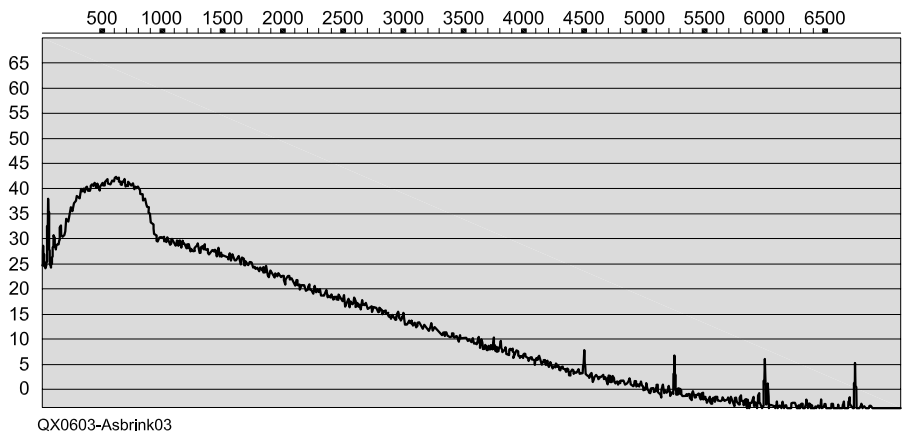


**Figure 3 — The loudspeaker output from an FT-1000D with a noise source at the antenna input. All settings are identical to those of Figure 1.**

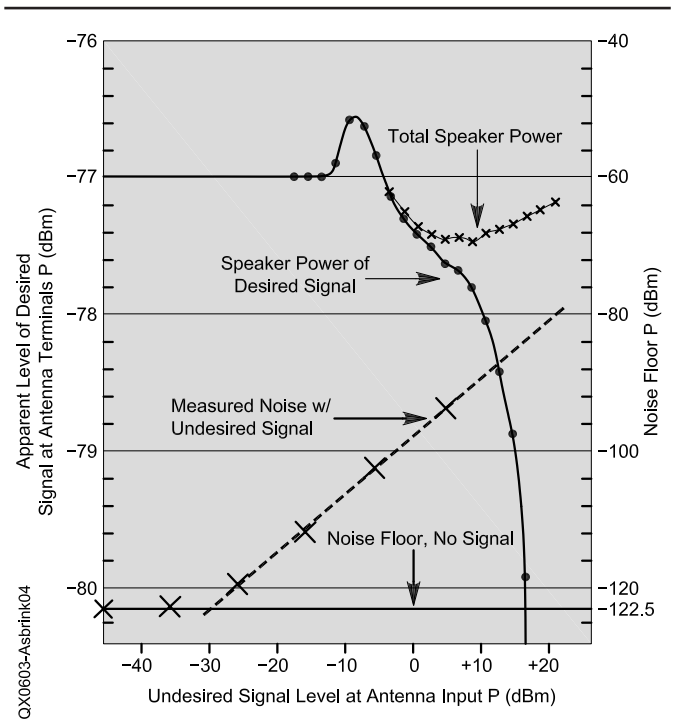


**Figure 4 — The loudspeaker output of an FT-1000D with a 14.138-MHz on-channel signal at a level of –77 dBm (10 dB below the on-channel CP1) as a function of the off-channel signal level at 14.158 MHz. The dots are the on-channel signal level measured at 5 Hz bandwidth, the small crosses are the power (10 Hz to 24 kHz) and the big crosses are the power measured without the on-channel signal.**

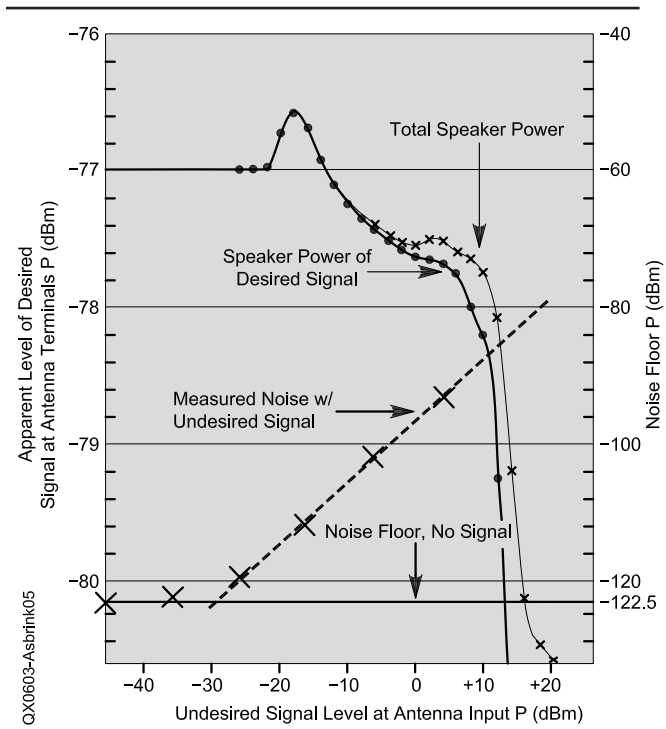


**Figure 5 — The loudspeaker output of an FT-1000D with a 14.178 MHz on-channel signal at a level of –77 dBm (10 dB below the on-channel CP1) as a function of the off-channel signal level at 14.158 MHz. The dots are the on-channel signal level measured at 5Hz bandwidth, the small crosses are the power (10 Hz to 24 kHz) and the big crosses are the power measured without the on-channel signal.**

### Measurement Accuracy Issues with the Weakest Signal

Finding the noise floor by connecting an RMS voltmeter to the audio output may give inaccurate results. The human ear does not respond well to hum from the ac mains frequency of 50 or 60 Hz. Figure 1 shows the loudspeaker output from a Yaesu FT-1000D HF transceiver that had a very leaky transformer placed close to it. This pure 50-Hz hum is absolutely inaudible despite the fact that it is about 30 dB above the noise floor in the spectrum, which has a bin width of 12 Hz. This inaudible 50-Hz hum dominates the loudspeaker signal. It actually lifts the reading of a typical RMS voltmeter by 12 dB and its presence degrades the MDS value by the same amount. The FT-1000D performs absolutely as well with the leaky transformer next to it; there is no audible difference whatsoever and the huge sensitivity difference is an artifact of the measurement procedure.

Even without the leaky transformer, there are some low-frequency spurs in the FT-1000D, as can be seen in Figure 2. This signal is 27 dB weaker than the 50-Hz hum caused by the leaky transformer, so it is only about 2.5% of the total power that reaches the loudspeaker and the error it introduces is only about 0.1 dB. Figures 1 and 2 were recorded in CW mode with the FT-1000D bandwidth set to 500 Hz. It is pretty obvious from Figure 2 that noise outside the desired bandwidth gives a noticeable contribution to the total power seen by an RMS voltmeter. The passband is well visible in Figure 3, where a noise source is connected to the antenna input. From Figure 3 we can estimate the noise floor in a 500-Hz window above the passband to be about 28 dB on the relative dB scale. From Figure 2, we can read the noise floor within the passband as 35 dB. That means that the noise power in the range 900 to 1400 Hz is only 7 dB below the noise power within the desired passband, and therefore causes a reading that is about 20% higher than it would be if a selective voltmeter were used. The noise above the passband is well audible, but it is not really disturbing and it does certainly not degrade the effective sensitivity of the FT-1000D by as much as 20%, as the MDS value would indicate.

By use of exactly the same settings as for Figures 1 to 3: Preamp off (IPO), AGC off, max RF gain, 50% AF gain, 500 Hz bandwidth in CW mode, MDS was measured at 14.120 MHz as described in Note 2 using an RMS voltmeter that was flat from 10 Hz to 24 kHz. The measurement was made with and without the very leaky transformer that makes the difference between Figures 1 and 2. The results are shown in Table 1, which shows the noise power density (NPD) referenced to the antenna input. These settings form kind of standard settings for a transceiver test and they are used in all measurements presented in this article.

The noise power density is 22.2 dB above –174 dBm/Hz, which means that the noise figure of this particular receiver is 22.2 ±1.2 dB with the controls set as in this test. The noise power density can be used to compute the noise power that would pass an ideal filter with a bandwidth of 500 Hz. The result is –124.8 dBm which is 2.3 dB better than the result obtained in the MDS measurement with the RMS voltmeter. The noise power density is a selective measurement and any 50-Hz hum does not affect it at all.

Since the actual detection is done in a much narrower bandwidth than 500 Hz either by machine or by a human being, I argue that the noise power density in the vicinity of the signal is the true noise floor for an MDS measurement. Any wideband noise, hum or high-frequency audio signal that may add several dB to an RMS voltmeter measurement is insignificant — and in those cases where it is audible, there should be a note saying, "This radio suffers from hum or high frequency noise." It may be appropriate to mention here that the mains hum originating in poorly filtered power supplies typically is a pulse train at twice the mains frequency. Contrary to the magnetically coupled pure 50/60-Hz sinewave, 100/120-Hz pulse trains are well audible.

The noise power density can be measured easily with a spectrum analyzer that will give the noise surrounding a carrier in dBc/Hz. With a carrier of known power at the antenna input, the noise power density comes out directly.

### Measurement Accuracy Issues with the Strongest Signal

If the BDR definition in terms of SNR loss for a weak signal is chosen, there are no accuracy problems because the definition requires SNR for a weak signal to be monitored. The definition in Note 2, where the reading of an RMS voltmeter is monitored while the off-channel signal is increased, that may lead to unexpected results sometimes.

To illustrate the problems, the BDR of the FT-1000D was measured with the procedure in Note 2. The loudspeaker output was also monitored on a spectrum analyzer on which the level of the on-channel signal was measured. The on-channel response of the FT-1000D is linear from the noise floor at –122.5 dBm up to –70 dBm. The point of 1-dB compression is –67 dBm. Following the procedure in Note 2, the on-channel signal level was set to –77 dBm. Figures 4 and 5 show the result of the measurement at a frequency separation of 20 kHz above and below the desired frequency.

An inspection of Figures 4 and 5 shows that the reciprocal mixing noise is equal to the noise floor power (MDS) for an off-channel signal level of –26 dBm regardless of whether the on-channel signal is above or below the off-channel signal. The dynamic range is therefore –26 dBm – (–122.5 dBm) = 96.5 dB. If the noise floor (MDS) were measured by means of the noise power density, the same dynamic range would result because then the reciprocal mixing noise power density would equal the FT-1000D noise power density at a signal level of –28.3 dBm.

The FT-1000D has lost sensitivity by 3 dB at a signal level of –28.3 dBm although the gain is unaffected up to –22 dBm (20 kHz below) and –14 dBm (20 kHz above) an off-channel signal. The first nonlinear phenomenon that happens is that the gain increases. The point of 1-dB compression as measured with a selective voltmeter is +8 and +10 dBm, respectively. When measuring the loudspeaker output with an RMS voltmeter, 1 dB compression occurs at +12 dBm when the on-channel signal is 20 kHz above the off-channel signal; but when the on-channel signal is 20 kHz below the interference,

**Table 1**

**MDS measured with a wideband RMS voltmeter and noise power in 1 Hz bandwidth as measured with a spectrum analyzer in the loudspeaker output.**

| | *Transformer* | |
|---|---|---|
| | *ON* | *OFF* |
| MDS(dBm) | –110.3 | –122.5 |
| NPD(dBm/Hz) | –151.8 | –151.8 |

the reading of the RMS voltmeter remains constant within 0.5 dB all the way up to an interference power level of +20 dBm (100 mW). It would probably remain constant at much higher input levels until the front end was damaged.

It should be quite clear from Figures 4 and 5 that the procedure used up to now at the ARRL Lab may give very inaccurate results because the RMS voltmeter does not distinguish between the desired signal and noise. Using the average from 20 kHz above and 20 kHz below, BDR as defined from the point of 1-dB saturation is 131.5 ±2.2 dB above MDS using the ARRL definition for MDS, or 133.8 ±2.2 dB when MDS is defined in terms of the noise floor power density. The much higher values reported in *QST* is caused by the use of an RMS voltmeter.[3]

**Conclusions**

When using the concept of dynamic range in Amateur Radio, we should refer to signals present simultaneously at the antenna input. This means that BDR — implying that blocking means that the ability to copy the desired signal as blocked by a strong off-channel signal — for the FT-1000D is 96.5 dB. When the desired signal is placed at –77 dBm (see Note 2), the point of saturation, which was +20 dBm in *QST* (see Note 3) has to be compared to –77 dBm for a dynamic range of 97 dB, not to the MDS value measured under quite different circumstances. The value of 150 dB reported in *QST* is not the dynamic range for two simultaneously present signals. It is the dynamic range for a single signal and is not of much interest to a radio amateur. The point of 1-dB saturation is 133.8 dB above the noise floor, which means that the operator can place the system noise floor up to 37 dB above the internal noise floor of the FT-1000D without serious problems because of gain compression on strong signals. This leaves adequate margin for a VHF enthusiast who uses the FT-1000D together with a transverter that might lift the noise floor by 10 dB and a mast mounted preamplifier that has to lift the noise floor by another 16 dB to get a system noise figure that is within 0.1 dB of the preamplifier itself.

Both BDR definitions convey important information on the usefulness of a receiver. ARRL is considering the use of an AF spectrum analyzer and the reporting of both measurements in future product reviews.

*Editor's note: Leif's observations about human vision form an apt analogy to receiver dynamic range. The baseball outfielder who drops a fly ball when the Sun shines in his eyes knows about blocking effects. He employs an attenuator (his sunglasses) to reduce the interference but the attenuation may, in fact, put the image of the desired signal (the baseball) below his noise floor. That's the same as what a front-end AGC does to your receiver: It raises the noise figure and may actually make it harder to recognize the desired signal.*

*The point is that you must measure the small-signal end of dynamic range under the same interference conditions used to measure the large-signal end. Only then do you truly measure dynamic range. In addition, the bandwidth in which noise-floor power is measured must be accurately known. It's not enough to dial in a nominal 500-Hz filter and assume its effective bandwidth is exactly 500 Hz. An uncertainty of ±150 Hz in bandwidth would result in additional uncertainty of at least 2.6 dB in noise powers between receivers. Passband and stopband shapes affect effective bandwidth. You cannot go by the 3-dB points alone.*

*As early as 1998, we noted the difference between blocking dynamic range and reciprocal-mixing dynamic range on these pages. Now it is a matter of how previously measured data are corrected or models recharacterized, and procedures updated, including measurement uncertainties. To the best of our abilities, we must adopt procedures that accurately measure real effects in receivers.*

*A 3rd-order IMD dynamic range measurement on an analog-to-digital converter, for example, may be superfluous when performance is dominated by overload instead. Likewise, another measurement, such as BDR, should not be characterized as "noise-limited" when the noise contribution can be discerned separately from the modeled effect.*

**Notes**

[1]M. Tracy, KC1SX, "Product Reviews — In Depth, In English," *QST*, Aug 2004, pp 32-36.
[2]Ed Hare, KA1CV (now W1RFI), "Swept Receiver Dynamic Range Testing in the ARRL Laboratory," *QEX*, Jun 1996, p 16.
[3]Product Review, *QST*, Mar 1991, pp 31-36.

*Leif was born in 1944 and licensed in 1961. He holds a PhD in physics and worked with research on molecular physics for 15 years at the Royal Institute of Technology. Since 1981, he has been running his own company developing various electronic products. He is the inventor of the magnetic intermodulation EAS system now owned by Checkpoint. Leif is essentially retired and works mainly with Amateur Radio related technical projects.* □□

# An Analysis of Stress in Guy-Wire Systems

*Have you ever thought about the forces on your tower guy lines? This article shows you how you can calculate those forces.*

By William Rynone, PhD, PE

**Introduction**

Because of our litigious society, I would like to state that my area of expertise is sparks and arcs rather than snaps and cracks. Therefore the following should be used as an educational tool rather than as an analysis or design format for specific tower installations.

My interest in antenna tower mechanical considerations was precipitated by my Amateur Radio club's interest in erecting one or two additional towers. It appears that tower and antenna manufacturers generally provide adequate information regarding tower installation parts and procedures, such as tower mounting base materials and construction, guy-wire size and pre-loading, anchor methods, etc. The recommended guy-wire specifications are given without mentioning the actual stress that the wires will experience under various load conditions. For example, if a tower manufacturer specifies 3000-lb guy-wire cable, I wondered what the actual stress would be. Typical cable specifications are those listed in Table 1, taken from literature that is supplied by the Wire Rope Corporation of America.[1]

Page 22-6 of *The ARRL Antenna Book*, 20th Edition, contains a brief description of guy-wire materials.[2] The book says, "At rated working loads, dry manila rope stretches about 5%, while nylon rope stretches about 20%. Solid galvanized steel wire is also widely used for guying. This wire has approximately twice the load ratings of similar sizes of copper-clad wire, but is more susceptible to corrosion. Stranded galvanized wire sold for guying TV masts is also suitable for light-duty applications, but is susceptible to corrosion. It is prudent to inspect the guys every six months for signs of deterioration or damage."

Since a wire rope manufacturer usually has a minimum order length or dollar value, and since the average Amateur Radio operator will only require small lengths of guy wire, buying directly from a manufacturer is usually not possible. However, some tower suppliers also sell ancillary equipment or parts to aid in the tower

PO Box 4445
Annapolis, MD 21403

[1]Notes appear on page 45.

installation. From the Texas Towers' web site (**www.texastowers.com**), both galvanized steel and a non-conductive cable, Phillystran, is available in various tension ratings and lengths. Also, the minimum length of galvanized steel cable that they will sell is 100 feet. From the Wirerope Works Structural Strand And Wire Rope Catalog, an Amateur Radio operator would also consider the following to be pertinent when installing a guyed tower.[3] "Assuming the applied tension does not exceed the elastic limit, structural strand and wire rope return to their original length once tension is released. Constructural stretch, on the other hand, results in a permanent set or increase in length."

**General Analysis of Guy-Wire Stress**

There are various forces creating tension in guy wires. For example, wind load on the tower and mounted antennas, pre-load in the guy wire, and to a lesser extent, wind load on the guy wire itself and the weight of the guy wire must all be considered.

The tower experiences various loads. These loads manifest themselves in compression, buckling and shear. Compression is due to the downward vertical force from the guy wires (due to all of the above-mentioned forces on the guy wire), the weight of the tower and the weight of the antennas. Shear is developed due to side loads on the tower and mounted antennas. It is possible that because of varying wind loads and variations in guy-wire tensioning, at a particular instant, one section of an antenna tower will be tending to bend in one direction while another section will be tending to bend in the opposite direction. I estimate that investigating all of these loads would generate sufficient data and descriptions to create a textbook (which may already exist).

The following is just the analysis of the load on the guy wires due to wind load on the tower and antenna. Usually a single set of guy wires is employed for towers of height equal to or less than 40 feet. To minimize the complexity of this analysis, this condition will be analyzed with only a single-layer dipole antenna. Also, tower twisting due to an asymmetric antenna load is not examined.

The associated computer program enables the user to input various tower and antenna dimensions and a wind speed. The program then computes the guy-wire tension for various guy-wire radial distances from the tower base. The program neglects the contribution to the total guy-wire tension due to wind loading on the guy wire and weight of the guy wire.

It is appropriate to mention that the guy wire pre-load is a trade-off. The greater the pre-load, the less tower sway due to varying wind speeds and directions, but at the sacrifice of a greater compression load on the tower and tension in the guys. *The ARRL Antenna Book* contains the following statement: "Many troubles encountered in mast guying are a result of pulling the guy wires too tight. Guy-wire tension should never be more than necessary to correct for obvious bowing or movement under wind pressure."[4]

To perform this analysis, the following tasks must be accomplished. Evaluate the:

1. pressure developed on the antenna due to the wind.
2. transverse antenna tower torque due to the antenna force.
3. transverse antenna tower torque due to wind pressure on the horizontal members of the supporting web.
4. transverse torque due to wind pressure on the three vertical members.
5. transverse torque due to wind pressure on the diagonal members of the supporting web.
6. total torque and the resulting horizontal force at the top of the tower where the guy wires are attached.
7. force generated in the guy wire for various declination angles.

*Equation Symbols:*

Antenna —

*HA* = Height of Antenna (ft).

*ED* = Element Diameter (ft).

*EL* = Antenna Element Length (ft).

*FA* = Force that the Antenna applies to the antenna tower (lbs).

*TA*= Torque due to the antenna (ft lbs).

Vertical members —

*VD* = Vertical member Diameter (ft).

*TVM* = transverse Torque due to a Vertical Member (ft lbs).

*HT* = Height of Tower (also equals vertical member height) (ft).

Web members —

*WW* = Web Width (horizontal space between vertical members) (ft).

*WH* = Web Height (vertical space between adjacent webs) (ft).

*RD* = Rebar Diameter (ft).

*THW* = Torque due to all Horizontal Web members (ft lbs).

*TDM* =Torque due to Diagonal Members (ft lbs).

*HWM* = Horizontal Web Member.

Tower —

*GWFP* = Guy-Wire Force Perpendicular to tower (lbs).

*GWTF* = Guy-Wire Tension Force (lbs).

**Table 1**

**Physical Properties of Zinc-Coated Steel Wire Strand**

| | | | | *Minimum Breaking Strength of Strand (lbs)* | | |
|---|---|---|---|---|---|---|
| *Nominal diameter of strand (in.)* | *Number of wires* | *Nominal diameter of coated wires (in.)* | *Approximate wt. of strand (lb/1000 ft)* | *Utilities Grade* | *High Strength* | *Extra High Strength* |
| 3/16 | 7 | 0.062 | 73 | — | 2850 | 3990 |
| 7/32 | 7 | 0.072 | 98 | — | 3850 | 5400 |
| 1/4 | 7 | 0.080 | 121 | — | 4750 | 6650 |
| 9/32 | 7 | 0.093 | 164 | — | 6400 | 8950 |
| 5/16 | 7 | 0.104 | 205 | — | 8000 | 11200 |

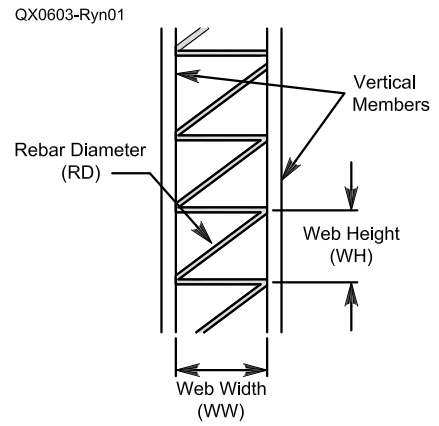


**Figure 1 — This drawing of a cross section of Rohn tower illustrates the dimensions needed for wind-load calculations.**

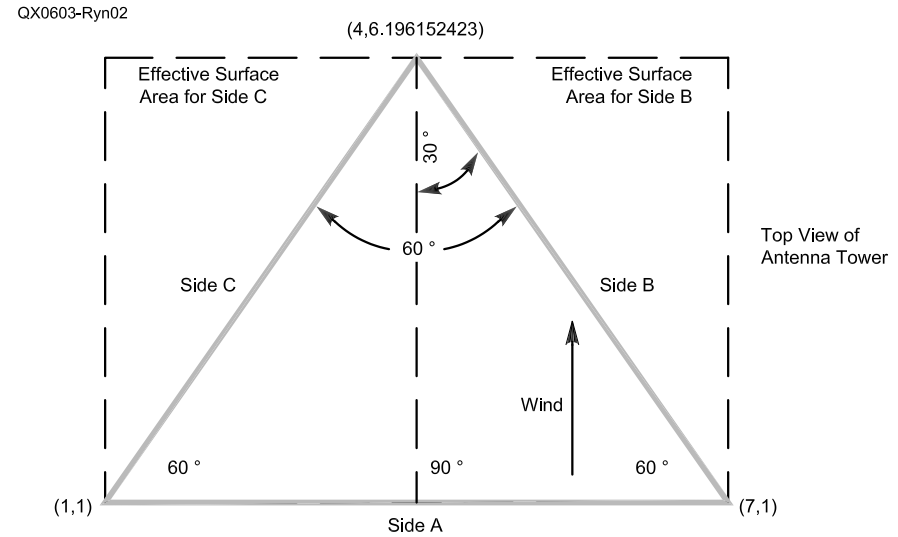


**Figure 2 — This drawing shows how the effective surface area of the tower legs affects wind loading.**

$V$ = Wind Speed (Velocity) (mph).
$P$ = Wind Pressure applied to antenna and tower (lb / ft$^2$).
$R$ = Radius of guy-wire anchors to tower base (ft).
$TT$ = Total transverse Torque due to wind (ft lb).
$Cd$ = Coefficient of drag.

*Analyses:*

1. Pressure developed on the antenna due to wind. (This analysis only deals with a steady wind.)

The Wirerope Works literature has an old publication that gives the pressure developed on square and round smoke stacks:[5]

$P = 0.0042 \times V^2$ (Square) and
$P = 0.0025 \times V^2$ (Round).

The equation for a round smoke stack is similar to one given in EIA-222-F for cylindrical surfaces.[6]

The force developed on one antenna element due to a wind that is perpendicular to the element, is given by $FA = A \times P \times Cd$.
Where:
$Cd$ = 1.2 for long cylinders (such as antenna beam elements). Re-writing:

$$FA = EL \times ED \times P \times Cd$$

2. Transverse antenna tower torque due to antenna force:

$$TA = M \times FA \times HA$$
$$TA = M \times EL \times ED \times P \times Cd \times HA \qquad \text{(Eq 1)}$$

Where
$M$ = the number of horizontal antenna elements.

3. Transverse antenna tower torque due to wind pressure on the horizontal members of the supporting web:

The number of webs, NW is determined by dividing the tower height by the web height.

$$NW = HT / WH$$

Each web cell has one horizontal element. See Figure 1.

The wind pressure on each horizontal web member is given by $P = 0.0025 \times V^2$

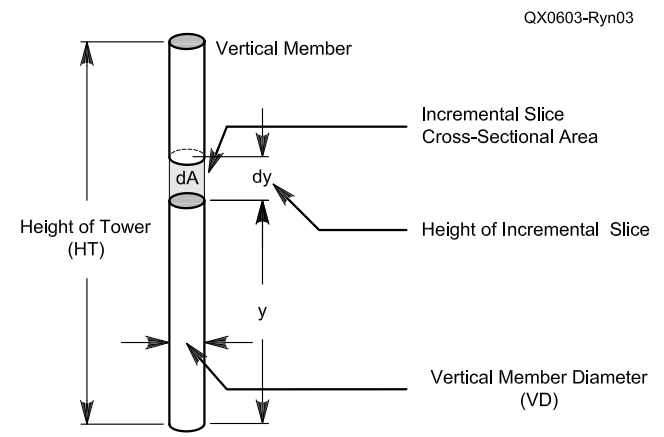


**Figure 3 — By calculating the wind loading on a small section of each tower leg and then adding all those effects for the full tower height, you can calculate the total wind-loading effects.**

The force on each web member due to the pressure is given by:

$FW$ = Area × Pressure × Coefficient of Drag = $WW \times RD \times P \times Cd$

The torque is the force times the lever arm, where each horizontal web member force is equal, but the lever arm (as measured from the antenna base), increments by the web height.

$$THWM = \sum_{1}^{NW} FW \times N \times WH = FW \times WH \times \sum_{1}^{NW} N$$

$$THWM = FW \times WH \times \frac{[NW \times (NW + 1)]}{2}$$

Figure 2 shows the sum of the forces generated on the two rear members is equal to the force on the member facing the wind.
Therefore, for three sets of webs,

$$THWM = FW \times WH \times [NW \times (NW + 1)] \quad \text{(Eq 2)}$$

4. Transverse torque due to wind pressure on the three vertical members:

Analyzing the torque due to one vertical member, Figure 3 illustrates the pressure on a single vertical member.

The incremental torque due to the wind pressure is given by:

$$dT = y \times dF = y \times P \times dA = \text{lever arm} \times \text{Pressure} \times \text{width} \times y$$

$$dT = y \times P \times VD \times dy$$

Where:
$y$ = Height from antenna base to an incremental area of the vertical member
$dF$ = An incremental force due to wind pressure on an incremental area of the vertical member
$dA$ = Incremental Area
Solving the above:

$$\int dT = \mathrm{T} = \int_0^{HT} y \times P \times VD \times dy = P \times VD \times \int_0^{HT} y \times dy = P \times VD \times \frac{y^2}{2}\Big|_0^{HT}$$

$$T = \frac{P \times VD}{2} \times y^2 \Big|_0^{HT}$$

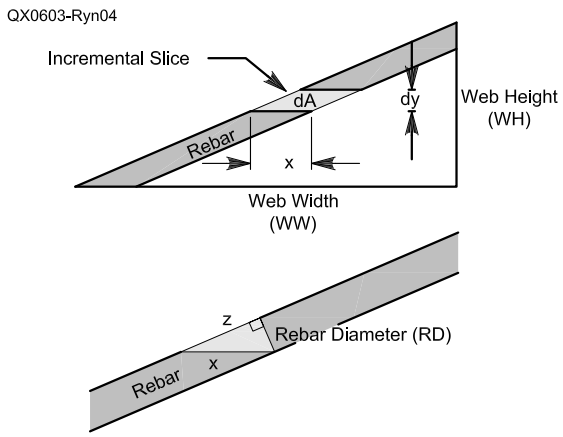


**Figure 4 — The diagonal cross braces between tower legs have an effect on wind loading. Again, you can add the effects on each small segment to calculate the total wind loading.**

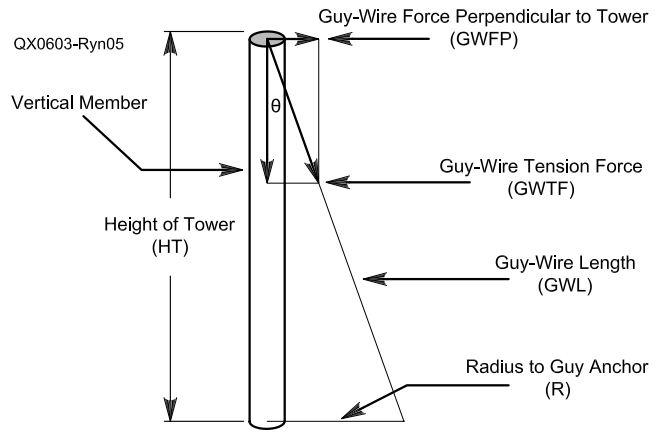


**Figure 5 — This diagram shows the horizontal and vertical forces exerted by the guy wires on the tower.**

**Table 2**

**Data Output From the Author's WIND_LOD.EXE Computer Program**

*For a Tower Height of 40 Feet and a Wind Speed of 60 mph*

| *X* | *Radius (ft)* | *Wire Length (ft)* | *Mast Angle (Degrees)* | *Ground Angle (Degrees)* | *Guy Tension (lb)* |
|---|---|---|---|---|---|
| 1 | 40.0 | 56.6 | 45.00 | 45.00 | 298.2 |
| 2 | 38.0 | 55.2 | 43.5 | 46.47 | 306.1 |
| 3 | 36.0 | 53.8 | 41.99 | 48.01 | 315.2 |
| 4 | 34.0 | 52.5 | 40.36 | 49.64 | 325.5 |
| 5 | 32.0 | 51.2 | 38.66 | 51.34 | 337.5 |
| 6 | 30.0 | 50.0 | 36.87 | 53.13 | 351.4 |
| 7 | 28.0 | 48.8 | 32.99 | 55.01 | 367.6 |
| 8 | 26.0 | 47.7 | 33.02 | 56.98 | 386.8 |
| 9 | 24.0 | 46.6 | 30.96 | 59.04 | 409.8 |
| 10 | 22.0 | 45.7 | 28.81 | 61.19 | 437.5 |
| 11 | 20.0 | 44.7 | 26.57 | 63.43 | 471.4 |
| 12 | 18.0 | 43.9 | 24.23 | 65.77 | 513.8 |
| 13 | 16.0 | 43.1 | 21.80 | 68.20 | 567.7 |
| 14 | 14.0 | 42.4 | 19.29 | 70.71 | 638.2 |
| 15 | 12.0 | 41.8 | 16.70 | 73.30 | 733.7 |
| 16 | 10.0 | 41.2 | 14.04 | 75.96 | 869.3 |
| 17 | 8.0 | 40.8 | 11.31 | 78.69 | 1075.0 |
| 18 | 6.0 | 40.4 | 8.53 | 81.47 | 1421.2 |
| 19 | 4.0 | 40.2 | 5.71 | 84.29 | 2118.8 |
| 20 | 2.0 | 40.0 | 2.86 | 87.14 | 4221.8 |

$$TVM = \frac{P \times VD}{2} \times HT^2$$

Where:
$P$ = K × $V^2$ (From Wirerope Works, Inc, Bethlehem Wire Rope Applications Notes)[3] and
$K$ = 0.0042 for flat stacks and 0.0025 for circular stacks.
For all three members,

$$TVM = \frac{3}{2} \times P \times VD \times HT^2 \quad \text{(Eq 3)}$$

5. Transverse torque due to wind pressure on the diagonal members of the supporting web:

The total torsional effect of discrete diagonal members of each web cell may be treated as a single long ribbon that extends from the ground to a height equal to the tower height. Figure 4 shows a cross-section of a diagonal rebar member. From that drawing we note that:

$$z^2 + RD^2 = x^2$$

$$z^2 = x^2 - RD^2$$

$$z = \sqrt{x^2 - RD^2}$$

Referring to a diagonal section of the webbing,

$$\frac{z}{WW} = \frac{RD}{WH}$$ Substituting

$$\frac{\sqrt{x^2 - RD^2}}{WW} = \frac{RD}{WH}$$

$$\sqrt{x^2 - RD^2} = \frac{WW}{WH} \times RD$$

$$x^2 - RD^2 = \frac{WW^2}{WH^2} \times RD^2$$

$$x^2 = \frac{WW^2}{WH^2} \times RD^2 + RD^2$$

$$x = RD\sqrt{\frac{WW^2}{WH^2} + 1}$$

However,

$$dA = x\,dy$$

$$dF = P \times dA$$

$$dT = y \times dF$$

$$dT = y \times P \times dA$$

$$dT = y \times P \times x \times dy$$

From the above,

$$dT = y \times P \times RD \times \sqrt{\frac{WW^2}{WH^2} + 1} \times dy$$

$$T = \int dT = \int_0^{HT} y \times P \times RD \times \sqrt{\frac{WW^2}{WH^2} + 1} \times dy$$

$$T = P \times RD \times \sqrt{\frac{WW^2}{WH^2} + 1} \times \int_0^{HT} y \times dy$$

$$T = P \times RD \times \sqrt{\frac{WW^2}{WH^2} + 1} \times \frac{y^2}{2}\Big|_0^{HT}$$

$$T = P \times RD \times \sqrt{\frac{WW^2}{WH^2} + 1} \times \frac{HT^2}{2}$$

For three sets of webs,

$$TDIAG = P \times RD \times \sqrt{\frac{WW^2}{WH^2} + 1} \times HT^2 \quad \text{(Eq 4)}$$

At this point, the total tangential torque is simply the sum of each of the individual torques:

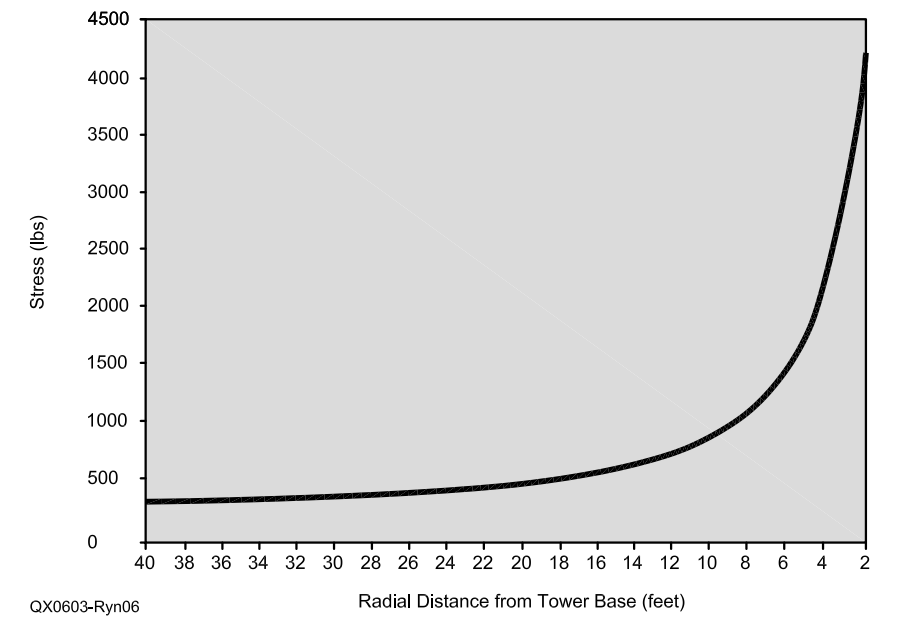


**Figure 6 — This graph shows the exponential increase in guy-wire stress as the radial distance from the tower decreases from a distance equal to the tower height.**

$TT = TA + THWM + \text{TVM} + TDIAG$

The perpendicular force applied to the top of the tower by a guy wire attached at the top may be calculated by recalling that the torque is equal to the product of force times lever arm:

$TT = GWFP \times HT$

Solving for the force:

$$GWFP = \frac{TT}{HT}$$

Figure 5 illustrates the guy-wire length calculation.

$$\text{Guy Wire Length} = GWL = \sqrt{(HT)^2 + R^2}$$

$\theta$ = Angle at top of tower between tower and guy wire

$$= \arctan\frac{R}{(HT)}$$

Also, to determine the guy-wire-tension force, *GWTF*:

$$\sin\theta = \frac{GWFP}{GWTF}$$

$$\therefore GWTF = \frac{GWFP}{\sin\theta}$$

This formula is incorporated into a computer program, *WIND_LOD.EXE* that enables the user to input wind speed, tower height, tower width and effective cross sectional area. The resulting output data consists of guy-wire tension versus various distances between the tower base and guy-wire anchor point. Table 2 is a sample of the output data.

Figure 6 is a plot of the data from Table 2, and is included to emphasize the importance of using an adequate spacing between the antenna base and the guy-wire-anchor location. The reader will note that the guy-wire stress increases exponentially as the spacing decreases. Some articles pertaining to guy-wire installation recommend that the minimum spacing be equal to or greater than 1/2 the antenna height, assuming that the guy wire is attached to the top. Referring to Figure 6, where the antenna height is 40 feet, you will note that for spacing of less than 20 feet, the stress begins to increase rapidly.

The author's computer program, *WIND_LOD.EXE* is available for download from the *QEX* file section of the ARRL Web page.[7]

**Acknowledgments**

Mr Norm Chipps made practical suggestions, Mr Jonathan Girard, Engineer, Rohn Products, supplied technical information. Mr Oscar Ramsey reviewed the text. Mr Tom Hughes and Mr Tom Secules of Wirerope Works, Inc kindly supplied technical information. Tim Klein of Wire Rope Corporation of America discussed technical aspects of wire rope.

[*Dr. Rynone is an Extra class radio amateur, WB2EIQ.* — Ed.]

**Notes**

[1]Wire Rope Corporation of America, **www.wrca.com**.
[2]R. Dean Straw, N6BV, ed, *The ARRL Antenna Book*, 20th Edition, p 22-6.
[3]Wirerope Works, Inc, **www.wwwrope.com**.
[4]R. Dean Straw, N6BV, ed, *The ARRL Antenna Book*, 20th Edition, p 22-7.
[5]*Guying of Stacks*, Wirerope Works, Inc.
[6]Kurt Andress, K7NV, *Mechanical Notes from K7NV, Wind Loads*, Array Solutions, **www.arraysolutions.com/Products/windloads.htm**.
[7]You can download the *WIND_LOD.EXE* program file from the ARRL Web at **www.arrl.org/qexfiles/**. Look for 3x06Rynone.zip.

□□

# An Accidental Discovery Put To Work

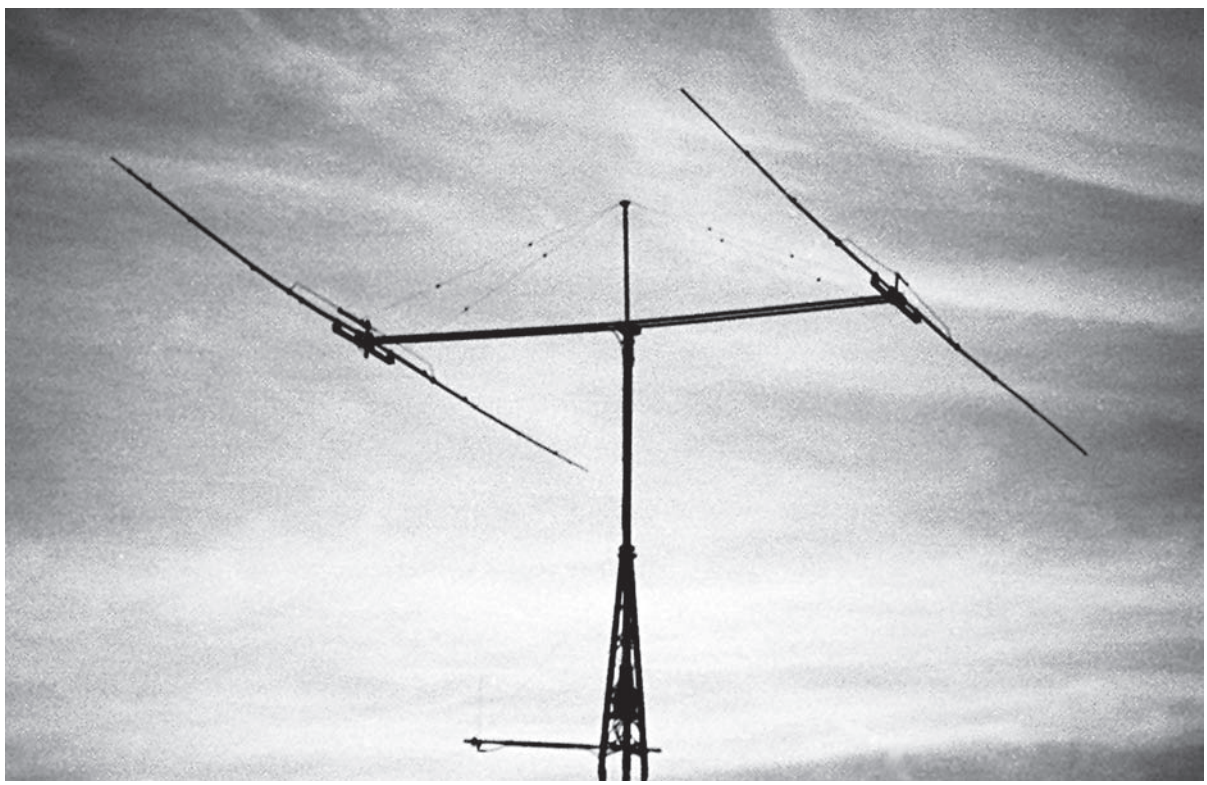

By Vidi la Grange, ZS1EL

*The author added 15-m performance to a monoband 20-m Yagi by using linear resonators. Learn how he built the resonators in this article.*

As a young physics student, I received my first ham license in 1956. A common student problem was that pocket money was not in abundance and I had to provide for both hobby and social activities. In this situation very delicate decisions had to be faced, especially when young ladies came into the picture. Vacation work at the Entomology Department of the University of Stellenbosch made it possible to buy a battered Hallicrafters SX-43 and a few pieces of surplus equipment, around which a CW transmitter could be built. Two bamboo poles held up the ends of a Windom antenna. DX contacts were few and far between but with some perseverance soon became great fun and provided for big thrills. It seems like only yesterday, I was listening with envy to other more established local operators, working DX with S9+ reports both ways. I could not believe that a Yagi made such a big difference compared to a wire antenna and dreams of having one of my own became stronger and stronger.

My heart nearly left my rib cage in one big beat the day my Elmer, Jack Snyman, ZS1OU, phoned to say that he would like to give me his old home-built Yagi. He no longer needed it, after buying a brand new, shiny, Moseley in a box! A copy of *CQ Antenna Roundup*, published in 1963 carried a detailed description of my new toy.[1] It was an ingenious antenna pioneered by Captain G. A. Bird, dubbed the "G4ZU Mini Beam." In the '60s and '70s, before

PO Box 301
Somerset Mall 7137
Republic of South Africa
**zs6al@mweb.co.za**

[1]Notes appear on page 50.

commercial trap Yagis appeared on the market, the G4ZU was a very popular triband Yagi, built by hams the world over. A commercial version was also available for a short while.

The design used a unique 3.5-m-long double boom. Parasitic element resonances on three bands were cleverly found by using a part of the twin boom, tuned in a trombone fashion. This section of the twin boom was automatically switched in and out by quarter-wavelength stubs made of 300-Ω line, depending on the operating band. The stubs were tucked conveniently into the boom, and to prevent their detuning by touching the boom, were threaded through corks like a string of evenly spaced beads. Living in the heart of South Africa's wine country at that time, corks were available in a big variety of flavors!

I was only able to really enjoy this antenna several years later, after finding a lightweight 12-m tower. As did many others, I soon discovered that the Mini Beam's major shortcoming was a serious lack of gain and directivity on 20 m. In contrast, performance on 15 and 10 m was quite remarkable.

In time, the poor performance on 20 m became more and more of an issue, especially when 10 and 15 m faded because of a low point in the sunspot cycle. Lots of time was spent to fine tune the switching stubs and accurately adjust the twin boom "trombones" in efforts to improve performance on 20 m. Before long quite a few short pieces of 300-Ω feed line cutoffs lay scattered around the antenna as proof of all my futile efforts. Had computers and modeling software been available in those years, a lot of time and 300-Ω line would have been saved and put to better use! It was great fun, nevertheless. After every attempted refinement I eagerly tested the antenna on the air, only to discover that it was still the same old story!

I finally decided that improved performance on 20 m was only possible by changing the G4ZU into a two-element, 20-m monoband antenna, thereby sacrificing the two higher-frequency bands. A quick survey of what material I had available in the G4ZU showed that very little extra aluminum tubing was needed to make up the two full sized 20-m elements. The original boom had very solid element mounting brackets and it made sense to use it as is, for the monoband antenna. An attractive feature of this mounting method was that the elements were insulated from the boom and split at the center, ideal for experimental work. Once completed and back on the tower, this antenna performed streets better on 20 m compared to the G4ZU. I could at long last enjoy more consistent S9+ signal reports both ways and work the weak ones on the ever-faithful 20-m band. In many tests on the air, the front-to-back ratio was on the order of two S units and front-to-side rejection was like a deep, complete null.

Quite predictably, over some time, 15 m and 10 m started showing signs of activity again! For a while, having a monobander was not much of a handicap because there was always something to do on the 20 m band. However, listening to mouth-watering DX on 15 and 10 m, it became clear that I had to do something about the two higher-frequency bands. Wheels kept turning in my mind, searching for an idea to add at least one more band without resorting to traps, trombone tuning, 300-Ω switching stubs or adding interlaced elements.

Les Moxon's book, *HF Antennas for All Locations* contains a myriad of antenna ideas, many of which are still well known and widely used, even 20 years after this publication first appeared on Amateur Radio operator's bookshelves.

One of Moxon's concepts, which immediately reached out to me, was his "accidental discovery" that the addition of a linear resonator, resonant on 21 MHz had very little influence on a basic 14 MHz element.[2] So, I asked myself the question: *What is a linear resonator and how can I make it work for me?*

A linear resonator is an LC circuit consisting of a one-turn, rectangular-shaped, linear inductor, shown in Figure 1 as B - C - E - F, and having its resonating capacitor at D. Half of the inductor, B - F, is common to the basic element A - G. Resonance is therefore shared by the linear inductor and the basic element, thereby showing two distinct resonant frequencies. The basic element frequency is determined by its physical length A - G, and the second, higher resonance by the added LC circuit, B - C - D - E - F.

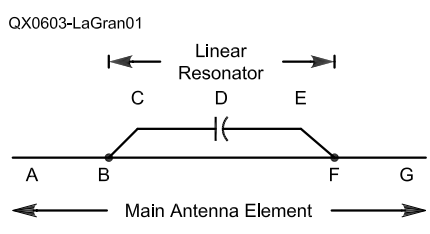


**Figure 1 — This drawing illustrates the principle of a linear resonator, as described by Les Moxon in *HF Antennas for All Locations*.**

This means that a full-sized 20-m element can also be resonant on 15 m. The following very attractive features were realized immediately:

- Hardware needed for adding a linear resonator to an existing 20-m element can be lightweight and much simpler than any other method of adding a second band.
- An entire 20-m element would resonate on 15 m and not only 66% of it, had traps been used to isolate the unwanted parts of the element.
- No interlaced elements were needed to clutter, or add wind resistance to a lean, two-element Yagi.

Les Moxon refers to linear resonators in more than one chapter of his book but he does not give much detailed guidance for building and adjusting them. Despite this, and no matter how sketchy the notes were, I could not wait to build a first test set up.

Geared with a full-sized two-element 20-m Yagi, a length of 4-mm OD aluminum rod and an absorption dip meter for checking resonances, I tackled this new approach with a great deal of enthusiasm. But, in the back of my mind was the memory of all the futile experiments with the G4ZU, which reminded me that this could turn out the same way.

To describe the building of a dual-resonant Yagi using linear resonators, let us take the reflector as an example.

### Basic Element

The basic element (A - G in Figure 1) is made of aluminum tubing tapering from 25-mm OD in the middle to 19 mm at the tips, with a total length of 11 m. Mounting of the element can be plumbers delight in theory, but I preferred insulated element-to-boom mounting, so that I could measure its resonance and make adjustments if needed during early experiments.

### The Inductor

The linear resonator inductor consists of two 4-mm OD aluminum rods of 1.2-m length each, B - C - D and D - E - F respectively, in Figure 1. They are mounted in line and parallel to the main element. Figure 2 shows one half of a resonator and its connection to the main element. One rod connects to the left and its mirror image to the right of the basic element, spaced at a

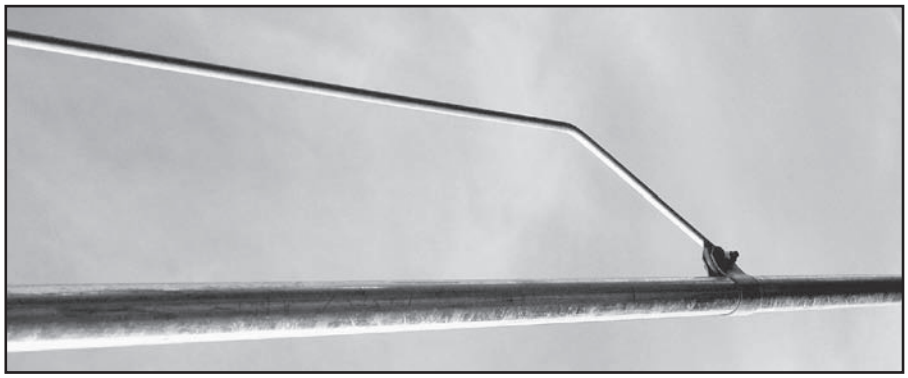

**Figure 2 — This photo shows one of the linear resonator rods attached to the main antenna element.**

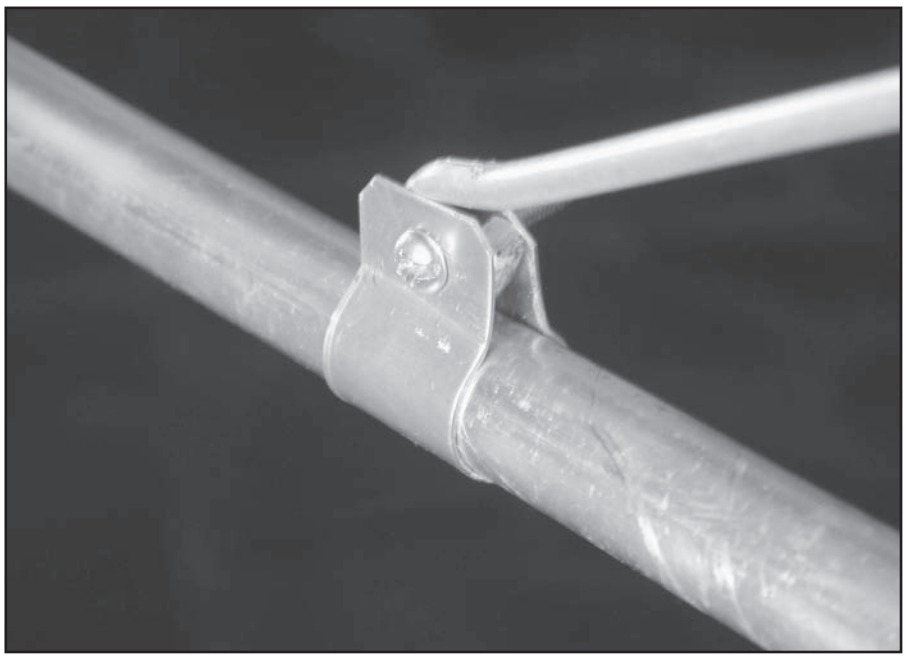

**Figure 3 — Here is a close-up view of a mounting clamp and resonator rod.**

**Figure 4 — This photo is a close-up view of the sliding coaxial capacitor.**

vertical distance of 100 mm from the main element. At point D in Figure 1 there is a gap of 20 mm between the left and right-hand rods, bridged by the adjustable tuning capacitor described later. At this position an insulated support made of clear plastic keeps the left and right rods in position. The far ends of these two rods are mounted to the main element by bending the last 150 mm of each rod at 45° towards the element.

A small loop at each bent-down tip provides a mechanical and electrical anchor point to the main element. Clamps bent out of 20-mm-wide aluminum strip and 4 mm × 15 mm stainless steel hardware secures each linear resonator tip to the elements, as shown in Figure 3.

### The Capacitor

A coaxial type capacitor was devised, which had the necessary adjustment range and is ideally suited for this application. It is positioned in the middle of the linear inductor, supported by the plastic insulator mentioned earlier.

The dielectric is a 300-mm length of clear automotive fuel pipe, which passed the microwave test. This fits snugly over the end of one of the rods, say the left, thereby forming the inner electrode of the coaxial capacitor. The outer electrode consists of a 16-mm OD aluminum tube, 250 mm long and having a 1.2-mm wall thickness. This slides over the dielectric like a sleeve. A grub screw at the right end of this sleeve provides mechanical and electrical connection to the right hand rod, shown in Figure 4. An exploded view of the capacitor is shown in Figure 5.

By moving this sleeve from left to right, capacitance varies over a sufficient range. Minimum capacitance is with the sleeve moved to the extreme right shown in Figure 6 and maximum capacitance has the sleeve to the extreme left, as shown in Figure 7. The grub screw locks the sleeve securely in any particular position when the correct setting is found. The dielectric has a wall thickness of about 3 mm, which leaves a lot of space between the capacitor electrodes. This allows rain water ingress without any noticeable change in capacitance. It also allows movement in windy conditions. A few holes were made in the outer pipe for drainage. It is a good idea to seal off the ends of the dielectric with self vulcanizing tape.

### Tuning the Resonator

With the linear resonator in posi-

tion on the 14-MHz reflector, the next step is to fine tune it to 20.5 MHz. This is, according to literature, the rule-of-thumb resonant frequency of a 15 m reflector. Armed with a dip meter, this is where the fun starts! Checking resonance of the linear resonator at first will probably be a bit tricky, but the sweet spot will be found near either extreme of the linear resonator, in the area of the 45° bends. See Figure 8.

### Checking Resonance of the Main Element

According to Les Moxon, the basic resonance of the element is not affected by the addition of the linear resonator. Since I had a split element to start with, verification of this was fairly simple. A single-turn loop made of heavy aluminum wire was placed over the 20 mm gap between left and right halves of the main element at the element to boom mounting bracket. The dip meter coupled to this loop confirmed that the basic resonance of the element was not affected by the linear resonator. This step was therefore omitted in further applications.

### Confirming Resonances with Modeling Software

After antenna-modeling software became available, the configuration and resonances of the 20 and 15-m elements were verified. Figure 9 is an *EZNEC 3.0* SWR plot. The following interesting facts came to light:

- The second resonance of a basic element obtained by addition of a linear resonator has to be at least 40% higher than the basic element resonant frequency. For example, efforts to tune a 14-MHz element to 18 MHz were not possible, while 21-MHz resonance could be found without any problem. This phenomenon has to be recognized in other applications.
- The LC ratio and shape of a linear

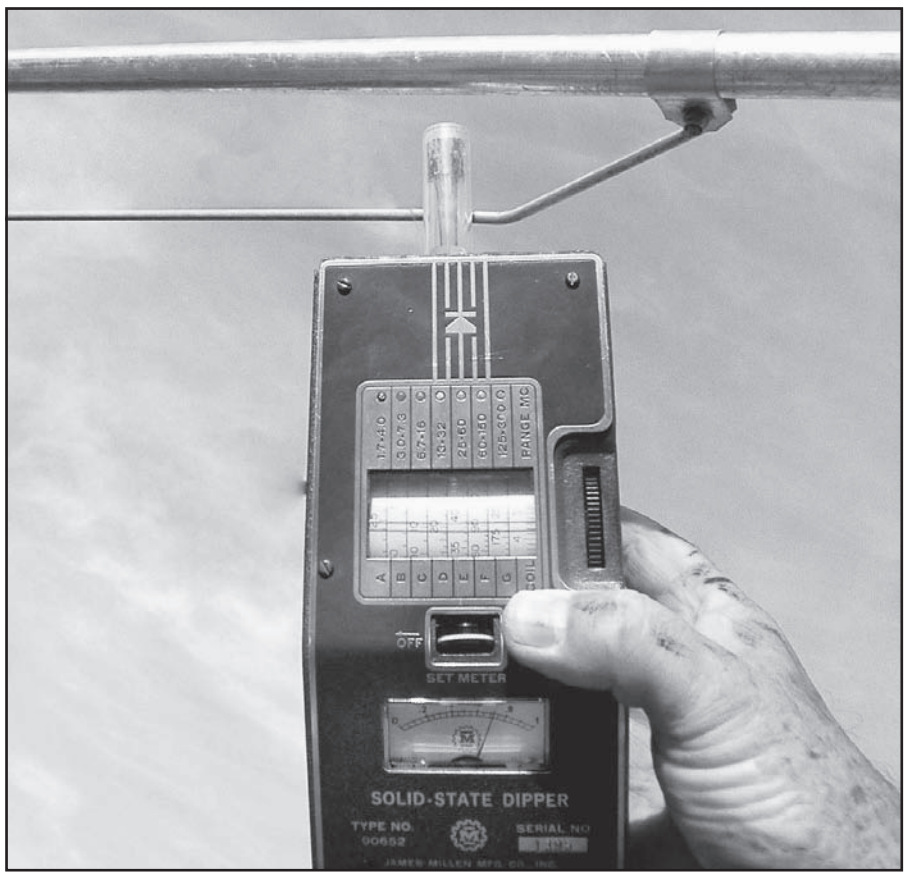


**Figure 8 — Use a dip meter to adjust the capacitor for the desired operating resonance.**

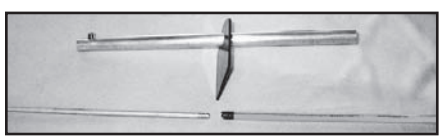

**Figure 5 — The capacitor pieces are laid out ready for assembly. The plastic spacer is on the outer-sleeve tubing and will also attach to the main antenna-element tubing.**

**Figure 6 — In this case the capacitor is set for minimum capacitance, with the outer sleeve pulled back as far as possible.**

**Figure 7 — Here the outer sleeve of the capacitor is pushed fully on to the inner section for maximum capacitance.**

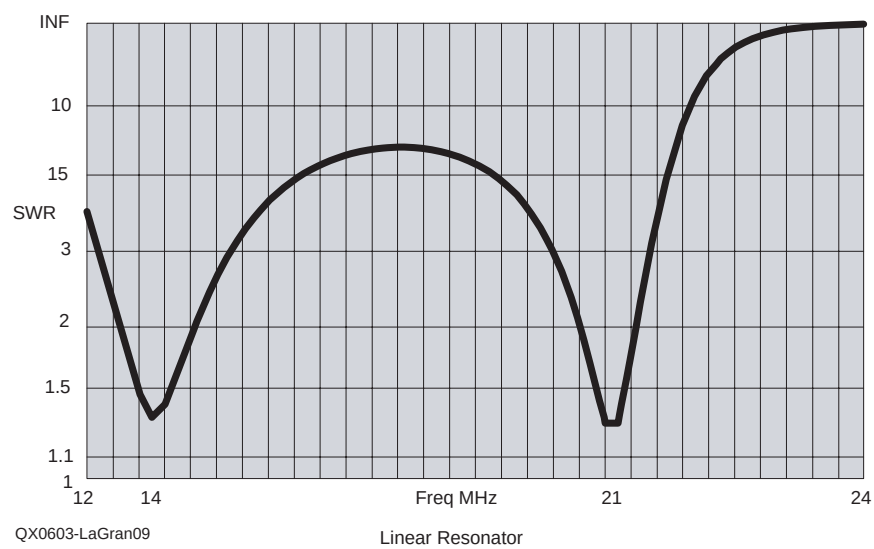


**Figure 9 — This graph shows the double resonance of the antenna, as predicted by the *EZNEC 3.0* antenna modelling software.**

resonator — for example the length C - E and the spacing from the main element B - C, as shown in Figure 1, is quite critical but can be verified by modeling software.

- The influence of a linear resonator on an existing element's normal resonance is negligible. If anything, it might drop the basic element resonance slightly due to inductive center loading.

**Feeding the Yagi**

Construction of the driven element was similar to that of the reflector and was split at the center. A 6-turn coil of 50-Ω coaxial cable was used as an RF choke at the feed point, with pigtails of about 75 mm per side connected to the left and right-hand halves of the main element.

Matching was checked by measuring SWR close to the driven element while the antenna was supported 3 m above ground in a temporary test set up. Fine tuning of the element length and adjustment of the resonating capacitor made it possible to obtain a match of better than 1.3:1 SWR at band centers. There was a frequency range of roughly 800 kHz between 2:1 SWR points.

**On-the-Air Performance**

During several years of use and reports from numerous DX stations, I found that the forward gain was similar to, or marginally better than commercial three-element trap triband Yagis used by friends in the neighborhood. The side-null on the dual band antenna was very deep but the front-to-back ratio was not as dramatic as in the case of a commercial trapped tribander. The general average F/B ratio was 2 S units, although under certain conditions much greater ratios were found. As a matter of fact I found it a bonus to be able to be more aware of what is going on "behind" me while the two sharp side nulls were sufficient to eliminate strong QRM.

Reflecting back on my many years as an Amateur Radio operator, the influence of people like my Elmer, ZS1OU, the G4ZU Mini beam and Les Moxon's "accidental discovery," this very successful two-element Yagi for 20 and 15 m is an outstanding example of a young ham's dream come true, albeit several decades later.

**Notes**

[1] *CQ Antenna Roundup*, Cowan Publishing Corp, 1963.

[2] Les Moxon, *HF Antennas for All Locations*, RSGB, 1993, p 134.

*Vidi la Grange, ZS1EL, ZS6AL and K1VL was born in George, South Africa on 24 May 1936.*

*He studied at the University of Stellenbosch and graduated with a degree in Physics in 1961. He obtained his first Amateur Radio call sign, ZS1AL, during that time. His interests in Amateur Radio centered mainly around experimental antenna work and building of various pieces of station gear. His favorite mode of operating is CW and he has been member of the First Class CW Operators Club (FOC) since April 1960.*

*He worked as a Research Officer at the Johannesburg Satellite Tracking and Data Acquisition Facility. Here, data was collected for various research projects conducted by NASA in the early days of space research. Vidi gained a lot of practical electronic knowledge and experience during this part of his career.*

*In 1972 he accepted a position as Production Engineer at the South African Iron and Steel Corporation, at their steel rolling mill south of Johannesburg. While there, he obtained a further academic qualification in Management. Before retiring from the steel industry in 1994, Vidi held the position of Manager, Tin-plate Technology.*

*After retirement from the steel industry, he accepted a position as Quality Systems Manager at a company producing plastic and resin automotive components. He was instrumental in getting their first ISO 9001 listing in 1996.*

*During early 1994 Vidi met Hester, N4MPQ, on 20 m CW. She was living in Hendersonville, North Carolina at the time. After a rather lengthy DX romance, they were married in 1996. Vidi and Hester live in Somerset West, a village about 35 km from Cape Town, South Africa.*

*Recently, Vidi has spent time applying his years of practical experience in linear resonators to a Force 12, C3S antenna. The end result is very exciting because he managed to get true two-element performance on each of five bands. Details of this work may be subject matter for a follow-up article.* □□

# *Antenna Options*

By L. B. Cebik, W4RNL

### Wire and the HF Horizon: the Ys and Wherefores

The ½-λ dipole and its kin (the inverted-V, the quadrant, etc) are far more competent antennas than many folks give them credit for being. They provide good gain with a fairly wide beamwidth and are bi-directional. In fact, if we rotate a ½-λ dipole in 120° increments, we obtain full horizon coverage with only a small gain deficit in the pattern overlap region, as shown on the left in Figure 1. With an antenna tuner and parallel feed lines, we can use the antenna at higher frequencies. Up to about 1.5 times the resonant frequency, the beamwidth is still great enough to give us less than a 3-dB gain deficit in the pattern overlap region. See the right side of Figure 1. For full-horizon coverage with no more than a 3-dB gain deficit (about ½ S-unit), we need a half-power beamwidth of about 60° from each of the three antenna positions.

Now let's give ourselves a limitation. We shall take away the rotator and use wire for the dipole. We end up with a very inexpensive but fixed antenna. For full-horizon coverage, we shall need at least three dipoles at approximately 120° angles to each other. The question then becomes how to arrange the three dipoles. The arrangement must activate one dipole, leaving the other two inert or inactive. Figure 2 shows full-Y

1434 High Mesa Dr
Knoxville, TN 37938-4443
**cebik@cebik.com**

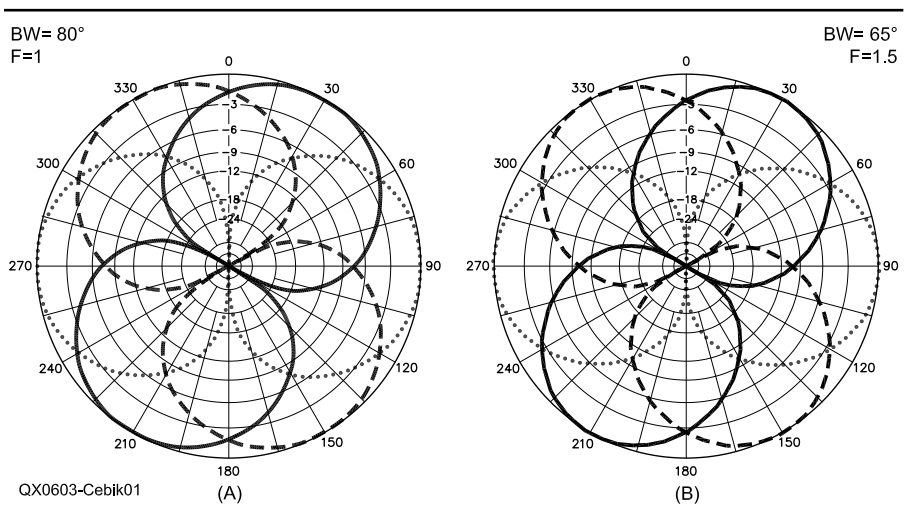


**Figure 1 — Ideal horizon coverage from three ½-λ dipoles at 120° angles to each other at the fundamental frequency (A) and at 1.5 times the fundamental frequency (B).**

and triangular (or delta, Δ) arrangements. The sketches assume that each dipole has a feed line, and that all feed lines are the same length. They run from the feed points to a central location. That location may be at the station equipment or a remote switch at the center of the arrays.

The full-Y array requires four supports, with one at the center and three for the far dipole ends. The triangle only needs three supports, since each support handles two dipole ends. However, if we wish to use the arrays at or very near to their resonant frequencies, we hit a snag in the form of very non-dipole patterns. Since the antennas are near their resonant frequencies on the lowest frequency of use, the two most obvious schemes fail us.

On the left in Figure 3, the full-Y array produces a bi-directional pattern with a narrow beamwidth. Interaction with the inactive dipoles produces north-south bulges and narrows the east-west pattern. In contrast, the inactive dipoles in the triangular array form reflectors to produce a spade-shaped pattern in one direction. In other applications, we might capitalize on this pattern, but for our project, it defeats the goal of covering the entire horizon. Most of the interactive effects disappear if the operating frequency is more than about 30% distant from resonance. However, that requirement would defeat our desire to have a three-dipole array that is highly usable on several ham bands and able to cover the horizon.

There are alternative array configurations that do not result in interactions of the type we obtain from the full-Y and delta arrays. In the 1930s, some operators used a half-Y formation. The Y was full, but each element was half of a dipole. Each half-dipole leg came together at a center point and each had one of the feed lines already connected. Hence, the array ended up with three feed lines. To select a dipole, we simply used two of the three lines. Many of these early operators used the antenna on a single band. Therefore, they created twisted triplets for the feed line. The close spacing and wire insulation on

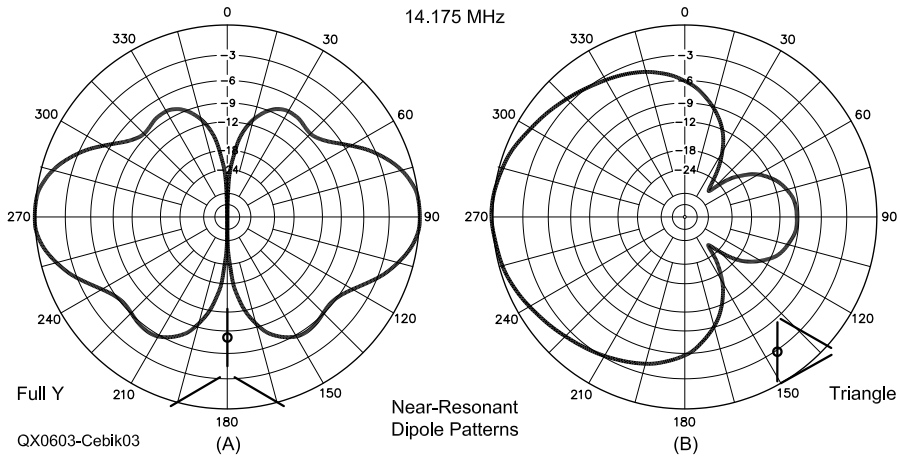


**Figure 3 — Radiation pattern limitations of the full-Y (A) and triangle (B) arrangements of dipoles resulting from interactions near dipole self-resonance. Antenna outline inserts are oriented correctly for the patterns shown. The active wire element has a circle indicating the feed point.**

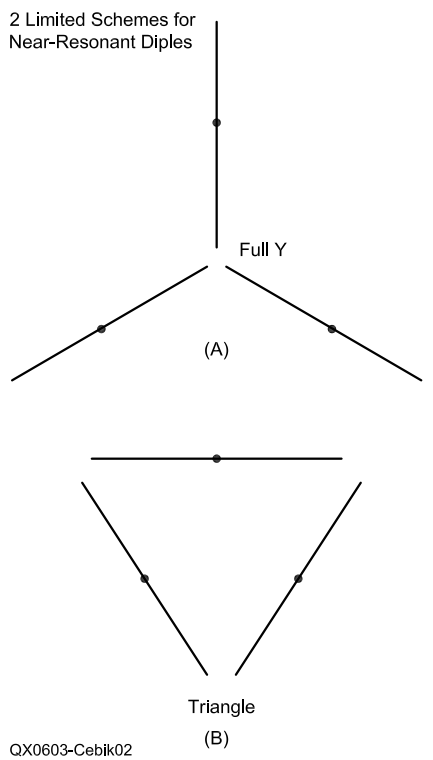


**Figure 2 — Full-Y and triangle arrays of dipoles. See Figure 3 and the text for limitations.**

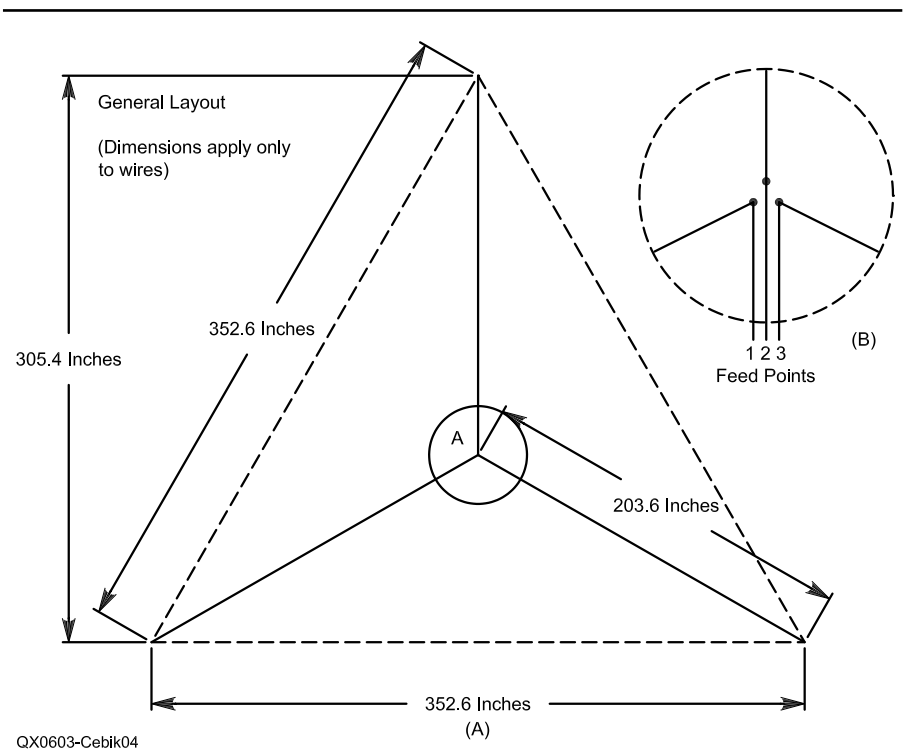


**Figure 4 — General outline (with wire dimensions) of a 20-meter Y-dipole array. The array is sometimes called the "half-Y" array, since each leg is ½ of a bent dipole. Part B shows the feed-point region and the triple feed line.**

the feed lines gave a reasonably constant and fairly low characteristic impedance for any wire-pair in the group. Determining the correct dipole to use simply required selecting the feed line pair that yielded the strongest signal.

Figure 4 provides an outline sketch of the wire portion of the array cut for 20 meters. The dimensions are overly precise, since we shall be using the array with parallel feed line and an antenna tuner. However, the dimensions are based on first resonating the dipoles in free space and then transferring those dimensions to a model over ground. Any equal wire lengths within a few inches of the values in the figure will work as well. Table 1 provides a recap of the critical dimensions, along with the dimensions of some other versions of the half-Y array.

The pair of wires that we select forms a dipole that is bent to include a 120° angle. Like any antenna with a slight V, we lose a bit of gain and some of the side null depth of a standard dipole. As shown in the top lines of Table 2, that gain loss relative to a standard dipole is under a half dB at 20 meters. However, in exchange for the maximum gain deficit, we obtain very workable patterns for many bands. The left portion of Figure 5 overlays patterns from 20 through 10 meters. The gain is remarkably consistent from one band to the next. Only on 10 meters do we find sufficient interaction between the two active wires and the inactive wire to produce a 0.9-dB front-to-back ratio.

Operation on 10 meters presses the array to its limits as a means of covering the entire horizon with three bi-directional patterns. The right side of Figure 5 shows the deeper nulls in the overlap region between maximum gain points. As well, there are other cautions to observe when using the half-Y array in multiband service. Table 4 lists some of the modeled performance figures, as well as indicating the bands most likely to yield excellent performance. Below 20 meters, we obtain an even broader beamwidth. However, the source impedance has a low resistance and a very high reactance. With the standard high impedance lines that we are likely to use for the array, this situation will likely result in a challenging matching situation for most tuners and introduce significant line losses. On 12 and 10 meters, the source impedance values reach levels that may challenge tuners in the other direction, depending upon the impedance components that exist at the terminals as a result of the line length and characteristic impedance. However, consistent operation on 20 through 15 meters — with 12 meters also a possibility — should be easy.

For the upper HF region, installing the half-Y should require only three supports, one at each dipole end. The triple feed line that forms an equilateral triangle as a cross-section can simply drop from the center point. If the curve that the line forms on its way to the shack entry is shallow enough, you can maintain equal-length lines along the entire feed line run. Under these conditions, you should not need significant retuning when switching from one pair of dipole legs to the next. Hence, a simple switching scheme should give instant recognition of which dipole pair yields the strongest signal.

There will be a temptation to use a center support and to place the feedline wires symmetrically around the support. This method will work if the support does not form a conductor or semiconductor. Trees and telephone poles notoriously change their conductive properties with the weather and the seasons. They can create losses along the line that take up much of the energy before it ever reaches the antenna. Unless the center support is certifiably non-conductive for the HF region in all weather, it may be better to offset the three feed lines from the support and to maintain sufficient

**Table 1**

**Dimensions of 20-Meter AWG No. 12 Dipole, Square and Rectangle Y-Arrays**

*Note: All dimensions in inches for AWG no. 12 copper wire. Multiply by 0.0254 for length in meters. See Figure 6 for abbreviations applied to a diagram of the square and rectangular arrays.*

| | *Dipole* | *Square* | *Rectangle* |
|---|---|---|---|
| Horizontal Length from Center (Hd, Hs, Hr) | 203.6" | 110.0" | 80.0" |
| Corner-to-Corner Length (Ld, Ls, Lr) | 352.6" | 190.7" | 138.6" |
| Perpendicular (Mid-Side to Apex: Pd, Ps, Pr) | 305.4" | 165.0" | 120.0" |
| Vertical Side Length (Ss, Sr) | —— | 220.0" | 278.6" |

**Table 2**

**Modeled Performance of 20-Meter Y-Arrays in Free Space and Over Ground**

*Free Space*

| *Array Type* | *Maximum Gain dBi* | *Beamwidth degrees* | *Source Impedance R ± jX Ω* |
|---|---|---|---|
| Dipole | 1.71 | 85 | 59.1 – *j*0.2 |
| Square | 3.02 | 88 | 99.2 – *j*0.9 |
| Rectangle | 3.75 | 87 | 49.3 – *j*0.8 |

*50' Above Average Ground*

| *Array Type* | *Maximum Gain dBi* | *Take-Off Angle degrees* | *Beamwidth degrees* | *Source Impedance R ± jX Ω* |
|---|---|---|---|---|
| Dipole | 7.05 | 19 | 88 | 58.9 + *j*5.6 |
| Square | 7.99 | 22 | 90 | 92.0 – *j*3.2 |
| Rectangle | 8.14 | 23 | 91 | 47.9 – *j*2.8 |

**Table 3**

**Modeled Dimensions of Y-Arrays for 20 to 10 Meters**

*Note: Dimensions given are for one leg. Correlate remaining dimensions via Table 1. H indicates the horizontal dimension for all versions, and S indicates the vertical side dimension for the loops. All dimensions derived from NEC-4 with a source impedance within 0.5-Ω of 20-meter version. All dimensions in inches: multiply by 0.0254 for length in meters.*

| *Frequency MHz* | *Dipole Hd* | *Square Hs* | *Ss* | *Rectangle Hr* | *Sr* |
|---|---|---|---|---|---|
| 14.175 | 203.6" | 110.0" | 220.0" | 80.0" | 278.6" |
| 18.118 | 159.2" | 86.2" | 172.4" | 63.0" | 218.0" |
| 21.225 | 135.8" | 73.7" | 147.4" | 53.7" | 186.5" |
| 24.94 | 115.5" | 62.8" | 125.6" | 45.7" | 159.0" |
| 28.4 | 101.4" | 55.2" | 110.4" | 40.1" | 139.2" |

distance to minimize interactions between the support and the lines.

The half-dipole Y is not the only possible form for the array. Ron Wray, WB5HZE, wrote to me about some interesting possible variations to suit his needs. Instead of using ¼-λ legs for each branch of the Y, he considered using half loops. In effect, the active pair of half loops would form a 1-λ quad loop with a 120° V. He also suggested that we need not replicate the isolation of the inactive element at the top or unfed point. The result would be a set of loops that had special advantages. First, for the same top height as the dipoles, they would yield additional gain. Second, a single top junction would simplify construction. Third, the entire array would occupy only half the lateral space required by the ¼-λ dipole legs. Finally, if a builder desired to use tubing or similar materials, a single center support could hold the entire array. See Figure 6.

I modeled the revised system and ended up with the dimensions shown in the remaining lines of Table 1 for a 20-meter version of Ron's antenna. In addition to the standard square loop, we can also form a rectangle with a 50-Ω impedance on the fundamental band. The table also shows the dimensions for such a loop, with reduced lateral spread. The rectangle is only 40% as wide as the version using linear dipole legs. However, it is significantly longer from top to bottom.

Table 2 shows the free-space and 50 ft modeled 20-meter performance data for the three versions of the half-Y array. The square and rectangular loop versions lose about a quarter dB relative to flat versions of those antennas. The loops both form in-phase-fed pairs of horizontal elements and show gain over the single dipole. As well, the loops show slightly higher beamwidth values. I chose a certain maximum height (50 ft) for the comparisons because that is likely to be the factor limiting most antenna builders. With a maximum top-wire height, the loops show slightly higher take-off (TO) angles than the dipole version, since the element with the feed point is lower than for the linear element antenna. For any loop, the height that determines the TO angle — when referenced to a single linear element — is about ⅔ of the way from the lower to the upper loop wire. (The same approximation applies also to stacks of Yagis.)

The source of the added gain for the loops on the fundamental frequency becomes apparent from Figure 7. The graphic overlays the elevation patterns for the three versions of the loop with the 50 ft top-wire height. The square loop shows considerable suppression of high-angle radiation due to the use of two wires, one above the other. As we move toward the rectangle, the horizontal portions of the antenna come closer to a ½-λ spacing, at which point, radiation toward the zenith would disappear. It is not possible to reach a full ½ λ and still have a loop. However, the 50-Ω rectangle has about 10 dB lower levels of zenith radiation than the linear dipole. As a result, there is more energy for the lowest lobe.

You may choose any fundamental band for a half-Y array in any of the three forms shown in these notes. Table 3 provides a starting point by giving the free-space resonant dimensions for the arrays using no. 12 copper wire as a

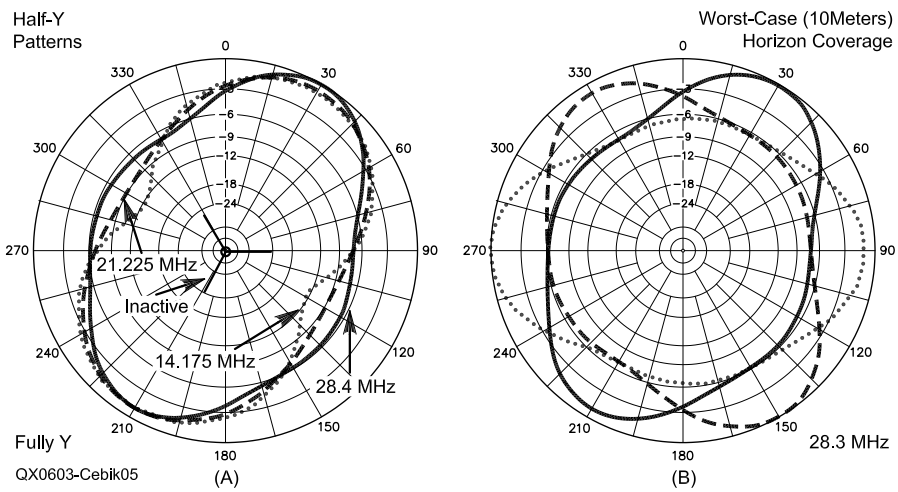


**Figure 5 — Typical (free-space) azimuth pattern produced by the Y-dipole array (A). Part B shows the worst case coverage on 10 meters. Primary-use bands extend through 12 meters.**

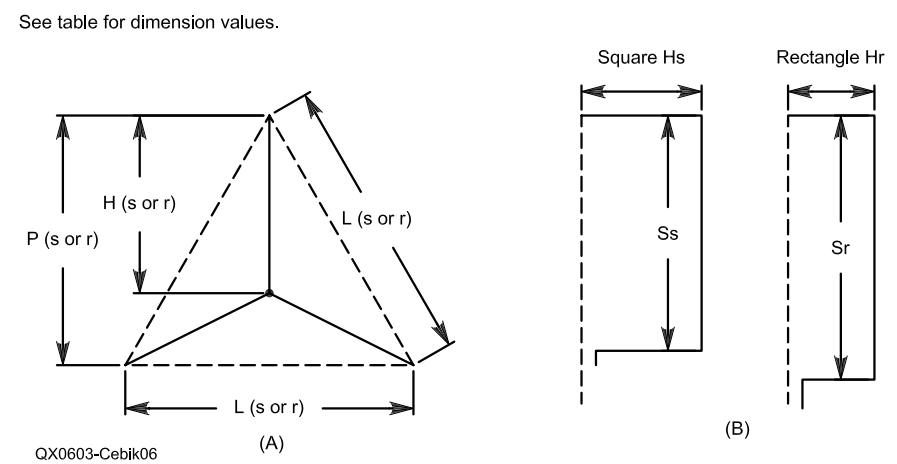


**Figure 6 — General layout for 20-meter Y-square and Y-rectangle arrays, originally suggested by Ron Wray, WB5HZE. See Table 3 for 20-meter wire dimensions.**

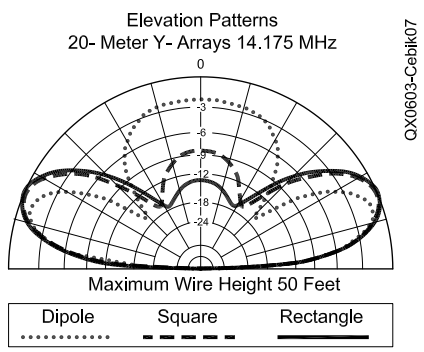


**Figure 7 — A comparison of elevation patterns for the dipole, square, and rectangle versions of the Y-array on 20 meters. Note the reduction of wasted high-angle radiation with the square and the rectangle at the selected top-wire height (about ¾ λ).**

material. Obviously, the higher the fundamental frequency of the loop, the easier it will be to form an array that requires only a single support. With some adjustment of the loop size, you can use tubular horizontals and wire vertical elements. You may also create a one-support structure by using a set of non-conductive horizontal supports with all-wire loops stretched between them. The variations are as unlimited as your creative adaptation of locally available materials.

Any of the three versions of the half-Y array will provide horizonal coverage on the primary bands because the unfed element is largely inert. The horizontal portions of the third element are at right angles to the active loop or dipole, despite the 120° V. Since the inactive element is also not fed, the current level remains near zero all along its length. Figure 8 shows an *EZNEC* portrayal of the relative current magnitude on the elements of both the Y-dipole and the Y-rectangle versions of the array on 20 meters, the fundamental frequency. Note that, for both versions of the antenna, the current level on the inactive element is completely insignificant, compared to the current on the active wires.

Table 4 provides the modeling data for all three versions of the array for a top-wire height of 50 ft above average ground. We have already noted the caution about operating the antennas at 30 meters, due to the low feed-point resistance and the high ratio of source reactance to resistance in all three antennas. For multiband operation, the dipole version of the half-Y array shows lower gain than the square and rectangular versions on 20 and 17 meters. However, the loop versions of the array lose any significant gain advantage on 15 meters. On 12 and 10 meters, the dipole array produces usable patterns, although the high feed-point resistance and reactance may present some antenna tuners with a challenge.

The loop versions of the Y-array show a steep decline in gain as the frequency climbs above 21 MHz. The situation is considerably worse on 12 and 10 meters than the gain values in the performance table indicate. Figure 9 shows the elevation and azimuth plots for the rectangular Y-array on both 15 and 12 meters. Similar patterns emerge for the square array and for the same set of reasons. At 21 MHz, the loops still show mainly broadside radiation, which is natural to a loop with a circumference in the vicinity of 1 λ. However, by the time the operating frequency reaches 24.94 MHz, the array is operating like a 2-λ loop, with strong radiation off the edges rather than broadside to the loop face. As a result of the change in operating conditions, the loop patterns show a very strong component directed straight upward as well as strong side-to-side radiation. In terms of total coverage of the horizon, the loop-based forms of the Y-array lose their utility as the loop circumferences grow to about 1.75 λ or larger.

The potential Y-array builder thus has to decide whether he or she wants more gain on 20 and 17 or the possibility of extended operation to include 12 and 10 meters. Since the final decision will likely also contain strong consideration of what will fit within a given antenna space and how many supports are available, I can only suggest careful planning before attempting to construct any version of the Y-array.

The planning should also include careful attention to the method of handling the triple feed line. If you plan the system as a monoband array, you can create your own twisted triplet of wires using well-insulated AWG no. 12 or larger wires. If you use good quality wire with one of the modern plastics for insulation, the feed line will likely have low — or at least acceptable — losses in the HF range. Do not use computer cabling, since the wires are likely too thin for even QRP power levels. The low-impedance line may not be a match for the source impedance, so you will still need a tuner. However, tuners built into modern transceivers may be all that you need to effect an adequate match.

For multiband use, the situation changes. Figure 10 shows the basic system of feeding the antenna with homemade transmission lines that have a relatively high characteristic impedance. With 1 inch spacing, AWG no. 12 or 14 wire will show close to 400 Ω as the characteristic impedance. It is possible to make periodic spacers from plastic discs. The goal is to hold all three wires in perfect alignment from the antenna source to the antenna tuner terminals or to some intervening switching system. If there is a center support, the wire-spacing disc can be the end portion of a larger piece of plastic material used to space the entire set of wires well away from the support. The plastic should have good RF properties in the upper HF region and be resistant to UV radiation. UV-protected polycarbonate is readily available from plastic supply houses and other sources.

If the run of line is fairly long and the spacers are anchored, you may also move the wire positions by one hole with

**Table 4**

**Modeled Anticipated Multiband Performance of Y-Arrays Resonant on 20 Meters for the Upper HF Amateur Bands**

*Note: All antennas have a maximum height of 50' above average ground and use AWG no. 12 copper wire. See Table 3 for dimensions. An asterisk (*) indicates the most usable bands. See text for cautions and exclusions.*

| *Frequency MHz* | *Max. Gain dBi* | *TO Angle degrees* | *Beamwidth degrees* | *Approximate Impedance R ± jX Ω* |
|---|---|---|---|---|
| *20-Meter Dipole Y-Array* | | | | |
| 10.125 | 7.0 | 27 | 95 | 20 – *j*460 |
| 14.175* | 7.1 | 19 | 88 | 60 + *j*6 |
| 18.118* | 7.0 | 15 | 82 | 160 + *j*440 |
| 21.225* | 7.2 | 13 | 77 | 340 + *j*960 |
| 24.94* | 7.2 | 11 | 68 | 1900 + *j*2000 |
| 28.4 | 8.1 | 10 | 58 | 3200 – *j*1900 |
| *20-Meter Square-Loop Y-Array* | | | | |
| 10.125 | 6.5 | 29 | 98 | 85 – *j*1100 |
| 14.175* | 8.0 | 22 | 90 | 90 – *j*3 |
| 18.118* | 8.3 | 18 | 89 | 380 + *j*1200 |
| 21.225* | 7.5 | 13 | 106 | 3600 – *j*3200 |
| 24.94 | 4.3 | 10 | 117 | 220 – *j*540 |
| 28.4 | 3.3 | 9 | 116 | 270 + *j*180 |
| *20-Meter Rectangular-Loop Y-Array* | | | | |
| 10.125 | 6.2 | 30 | 99 | 50 – *j*1100 |
| 14.175* | 8.1 | 23 | 91 | 50 – *j*2 |
| 18.118* | 8.9 | 18 | 91 | 190 + *j*1200 |
| 21.225* | 7.3 | 14 | 113 | 2200 – *j*4700 |
| 24.94 | 3.3 | 10 | 146 | 150 – *j*560 |
| 28.4 | 1.8 | 9 | 106 | 190 + *j*140 |

each new spacer. Make each position shift in the same direction, either clockwise or counterclockwise, so that the resulting line has a stiffening twist along its total length. The ultimate goal is a set of three possible line combinations such that, when switching from one combination to the next, no antenna tuner changes are necessary. The result will be the ability to switch from one combination to the next to determine instantly which one produces the strongest signal. The strongest received signal normally indicates the best setting for the strongest transmitted signal.

You may switch the system manually or remotely anywhere along the line. The top portion of Figure 11 shows a simplified manual switching system suitable for use in the shack near the tuner output terminals. The numbered lines are the three wires from the loop or dipole halves. The lines marked A and B represent the two-wire parallel feed line from the switch to the antenna tuner. Because the impedance at the switch may be either very high or very low, use as large of a ceramic rotary switch (two-pole, three-position) as you can obtain, depending on the power that you plan to use. The terminals should be well spaced and heavy to handle either high voltage or high currents. You may add a third wafer to ground the inactive line. A metal enclosure is not necessary, but the entire assembly should adhere to all safety precautions concerning unwanted contact by either the operator or shack visitors.

The lower portion of Figure 11 shows the bare bones of a remote relay-controlled switching system. In the sketch, the normally closed contacts are upward to simplify the drawing. The relay control switch is in the shack, while the relays might normally live very close to the array feed points. The schematic does not show the normal reversed diode across each relay and the extensive use of bypass capacitors and other components needed to keep the relay control lines free of RF. Like the manual switching sections, the relays need widely spaced contacts to handle high voltage and large contact surface areas to handle high currents. The remote system allows the use of one of the commercial parallel transmission lines for the run from the switching box to the antenna tuner. The relay system requires careful weather proofing. I prefer a double-shell system, with weep holes well separated. If one shell has a hidden leak, the second shell sustains protection. Debug the relay housing(s) at least once or twice per season.

The half-Y array is not an answer to every upper-HF operating need. Its goal is to provide full horizon coverage for the general operator with limited space and a budget that does not include a rotator. Antenna and feed-line switching with less expensive components substitutes for an expensive and high-maintenance rotator system. One or another version of the antenna may be suitable for potential use on any of the HF amateur bands as the fundamental frequency.

The triangular or Y-array concept is adaptable to many variations. For example, if you have a need for diverse target areas rather than whole horizon coverage, you might consider a triangle of extended lazy-H antennas. With sufficient separation, you can create a switchable triangle of Lazy-H arrays targeted by the best compromise relative to the broadside pattern of each one. The extended Lazy-H uses 1.25-λ elements on the highest frequency of use, with ½-λ to $^5/_8$-λ spacing between the upper and lower elements. A perfect triangle is not necessary, so you can modify the broadside direction of each Lazy-H to accommodate the narrower beamwidth that gives you the higher gain. As well, the longer elements will be more immune to interaction with the inactive antennas. If you begin with 1.25-λ elements and a vertical spacing of $^5/_8$ λ at 10 meters, you can cover several lower bands with good patterns and significant gain before the array approaches the size at which interactions with the inactive wires create pattern distortions. The array trades beamwidth for gain, so full horizon coverage cannot be a goal. However, you can obtain good signal strength to up to six target communication areas.

Alternatively, especially for the lower bands, you can create triangles of vertical dipoles. By judicious switching, you can drive one dipole and let the other two form a set of reflectors. The leads to a central remote switch can comprise inductively reactive loads for the reflectors, to create the right amount of

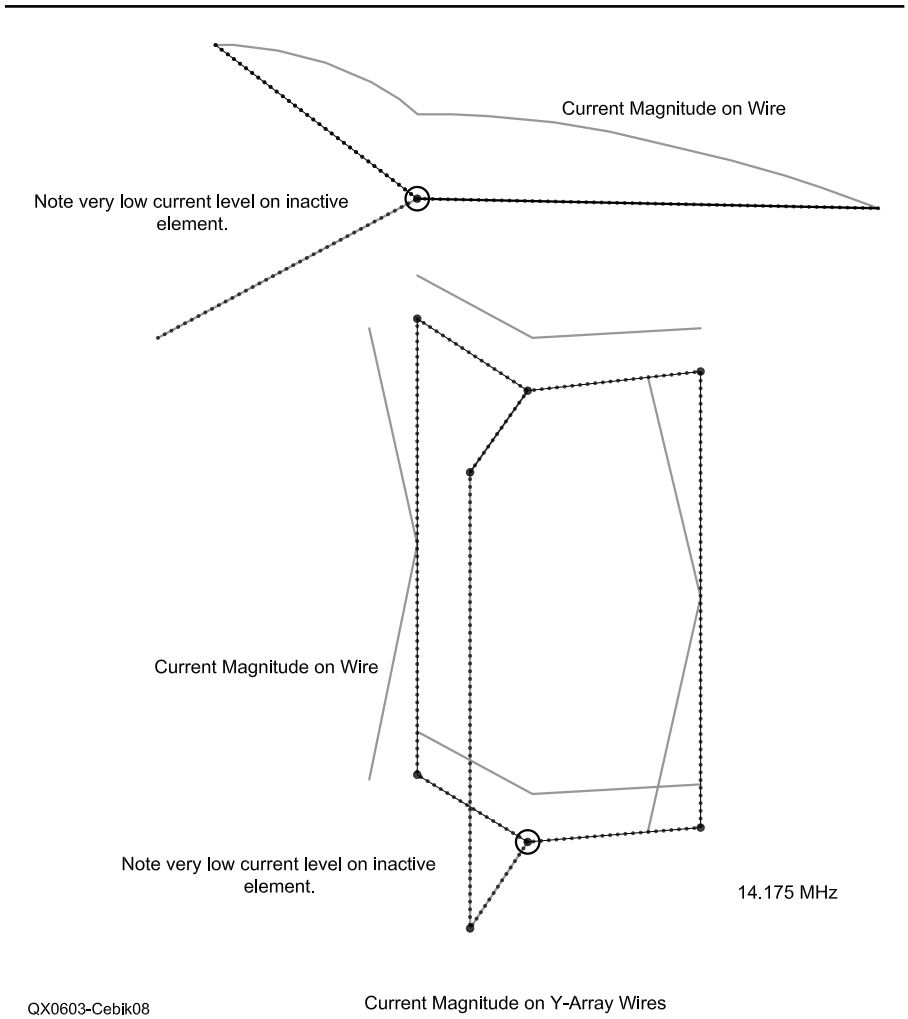


**Figure 8 — Relative current magnitudes on the active and inactive wires of a Y-array. Note the very low current magnitude on the inactive wires. The rectangular version has a common junction of top wires, and only the inactive lower wire is isolated from the active wires.**

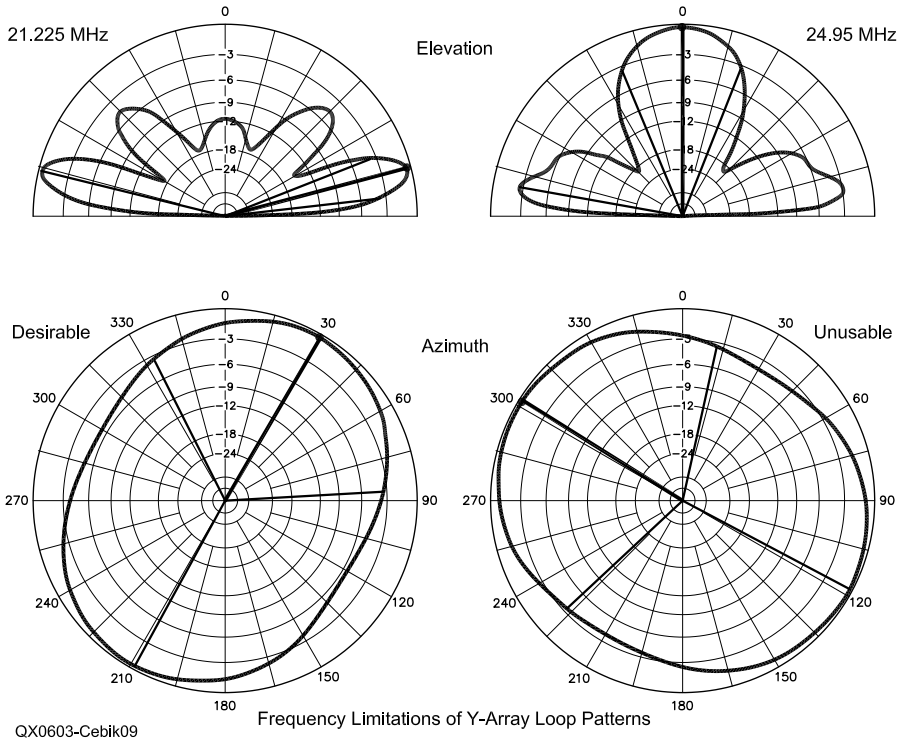


**Figure 9 — Elevation and azimuth patterns of the Y-rectangle array on 15 and 12 meters. The 15-meter pattern remains broadside to the loop face. The 12-meter pattern shows strong loop edge radiation, resulting in pattern changes in both plotting planes. The Y-square patterns are similar.**

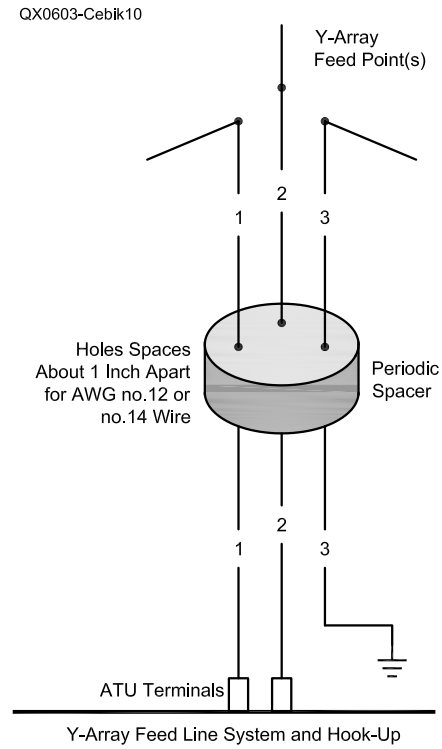


**Figure 10 — The general scheme for feeding a Y-array via an antenna tuner. The sketch shows that lines 1 and 2 are connected and active, with the inactive line (3) connected to an (optional but advisable) earth ground. See text and Figure 11 for possible switching schemes. Maintaining a constant spacing between the 3 feed-line wires is crucial to effective array operation.**

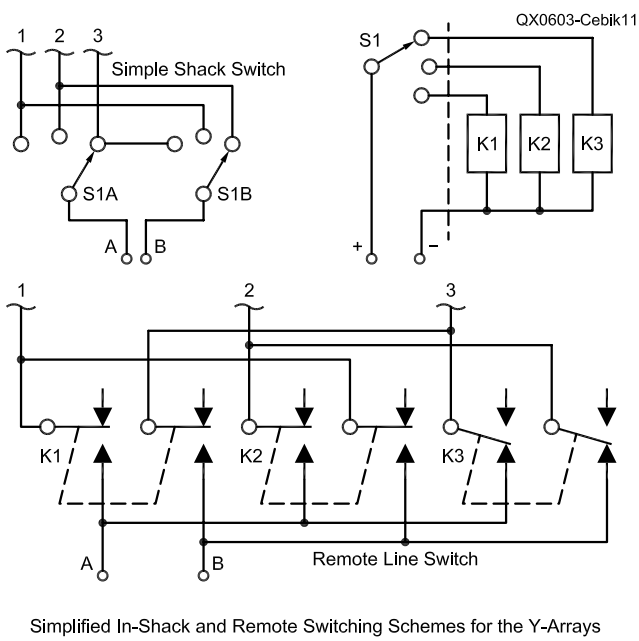


**Figure 11 — Simplified schematic diagrams for manual in-shack switching and for remote relay switching of the feed lines to select the active dipole. The diagram of the remote version does not show relay protection diodes and RF bypass capacitors for simplicity. Both schemes activate lines 2 and 3.**

lengthening for optimum parasitic reflector service. Vertical antenna patterns normally have a larger beamwidth than horizontal antenna patterns, and a 120° beamwidth is not difficult to obtain. Therefore, you can cover the entire horizon with just three vertical dipoles.

The Y-arrays and some of the possible triangles provide examples of what we can do with wire when faced with a limited budget and limited installation space. The basics for the arrays that we discussed have very old roots, but are ripe for re-use, refreshment, and contemporary adaptation to increase our antenna options. "Why" is a question, but for some operators, "Y" may be an answer.

[You can download the *EZNEC* antenna model files associated with this article from the ARRL Web at **www.arrl.org/qexfiles/**. Look for 3x06_Cebik.zip — *Ed.*] □□

# ARRL Handbook... 80 Years of Excellence!

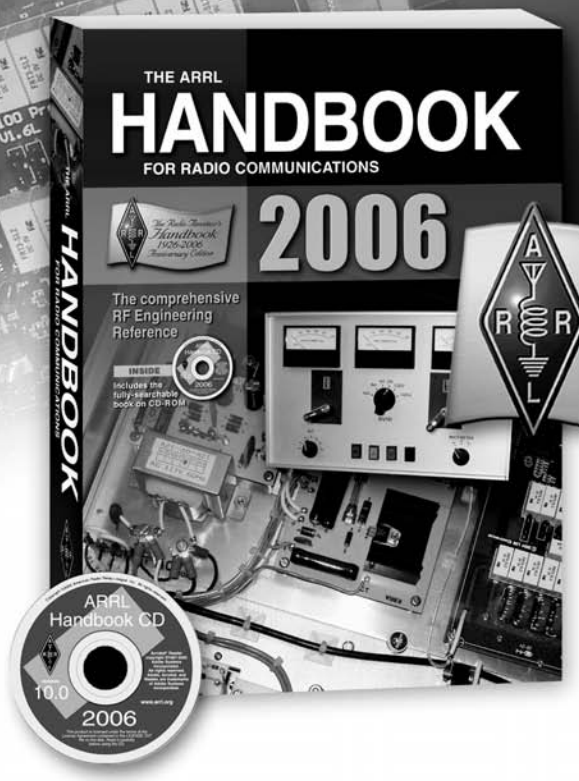


The Radio Amateur's Handbook 1926-2006 Anniversary Edition

Since 1926, generations of radio amateurs and experimenters have come to know **The ARRL Handbook** as THE standard in applied electronics and communications.

## About the 2006 Edition

**ALWAYS REVISED!** This 2006 edition builds on the extensive rewrite of the previous edition, and includes the most up-to-date theory, references and practical projects (including weekend-builds!) for receivers and transmitters, transceivers, power supplies, RF amplifiers, station accessories, and antennas.

**NEW HF AMP!** An impressive addition to **The ARRL Handbook** is a *brand-new*, high-power HF linear amplifier project using the new Eimac 3CX1500D7 power triode.

**CD-ROM INCLUDED!** This edition is bundled with **The ARRL Handbook CD (version 10.0)**—the complete and fully searchable book on CD-ROM, including many color images, additional software and reference material

**Order Today www.arrl.org/shop or Toll-Free 1-888-277-5289 (US)**

**Softcover.** Includes book and CD-ROM.
ARRL Order No. 9485 ..... **$39.95** plus s&h

**Hardcover.** Includes book and CD-ROM.
ARRL Order No. 9493 ..... **$54.95** plus s&h

Shipping and Handling charges apply. Sales Tax is required for orders shipped to CA, CT, VA, and Canada.

Prices and product availability are subject to change without notice.

### You get all this when you order:

- **The ARRL Handbook—2006 edition.** Up-to-date and always revised!
- **The ARRL Handbook on CD-ROM—version 10.0.** included with every book.

**ARRL** *The national association for AMATEUR RADIO*
225 Main Street, Newington, CT 06111-1494 USA

SHOP DIRECT *or call for a dealer near you.*
ONLINE WWW.ARRL.ORG/SHOP
ORDER TOLL-FREE 888/277-5289 (US)

## Complete Table of Contents

- Introduction to Amateur (Ham) Radio
- Activities in Amateur Radio
- Safety
- Electrical Fundamentals
- Electrical Signals and Components
- Real-World Component Characteristics
- Component Data and References
- Circuit Construction
- Modes and Systems
- Oscillators and Synthesizers
- Mixers, Modulators and Demodulators
- RF and AF Filters
- EMI/Direction Finding
- Receivers and Transmitters
- Transceivers, Transverters and Repeaters
- DSP and Software Radio Design
- Power Supplies
- RF Power Amplifiers
- Station Layout and Accessories
- Propagation of RF Signals
- Transmission Lines
- Antennas
- Space Communications
- Web, Wi-Fi, Wireless and PC Technology
- Test Procedures and Projects
- Troubleshooting and Repair

# Letters to the Editor

## RF Power Amplifier Output impedance Revisited (Jan/Feb 2005)

***Dear Sir:***

In my letter in the Mar/Apr 2005 issue of *QEX*, regarding Bob Craiglow's article, I referenced a simple mathematical proof that an RF power amplifier (RFPA) was conjugately matched with its load when *the load was adjusted to draw maximum power*. In his response in the May/Jun *QEX*, Bob dismissed this proof claiming I did not "…adequately model all the essential features of a nonlinear, non-time-stationary RF power amplifier." The quoted statement is true. I did not model **any** nonlinear features. But this is irrelevant. The proof is independent of any linearity arguments. The only assumptions required are that there is a maximum in the power-output-load resistance relation and that the output current be differentiable by the load resistance. The proof stands, and despite Bob's conclusions, RFPAs are conjugately matched with their load when the load is adjusted to draw a maximum power. See also the numerical calculations below.

Regarding the value of the equivalent source resistance, I now acknowledge that Bob is correct and that the equivalent source resistance for a PA operating with fixed bias is $R_S = \Delta E_p / \Delta I_{p1}$, given by the relation $2\pi r_p / (\theta + \sin\theta)$. The key to me was Bob's remark in private correspondence that $E_p$ should/could be regarded as the terminal voltage of a counter generator connected across the RFPA's output terminals. In this view, $E_p$ can clearly be taken as an independent variable and this eliminates my objection to his procedure in differentiating $E_p$ with respect to $I_{p1}$. For PAs operating with a fixed conduction angle, the equivalent source resistance is $2\pi r_p / (\theta + \sin\theta)$.

It is necessary to recognize that his equation (Eq B1) is correct in so far as it is a way to calculate the load current. In this equation, θ is a number. It is the operating angle of the RFPA. It is a parameter, not a variable.

The following results of numerical calculations illustrate these points. For these calculations I have taken $\mu E_g = 14.1493$ V, $\mu E_{bco} = -5.0$ V ($E_{bco}$ is the bias beyond cutoff), $r_p = 1.0\ \Omega$ and the operating angle at maximum output as 120°.

**Calculated RFPA characteristics, $P_{max}$ at θ = 120°.**

| θ | $R_S$ | $I_{p1}$ | $E_{p1}$ | $R_L$ | Power |
|---|---|---|---|---|---|
| 126.71 | 2.0852 | 2.5017 | 3.0 | 1.1992 | 3.753 |
| 123.99 | 2.0991 | 2.2627 | 3.5 | 1.5468 | 3.960 |
| 120.00 | 2.1224 | 1.9550 | 4.1493 | 2.1224 | 4.056 |
| 117.58 | 2.1382 | 1.7904 | 4.5 | 2.5134 | 4.028 |
| 113.75 | 2.1662 | 1.5880 | 5.0 | 3.2093 | 3.895 |

The output power is a maximum when the load resistance equals the source resistance. The RFPA is conjugately matched to its load at the load drawing maximum power.

In the immediate vicinity of the maximum power the RFPA is represented by a Thevenin equivalent circuit with an open circuit potential of 8.298 V and a series resistance of 2.1224 Ω.

However, the source resistance is not constant and the variation becomes appreciable for large changes in the load resistance, although on a plot of $E_p$ against $I_{p1}$ the deviation from linearity is difficult to identify.

Regarding Bob's Appendix C, his conclusion that if a test signal were phase displaced the source impedance would be reactive, leads to an impossible situation. If Bob is thinking (or perhaps if I am thinking that he is thinking) he will measure the impedance with a test signal with $\alpha = 0.0$, I will need a pure resistance to draw maximum power. But if he is thinking of making the measurement with a signal where $\alpha \neq 0$, I need a reactive load to draw maximum power. I note also that the magnitude of the source admittance changes with α, even when purely resistive.

For example at α of 0.0° and 90° the measured impedances, both resistive, are 2.1224 $r_p$ and 5.1151 $r_p$. Changing the phase of the test signal has changed the "source resistance" by a factor of more than two, with no change in the amplifier! Further, this effect is independent of the magnitude of the test signal. Even an *infinitesimal* test signal with $\alpha \neq 0$ causes the source impedance to break into resistive and reactive components and to change in magnitude as above. Bob's conclusions in this area are wrong. — *Bert Weller, WD8KBW,* **sodiumflame @sbcglobal.net**

***Dear Doug,***

Bert and I now agree that the source impedance is defined as $Zs = -\Delta E_p / \Delta I_p$. We also agree that the output or source resistance is $R_s = 2\pi r_{p1} / [\theta + \sin\theta]$ for a PA with fixed dc bias,[1] and $R_s = 2\pi r_p / [\theta - \sin\theta]$ if the bias, $E_{bco}$, is adjusted so as to hold the conduction angle, θ, constant with changes in $E_g$ and $E_p$.[2] Call the first case *fixed* $E_{bco}$ and the second *fixed* θ. Finally we agree that, for a *fixed* θ design, the load resistance that maximizes the power output for a fixed grid drive voltage, $R_{Ld}$, equals $R_s$ and therefore gives a conjugate match.

However, for a *fixed* $E_{bco}$ design, Bert maintains that the load that maximizes the power output is still equal to the source resistance and therefore still gives a conjugate match. However, I maintain that maximum output always occurs at $R_{Ld} = 2\pi r_p / [\theta - \sin\theta]$, which does not give a conjugate match for this case. The derivation of $R_{Ld}$ in Appendix B gives the load for maximum power output as $R_{Ld} = 2\pi r_p / [\theta - \sin\theta]$, which depends only on the fixed parameters $r_p$ and θ and is therefore applicable to both *fixed* $E_{bco}$, and *fixed* θ designs.

Below is a table, identical to Bert's *fixed* $E_{bco}$ table, except that it investigates the region around a nominal load impedance of $R_{Ld} = 5.115\ \Omega$ instead of the region around to $R_S = 2.122\ \Omega$. The bias voltage required to adjust θ to 120° with $\mu E_g = 14.149$ V is now $\mu E_{bco} = -3.537$ V. The maximum power output for $R_L = R_{Ld}$ is 4.893 W instead of 4.056 W for $R_L = R_S$, as shown in Bert's table. This shows that the power output is 20% greater for $R_L = R_{Ld}$ than for a conjugate match ($R_L = R_S$).

**Calculated RF PA characteristics.**

| θ | $R_S$ | $I_p$ | $E_p$ | $R_L$ | $P_{out}$ |
|---|---|---|---|---|---|
| 126.7 | 2.08 | 1.77 | 6.26 | 3.54 | 5.54 |
| 124.0 | 2.10 | 1.60 | 6.62 | 4.13 | 5.29 |
| 120.0 | 2.12 | 1.38 | 7.07 | 5.11 | 4.89 |
| 117.6 | 2.14 | 1.27 | 7.32 | 5.78 | 4.63 |
| 113.7 | 2.17 | 1.10 | 7.68 | 6.96 | 4.23 |

Bert's second criticism is that an RFPA's source impedance, $Z_S = -\Delta E_p / \Delta I_p$, cannot possibly be reactive. Certainly, $\Delta E_p$ is small and so is $\Delta I_p$ but this does not imply that their ratio is small. The instantaneous plate

[1]See Eq A1 with $E_{bco} = [E_c + E_b / m]$.

[2]See Eq A3 where the fixed bias term, $mE_{bco} = [mE_c + E_b]$, is replaced by Eq A2.

current, $i_p$, flows only during the conduction interval of $-\theta / 2 \le \phi \le \theta / 2$. Therefore, $\Delta I_p$ will tend to be somewhat in phase with $E_p$ and, if $\Delta E_p$ is not in-phase with $E_p$, $-D E_p / D I_p$ may have a reactive component.

The output admittance is $Y_S = G_S + jB_S = -\Delta I_p / \Delta E_t$ where $\Delta E_t = -\Delta E_p \cos(\phi + \alpha)$, $\Delta E_p$ is the magnitude of the test signal, and $\alpha$ is its phase relative to the ac grid voltage. For a *fixed* $E_{bco}$ design, the instantaneous plate current is given by Eq A1. When the small test voltage is added, the instantaneous current becomes $i_p = [\mu E_{bco} + (\mu E_g - E_p) \cos f - \Delta E_p \cos(\phi + \alpha)] / r_p$. Therefore the change in the instantaneous current is $\Delta i_p = -[\Delta E_p \cos(\phi + \alpha)] / r_p$. The corresponding change in the fundamental ac component of current, that is in-phase with the test voltage, is

$$\Delta I_{p_r} = 1/\pi \int_{-\theta/2}^{\theta/2} \Delta i_p \cdot \cos(\phi + \alpha) \cdot d\phi$$

so that

$$\Delta I_{p_r} = -\Delta E_p [(\theta + \cos(2\alpha)\sin(\theta)] / [2\pi \cdot r_p]$$

Therefore the conductance is $G_S = -\Delta I_{pI} / \Delta E_p = [\theta + \cos(2a) \sin(\theta)] / [2\pi r_p]$.

Similarly, the quadrature component of ac current, relative to the phase of the test voltage, is:

$$\Delta I_{p_o} = 1/\pi \int_{-\theta/2}^{\theta/2} \Delta i_p \cdot \sin(\phi + \alpha) \cdot d\phi$$

so that

$$\Delta I_{p_o} = -\Delta E_p [(\sin(2\alpha)\sin(\theta)] / [2\pi \cdot r_p]$$

Therefore the suseptance is $B_S = -\Delta I_{pQ} / \Delta E_p = [\sin(2\alpha) \sin(\theta)] / [2\pi r_p]$.

Most published RFPA analyses are for *fixed* θ designs while implementations are normally *fixed* $E_{bco}$ designs. It appears possible, at least in theory, to design a *linear*, class C, SSB, RFPA with a *fixed* θ design, using a grid bias control circuit based on feedback of the RF output envelope voltage. This appears to offer an opportunity to design a high efficiency, linear, class-C SSB PA.

*— Bob Craiglow,* **craiglowrl@juno.com**

***Gentlemen,***

I'm glad to see new information in your debate but theories need testing for confirmation. That's what we've lacked for the last several years.

Certain assertions previously advanced on these pages remain unchallenged and unconfirmed. They include:

1. Resistive load-variation testing cannot confirm a conjugate match because a magnitude-only measurement at the load measures only the magnitude of an amplifier's source impedance. That type of test can refute a conjugate match, however. (W. Bruene, W5OLY, "Letters to the Editor," *QEX*, Jan/Feb 2001, pp 59-61.)

2. Resistance in an amplifier's source impedance implies the conversion of energy from one form to another. Absent radiative effects, only an ohmic resistance that converts electromagnetic energy to heat can explain that resistance. The question is: Is a measurement of an amplifier's s22 (output reflection coefficient) equivalent to a measurement of its source impedance? Or is it a measurement of the conjugate of its optimal load impedance? (D. Smith, KF6DX, "Resistance — The Real Story," *QEX*, Jul/Aug 2004, pp 51-53.)

3. The establishment of the ratio of voltage to current at a source is an indication of the load impedance and not necessarily of the source impedance. Example: A 3-W night light might be plugged into a 120-V ac wall outlet. That ratio V / I is much more than that of a 3-kW amateur amplifier drawing its full current. Does that imply anything about source impedance?

I'd say it's time to lay it on the line *— Doug Smith, KF6DX,* QEX *Editor,* **kf6dx@arrl.org**.

**Quadrature Phase Concepts (Nov/Dec 2005)**

***Hi Doug,***

I felt uneasy about the conclusion that quadrature techniques cannot eliminate one sideband in a receiver. After all, the equivalent of Figure 2 is in fact frequently used to eliminate the unwanted sideband in direct-conversion receivers.

It seems that there is an error in how the 45° phase shift in the signal path (not the oscillator path) is taken into account. When a sine wave of frequency $f$, given by $\cos(2\pi ft)$, undergoes a phase shift, the result can be denoted by $\cos(2\pi ft + c)$, for some $c$. A positive phase shift corresponds to advancing time $t$, so a positive phase shift is represented by positive $c$ if $f > 0$, and negative $c$ if $f < 0$ — and conversely for a negative phase shift. KC7FHP, however, unconditionally represents a positive phase shift by a positive $c$ (first line of second column on page 21), even though the frequency here (in $F - O$) may be either positive or negative.

*— 73, Pieter-Tjerk, PA3FWM,* **pa3fwm@amsat.org**

***Hi Gary and Doug,***

In my opinion, the conclusions made in this article are wrong. Hundreds of amateur and professional realizations successfully use the phasing method to make SSB without passband filtering.

Here is the mistake, according to me:

[Eq 5] and [Eq 6] are actually only correct if $F - O > 0$, and Gary implicitly thinks that they remain the same when $F - O$ is negative. If $F - O < 0$, the equations in fact take another form. So when Gary says (p 21): "Assuming $F - O$ is positive or $F - O$ is negative, it doesn't matter…" It actually matters, because the equations are not the same in the two cases. This is why the demonstrations that follow are incorrect.

The fact that the equations are not the same for positive and negative frequencies comes from the Hilbert Transform properties, in which sign of frequency is of crucial importance. For example :

HT[cos(2 π F T)] = sin(2 π F T) if F > 0, and –sin(2 π F T) if F < 0

HT[sin(2 π F T)] = –cos(2 π F T) if F > 0, and cos(2 π F T) if F < 0

Note that in Figure 2, p 21, if Gary had made a difference instead of a sum at the end of the treatments, he would have obtained *zero*, and would have achieved what he wanted: eliminating part of the frequency spectrum! He speaks of "subtraction" in the modulator (p 20), but unfortunately not in the demodulator!

Thank you for this article. It was a good opportunity for everybody to dive deeply into Hilbert Transform theory!

*— 73, Christophe Bourguignat, F4DAN, 15, rue Poirier de Narçay, 75014, Paris, France*

**Source Coding and Digital Voice for PSK31 (Nov/Dec 2005)**

***Hi,***

I just read your interesting article on using PSK31 to transmit speech. In your system, unlike pure text-to-speech systems, you really do have access to the original accent, phrasing, and intonation information. You also have access to the timing info. In fact, the "time warping" goes to great length to remove this info, so it must be detecting it. Therefore, it doesn't seem unreasonable to encode some of this information with the signal, at some increase in bandwidth. One idea would be to have a special message that says "the next word is accented" or "the pitch curve slope is such-and-such" or "the playback rate slope is such-and-such." To determine how feasible this would be for the extreme

case of PSK31, a "thought experiment" such as you did would be required. Yet another idea for increasing fidelity would be to make a pitch range and spectral characterization of the source voice and transmit that as a header; this could be used to pick a synthesis voice that partially matches the original. At the very least it could be used to select between female and male voice synthesis.
*— Best regards, David A. Jaffe, K6DAJ,* **David.Jaffe@analog.com**

***Hi David,***

Thanks for your note. You're right that additional information could be transmitted to take care of the things you mention. I'm glad to see you're thinking about that. As you did, I also thought about transmitting information that would allow the synthesized voice to match the original. Of course, many methods exist for it that are well-documented.

Other neat things you can do with digital voice include: adding header information to CQs that indicates the interests of the caller, establishing store-and-forward operation phonegrams, which would be neat for soldiers overseas), interspersing image data and so forth. The ARRL regulation-by-BW proposal has something to say about all that, I think. Other ideas can be found in the reports of the ARRL Digital Voice Working Group, under Committee Reports from the last five years in the Announce territory of **www.arrl.org**.

As I've stated before, standards are firmly established only by their popularity, and not just by committees. It remains, therefore, for someone to get interested enough to start coding. I wish I had the time for it.
*— 73, Doug, KF6DX*

**Quantifying SETI (Jan/Feb 2006)**

One reader reports that he was referred to the following Web pages by author H. Paul Shuch, N6TX, to learn how to build an amateur SETI station and more: **www.setileague.org/editor/magic.htm** and **www.setileague.org/articles/minimeta.htm**. We're happy to pass those URLs along. *— Doug, KF6DX*

**Pspice for the Masses (Jan/Feb 2006)**

***Hi Doug,***

Just got the new issue — as usual, interesting. Though of no great consequence, the curve identifications in Figure 4 are reversed. Most readers will hopefully recognize this.
*— 73, Bob Hicks, W5TX,* **w5tx@w5tx.com**

**Tech Notes (Jan/Feb 2006)**

We want to clarify that in last issue's Tech Notes, Eq 5 is properly called the standard deviation of the mean. The standard deviation of the mean is an estimate of the standard uncertainty to be associated with the mean, or average, of a set of measurements or calculations. *— Ed.* □□

*In the next issue of*

QEX

Our Italian friends Paolo Antoniazzi, IW2ACD, and Marco Arecco, IK2WAQ, return with a study of helical feeds with disk reflectors for Phase-3E parabolic antennas at 2.4 GHz. They also look at Phase-5A, 10-GHz possibilities for future Earth-Mars communications. Extensive computer modeling is balanced by the authors' experience in microwave antenna construction. Don't miss this one! □□

# *Upcoming Conferences*

**40th Anniversary CSVHFS Conference, 27 – 29 July, 2006 Bloomington, MN (Across from the Mall of America) Call for Papers**

The Central States VHF Society is soliciting papers, presentations, and Poster displays for the 40th Annual CSVHFS Conference to be held in Bloomington, Minnesota (across from the Mall of America) on 27 – 29 July, 2006. Papers, presentations, and Posters on all aspects of weak-signal VHF and higher-frequency Amateur Radio operation are requested. You do not need to attend the conference, nor present your paper, to have it published in the *Proceedings*. Posters will be displayed during the two days of the Conference.

**Topics of interest include (but are not limited to):**

- Antennas, including modeling/design, arrays, and control.
- Construction of equipment, such as transmitters, receivers, and transverters.
- RF amplifiers (power amps) including single-band and multi-band vaccum tube and solid-state preamplifiers (low noise).
- Propagation, including ducting, sporadic E, and meteor scatter, etc.
- Test Equipment, including homebrew, using, and making measurements.
- Regulatory topics.
- Operating, including contesting, roving, and DXpeditions.
- EME.
- Digital signal processing (DSP).
- Software-defined radio (SDR).
- Digitial modes such as WSJT, JT65, etc.

Generally, topics not related to weak signal VHF, such as FM repeates and packet radio are not accepted for presentation or publication. There are always exceptions, however.

Please contact either the Technical Program Chairman, Jon Platt, WØZQ, or the *Proceedings* Chairman, Donn Baker, WA2VOI/Ø at the the e-mail addresses below.

The deadline for submissions for the *Proceedings* is Monday, **1 May 2006**. For Presentations to be delivered at the conference the deadline is Monday, **3 July 2006**. The deadline for Posters to be displayed at the conference is Thursday, **27 July 2006**. (Bring your poster with you!)

Further information is available at the CSVHFS Web site (**www.csvhfs.org**). See "The 2006 Conference," and "Guidance for Proceedings Authors," "Guidance for Presenters," and "Guidance for Table-top/Poster Displays."

**Contacts**

Technical Program Chairman: Jon Platt, WØZQ at **w0zq@aol.com**.

Proceedings Chairman: Donn Baker, WA2VOI/Ø at **Proceedings.WA2VOI@OurTownUSA.net**. □□

# Electronics Officers
## Needed for U.S. Flag Commercial Ships Worldwide

Skills required: Computer, networking, instrumentation and analog electronics systems maintenance and operation.
Will assist in obtaining all licenses.
Outstanding pay and benefits.
Call, Fax or e-mail for more information.

**American Radio Association, AFL-CIO**
Phone: 504-831-9612
Fax: 775-828-6994
**arawest@earthlink.net**

# ELECTRONICS OFFICER TRAINING ACADEMY

**The Complete Package To Become A Marine Radio Officer/Electronics Officer**

ELKINS, with its 54-year history in the radio and communications field, is the only school in the country providing all the training and licensing certification needed to prepare for the exciting vocation of Radio Officer/Electronics Officer in the Merchant Marines.
Great Training | Great Jobs | Great Pay

Call, Fax or Email for More Information:

**ELKINS Marine Training International**
P.O. Box 2677; Santa Rosa, CA 95405
Phone: 800-821-0906, 707-792-5678
Fax: 707-792-5677
Email: info@elkinsmarine.com
Website: www.elkinsmarine.com

## Flash Crystal Frequency Synthesizer

- **Clean, Stable RF Signal Source** – Great for local oscillators and lab test equipment applications!
- **Several Models Available** – Covering from 7 MHz up to 148 MHz
- **Can Store Up to 10 Frequencies** – Board-mounted mini rotary dip switch for frequency selection
- **Completely Re-Programmable** – Program the 10 frequencies using any PC running *Hyperterminal* (included in *Windows* operating systems)
- **Economical** – A fraction of the cost of comparable lab-grade RF signal synthesizers
- **Outputs Approximately 5 mW (+7 dBm)** – Female SMA RF output connector
- **Fully Assembled, Tested, and Ready to Go!** – Just $80 (plus $4.30 S/H in US)
- **Super Compact** – Measures less than 2 by 2 inches!
- **Power Requirements** – 8 to 15V dc at approximately 55 mA

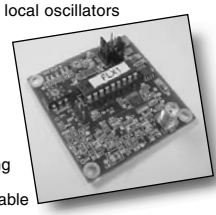

**For Further Details, Visit Our Web site for the Owners Manual**

### HC-49 Crystals
- Frequencies: 3535, 3560, 7030, 7038, 7040, 7042, 7058, 7122, 7190, 7195, 10106, 10125, 10700, 14057, 14058, 14060, 21060, 24906, 28060, 28238, 28258 kHz
- Specs: +/–100 ppm, 18 pf

### Cylindrical Crystals
- Frequencies: 3560, 7030, 7038, 7040, 7042, 7190, 10106, 10125, 14025, 14200, 14285, 18096, 21026, 21060, 24906, 28060 kHz.
- Specs: +/–100 ppm, 18 pF, 3x8 mm. (3560 crystal: 3x10 mm)

**Expanded Spectrum Systems • 6807 Oakdale Dr • Tampa, FL 33610**
**813-620-0062 • Fax 813-623-6142 • www.expandedspectrumsystems.com**

From MILLIWATTS to KILOWATTS
More Watts per Dollar

Taylor TUBES

## Quality Transmitting & Audio Tubes

Eimac

- COMMUNICATIONS
- BROADCAST
- INDUSTRY
- AMATEUR

Svetlana

*Immediate Shipment from Stock*

| | | | |
|---|---|---|---|
| 3CPX800A7 | 3CX15000A7 | 4CX5000A | 813 |
| 3CPX5000A7 | 3CX20000A7 | 4CX7500A | 833A |
| 3CW20000A7 | 4CX250B | 4CX10000A | 833C |
| 3CX100A5 | 4CX250BC | 4CX10000D | 845 |
| 3CX400A7 | 4CX250BT | 4CX15000A | 866-SS |
| 3CX400U7 | 4CX250FG | 4X150A | 872A-SS |
| 3CX800A7 | 4CX250R | YC-130 | 5867A |
| 3CX1200A7 | 4CX350A | YU-106 | 5868 |
| 3CX1200D7 | 4CX350F | YU-108 | 6146B |
| 3CX1200Z7 | 4CX400A | YU-148 | 7092 |
| 3CX1500A7 | 4CX800A | YU-157 | 3-500ZG |
| 3CX2500A3 | 4CX1000A | 572B | 4-400A |
| 3CX2500F3 | 4CX1500A | 807 | M328/TH328 |
| 3CX3000A7 | 4CX1500B | 810 | M338/TH338 |
| 3CX6000A7 | 4CX3000A | 811A | M347/TH347 |
| 3CX10000A7 | 4CX3500A | 812A | M382 |

*– TOO MANY TO LIST ALL –*

VISA MasterCard DISCOVER

**ORDERS ONLY:**
**800-RF-PARTS • 800-737-2787**
Se Habla Español • We Export

TECH HELP / ORDER / INFO: 760-744-0700

FAX: 760-744-1943 or 888-744-1943

*An Address to Remember:*
**www.rfparts.com**

*E-mail:*
rfp@rfparts.com

RF Since 1967

RF PARTS™ COMPANY

# 2006 Dayton Hamvention®

Sponsored by Dayton Amateur Radio Association Since 1952

Don't Miss Ham Radio's GREATEST SHOW!

## May 19 – 21, 2006 at Hara Arena, Dayton, Ohio

**Forums – 500 Inside Exhibit Spaces – 2,300 Flea Market Spaces**
**Over $50,000 in Prizes!**

**Buy Tickets and Flea Market Spaces on-line! No Change in prices!**

**www.hamvention.org**
**or call (937) 276-6930 or write to:**
**Dayton Hamvention, PO Box 964, Dayton, OH, 45401**

**For hotel info, see our web site or contact the Dayton Convention and Visitors Bureau at (800) 221-8235**

**If you don't see it at Hamvention, it simply doesn't exist!**

*And Featuring...*

# ARRL EXPO — 2006 —

SAVE the dates
May 19, 20 & 21

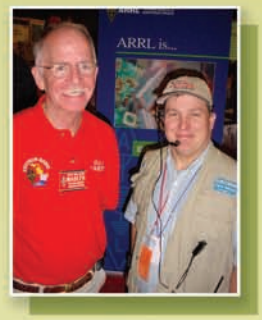


**Your Hamvention admission includes access to ARRL EXPO (located in the Hara Ballarena, near the 400-numbered booths).**

- Visit special ARRL exhibits and booths, including the huge ARRL bookstore!
- See live presentations on the ARRL Stage
- Meet ARRL staff and volunteers
- DXCC Card Checking
- Join or renew with ARRL – and receive a FREE GIFT



***Pick up your ARRL Passport***

***The ultimate convention scavenger hunt!***

**ARRL** *The national association for AMATEUR RADIO*

Visit **www.arrl.org/expo** for the latest ARRL EXPO 2006 news!

KENWOOD
Listen to the Future

# TS-480

## The Perfect Remote Base Transceiver

## Straight Out of the Box!


- The perfect internet base transceiver - straight out of the box!
- Easy to operate
- The size makes it great for base, mobile or portable operation.
- Free VoIP/Control software downloads at Kenwood.net.
- Incredible RX specifications.

**KENWOOD U.S.A. CORPORATION**
**Communications Sector Headquarters**
3975 Johns Creek Court, Suite 300, Suwanee, GA 30024-1265
**Customer Support/Distribution**
P.O. Box 22745, 2201 East Dominguez St., Long Beach, CA 90801-5745
Customer Support: (310) 639-4200 Fax: (310) 537-8235

INTERNET
**Kenwood News & Products**
http://www.kenwood.net
ADS#02406

JQA-1205 091-A
**ISO9001 Registered**
Communications Equipment Division
Kenwood Corporation
ISO9001 certification